

The Plaid Model and Outer Billiards on Kites

Richard Evan Schwartz *

October 12, 2015

Abstract

This paper establishes an affine quasi-isomorphism between the arithmetic graph associated to outer billiards on kites, and the plaid model, a combinatorial construction for producing embedded polygons in the plane.

1 Introduction

The purpose of this paper, which continues the study of the plaid model, is to prove the Quasi-Isomorphism Conjecture from [S1].

Theorem 1.1 (Quasi-Isomorphism) *Let $p/q \in (0, 1)$ be any rational such that pq is even. Let Π denote the plaid model at the parameter p/q . Let Γ denote the arithmetic graph associated to the special orbits of outer billiards on the kite $K_{p/q}$. Then Π and Γ are 2-affine-quasi-isomorphic.*

Quasi-Isomorphisms: First let me explain what the term *quasi-isomorphic* means. We say that two embedded polygons are *C-quasi-isomorphic* if they can be parametrized so that corresponding points are within C units of each other. We say that two unions Γ and Π of polygons are *C-quasi-isomorphic* if there is a bijection between the members of A and the members of Γ which pairs up *C-quasi-isomorphic* polygons. Finally, we say that A and B are *C-affine-quasi-isomorphic* if there is an affine transformation $T : \mathbf{R}^2 \rightarrow \mathbf{R}^2$ such that Π and $T(\Gamma)$ are *C-quasi-isomorphic*.

* Supported by N.S.F. Research Grant DMS-1204471

Example: Figure 1 shows the Quasi-Isomorphism Theorem in action for the parameter $p/q = 3/8$. The black polygons are part of the plaid model and the grey polygons are part of the affine image of the arithmetic graph.

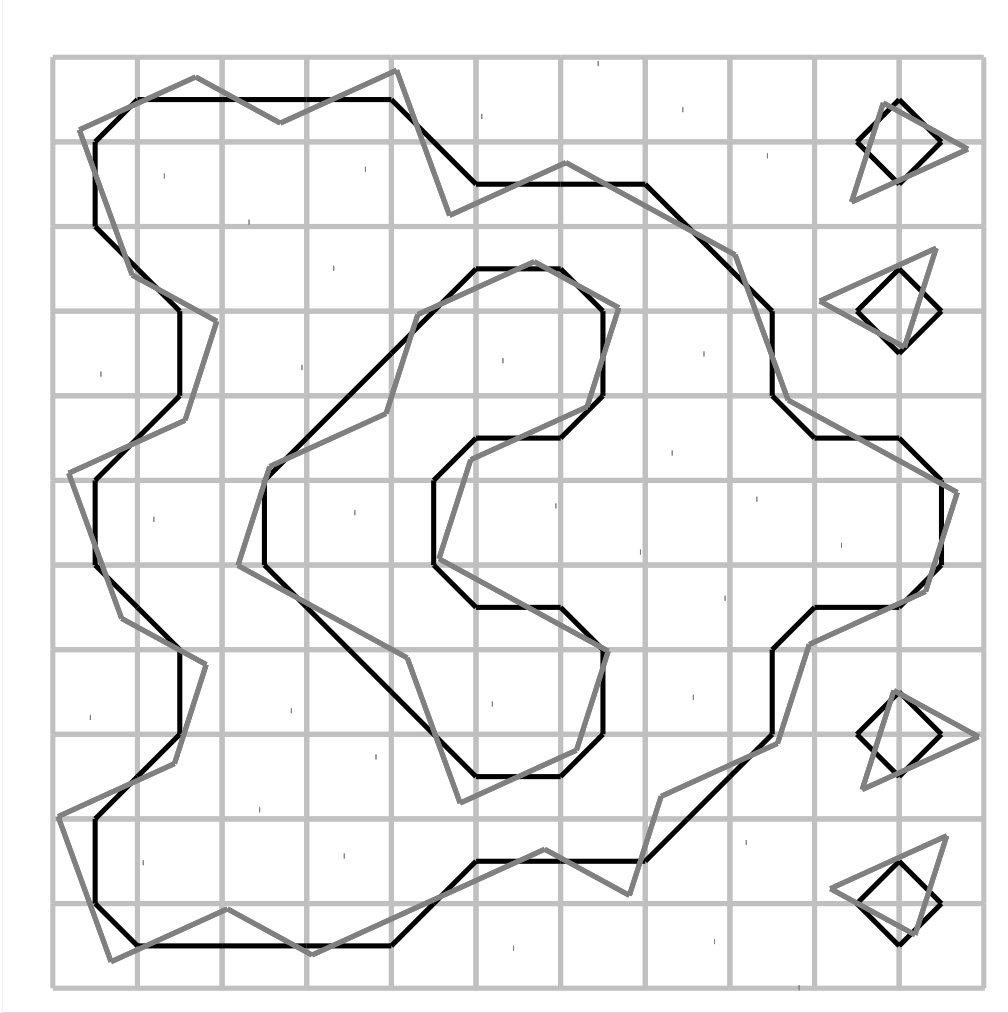


Figure 1: The Quasi-Isomorphism Theorem in action.

In general, the vertices of the black curves lie in the lattice $\frac{1}{2}\mathbb{Z}^2$, which has co-area $1/4$, whereas the vertices of the grey curves lie in a lattice having co-area $1 + p/q$. Even though the polygons line up in a global sense, their vertices lie on quite different lattices. This fact points to the highly nontrivial nature of quasi-isomorphism being established.

The Plaid Model: The plaid model, introduced in [S1], has a combinatorial flavor that is similar in spirit to corner percolation and P. Hooper's Truchet tile system [H]. I will give a precise definition in §2. The plaid model has a rich and inherently hierarchical structure which I explored in [S1] and [S2]. In [S2] I showed that the plaid model (which can be defined even for irrational parameters) has unbounded orbits for every irrational parameter. The significance of the Quasi-Isomorphism Theorem, aside from its intrinsic beauty, is that it allows one to use the plaid model as a tool for studying the dynamics of outer billiards on kites.

Outer Billiards: Outer billiards was introduced by B. H. Neumann in the late 1950s. See [N]. One of the central questions about outer billiards has been: Does there exist a compact convex set K (other than a line segment) and a point p_0 so that the orbit $\{p_n\}$ exits every compact set? This question, dating from around 1960, is called the Moser-Neumann question. See [M1] and [M2]. My monograph [S0] has a survey of the known results about this problem. See also [T1] and [T2]. The main work on this Moser-Neumann problem is contained in [B], [D], [VS], [K], [GS], [G], [S0], [DF].

In [S0] I showed that there are unbounded orbits with respect to any irrational kite. Any kite is affinely equivalent to the kite K_A with vertices

$$(-1, 0), \quad (0, 1), \quad (0, -1), \quad (A, 0), \quad A \in (0, 1). \quad (1)$$

K_A is rational if and only if $A \in \mathbf{Q}$. Outer billiards on K_A preserves the infinite family of horizontal lines $\mathbf{R} \times \mathbf{Z}_1$. Here \mathbf{Z}_1 is the set of odd integers. A *special orbit* is an orbit which lies in this set of horizontal lines.

Polytope Classifying Spaces: Say that a *grid* is an affine image of \mathbf{Z}^2 in the plane. Suppose that G is a grid and Γ is a collection of polygons and polygonal arcs having vertices in G . Suppose also that there are only finitely many local pictures for Γ , up to translation.

A *polytope classifying space* is a triple (X, Φ, \mathcal{P}) where X is some Euclidean manifold, $\Phi : G \rightarrow X$ is an affine map, and \mathcal{P} is a partition of X into polytopes, each one labeled by one of the local pictures for Γ . We say that the triple (X, Φ, \mathcal{P}) is a classifying space for Γ if the following is true for each $c \in G$. The point $\Phi(c)$ lies in the interior of one of the polytopes of \mathcal{P} and the local picture of Γ at c coincides with the label of the polytope containing $\Phi(c)$.

The Plaid Master Picture Theorem: Our Isomorphism Theorem from [S1] says that, for any even rational parameter $A \in (0, 1)$, the plaid model has a 3 dimensional classifying space $(X_A, \Phi_A, \mathcal{P}_A)$. The grid in question here is the set of centers of integer unit squares. We call this grid the *plaid grid*.

In hindsight, it would have been better to call the Isomorphism Theorem the Plaid Master Picture Theorem, and so I will rechristen it here.

The plaid classifying spaces fit together. There is a 3 dimensional group Λ of affine transformations acting on

$$\widehat{X} = \mathbf{R}^3 \times [0, 1],$$

together with a Λ invariant partition of \widehat{X} into integer convex polytopes such that the intersection of these objects with $\mathbf{R}^3 \times \{P\}$ gives the pair (X_A, \mathcal{P}_A) . Here $P = 2A/(1 + A)$.

I will also explain how to interpret the quotient \widehat{X}/Λ , together with the quotient partition, as a 4 dimensional affine polytope exchange transformation. This is the same as the *curve following dynamics* defined in [H].

The Graph Master Picture Theorem: Our (Graph) Master Picture Theorem from [S0] does for the arithmetic graph what the Plaid Master Picture Theorem does for the plaid model.

There are several minor differences between the plaid case and the graph case. First, the way the partition determines the local picture is different; in fact there are really two partitions in this case. Another difference is the way that the slices fit together. The pair (X_A, \mathcal{Q}_A) associated to the arithmetic graph at A is the slice at A , rather than the slice at P . This seemingly minor point turns out to be important and helpful.

Another difference is that we will compose the classifying map, Φ'_A with the affine map from the Quasi-Isomorphism Theorem, so that the Master Picture Theorem pertains directly to the set of polygons we wish to compare with the plaid model. We define the *graph grid* to be the affine image of \mathbf{Z}^2 under this affine map.

The classifying space picture for the arithmetic graph can also be interpreted in terms of affine polytope exchange transformations, but we will not dwell on this point. In the plaid case we really need the interpretation for some of our constructions, but in the graph case we can do without it.

The Projective Intertwiner: Let G_Π and G_Γ respectively denote the plaid grid and the graph grid. Let X_Π and X_Γ respectively denote the plaid PET and the graph PET. Let $\Phi_\Pi : G_\Pi \rightarrow X_\Pi$ and $\Phi_\Gamma : G_\Gamma \rightarrow X_\Gamma$ be the two intertwining maps. Technically, we should write $\Phi_\Pi = \Phi_{\Pi,A}$, and $G_{\Gamma,A}$, etc., to denote dependence on the parameter.

The grid G_Γ has the property that no point of G_Γ lies on the boundary of an integer unit square. This means that to each $b \in G_\Gamma$, there is a unique associated point $c(b) \in G_\Pi$. Here $c(b)$ is the center of the unit integer square containing b . We call $b \rightarrow c(b)$ the *centering map*. We will find a piecewise projective map $\Psi : X_\Pi \rightarrow X_\Gamma$ with the following property:

$$\Phi_\Gamma(b) = \Psi \circ \Phi_\Pi(c(b)), \quad \forall b \in G_\Gamma. \quad (2)$$

This equation is meant to hold true for each even rational parameter, but the map Ψ is globally defined and piecewise projective. That is, the restriction of Ψ to the interiors of suitable polytopes is a projective transformation. We call Ψ the *projective intertwiner*.

Main Idea: A plaid 3-arc is the portion of a connected component of the plaid model which occupies 3 consecutive integer unit squares. We will see that the plaid classifying space X_Π has a partitioned into finitely many polytopes, each one labeled by a plaid 3-arc. (This is where we use the dynamical interpretation.) For each point $a \in G_\Pi$, the plaid 3-arc centered at a is a translate of the label of the partition piece containing $\Phi_A(a)$. We call this auxiliary partition the *plaid triple partition*.

At the same time the graph classifying space X_Γ has a partition into finitely many polytopes, with the following properties: Each of these polytopes is labeled by a (combinatorial) length 2 polygonal arc with integer vertices. For each lattice point $b \in G_\Gamma$, the length 2 arc of the arithmetic graph centered at b is determined by the polytope label. We call this partition the *graph double partition*.

The way we prove the Quasi-Isomorphism Theorem is that we consider the image of the plaid triple partition under the projective intertwining map. We study how it sits with respect to the graph double partition. This allows us to line up the plaid model with the arithmetic graph piece by piece. We will see also that there is some amount of fussing when it comes to globally fitting the different pieces together.

Self-Containment: This paper is the culmination of several years of work, and about 8 years of thinking, about the structure of outer billiards on kites. The reader might wonder whether it is possible to read this paper without an enormous buildup of machinery and background. In one sense this paper is very far from self-contained, and in another sense, it is self-contained.

The proof of the Quasi-Isomorphism Theorem, as stated, is far from self-contained. It relies on the Plaid and Graph Master Picture Theorems. In this paper, I will state these results precisely, but I will not re-do the proofs. On the other hand, I will give a complete account of the relationship between the graph PET and the plaid PET. So, if one view the Quasi-Isomorphism Theorem as a statement about some kind of quasi-isomorphism between 4 dimensional affine PETs, then the paper is self-contained. The projective intertwining map Ψ is not a conjugacy between these two PETs, but for even rational parameters, it does induce a bijection between the orbits of the two systems which preserves periods up to a factor of 2. This seems to be a striking situation. I haven't seen anything like it in the study of PETs.

Paper Overview: Here is an overview of the paper.

- In §2, I will recall the definition of the plaid model.
- In §3, I will recall the definition of the arithmetic graph. I will also prove some geometric facts about the *graph grid*, which is the image of \mathbb{Z}^2 under the affine transformation implicit in the Quasi-Isomorphism Theorem.
- In §4 I will deduce the Quasi-Isomorphism from two other results, the Pixellation Theorem and the Bound Chain Lemma. The Pixellation Theorem, a 6-statement result, is the main thrust of the paper. It makes a statement to the effect that locally the polygons in the two collections follow each other. The Bound Chain Lemma provides the glue needed to match the local pictures together.
- In §5 I will deduce the Bound Chain Lemma from the Pixellation Theorem. The deduction is a tedious case by case analysis. Following §4-5, the rest of the paper is devoted to proving the Pixellation Theorem.
- In §6 I will give an account of the Plaid Master Picture Theorem, and I will also define the Plaid Triple Partition.

- In §7, I will give an account of the Graph Master Picture Theorem.
- In §8 I will introduce a formula, called the Reconstruction Formula, which gives information about the graph grid in terms of the graph classifying map. I will use this formula to prove Statement 1 of the Pixellation Theorem modulo some integer computer calculations.
- In §9 I will prove the existence of the projective intertwiner, the map which relates the Plaid and Graph Master Picture Theorems. The result is summarized in the Intertwining Theorem.
- In §10, I will combine the Plaid Master Picture Theorem, the Graph Master Picture Theorem, and the Intertwining Theorem to prove Statement 2 of the Pixellation Theorem, modulo some integer computer calculations. I will also set up the problems which one must solve in order to Prove the remaining statements of the Pixellation Theorem.
- In §11, I will introduce some auxiliary sets which augment the power of the machinery developed above. I will also give some sample arguments which illustrate most of the features of the general proof given in §12.
- In §12 I will combine all the machinery to prove Statements 3,4, and 5 of the Pixellation Theorem, modulo some integer computer calculations.
- In §13 I will explain the integer computer calculations used in §8,10,11. In §13.3, I will explain how to access the computer program which runs the proof.

Companion Program: This paper has a companion computer program. I checked essentially all the details of the paper on the computer program. I think that the reader would find this paper much easier to read if they also used the program. Most of the technical details of the paper are simply encoded into the computer program, where they are illustrated as colorful plots and pictures. In particular, the polytope partitions which form the backbone of our proof are much easier to understand when viewed with the program. Again, in §13.3, I explain how to access the program.

Acknowledgements: I would like to thank Pat Hooper, Sergei Tabachnikov, and Barak Weiss for helpful and interesting conversations related to this work.

2 The Plaid Model

2.1 The Mass and Capacity Labels

In [S1] we gave a general definition of the plaid model and explored its symmetries. Rather than repeat the definition from [S1] we will explain the plaid model for the parameter $p/q = 2/9$. The definition generalizes in a straightforward way to the other parameters. The parameter $2/9$ is small enough to allow us to present the whole definition concretely but large enough so that the definition isn't muddled by too many coincidences between small numbers. In any case, the planar definition of the plaid model is just given for the sake of completeness; we will use the PET definition given in §3.

So, we fix $p/q = 2/9$. We have the following auxiliary parameters:

$$\omega = p + q = 11, \quad P = \frac{2p}{p+q} = \frac{4}{11}, \quad Q = \frac{2q}{p+q} = \frac{18}{11}, \quad \tau = 3. \quad (3)$$

The parameter τ is the solution in $(0, \omega)$ to the equation $2p\tau \equiv 1 \pmod{\omega}$. In this case, we have $2(2)(3) = 12 \equiv 1 \pmod{11}$.

The plaid model is invariant under the action of the lattice generated by vectors $(0, 11)$ and $(11^2, 0)$. Moreover, the model does not intersect the boundaries of the 11 *blocks*

$$[0, 11]^2 + (11k, 0), \quad k = 0, \dots, 10.$$

So, it suffices to describe the plaid model in each of these 11 blocks.

We think of $[0, 11]^2$ as tiled by the 12×12 grid of unit integer squares. We introduce the *capacity labeling* on the integer points along the coordinate axes as follows.

- We give the labels $0, 2, 4, 6, 8, 10, -10, -8, -6, -4, -2, 0$ to the points $(0, 3), (0, 6), (0, 9), \dots, (0, 33)$.
- We extend the labels so that they are periodic with respect to translation by $(0, 11)$.
- We give the same labels to integer points along the x -axis, simply interchanging the roles of the x and y axes.

We now describe the *mass labeling* of the integer points along the y -axis. We let $[x]_{11}$ denote the point $x + 11k$ which lies in $(-11, 11)$. Here $k \in \mathbf{Z}$ is a suitably chosen integer. When $x \in 11\mathbf{Z}$ we set $[x]_{11} = \pm 11$. (This situation does not actually arise.) If $\mu \neq 0$ is a capacity label of some point, then exactly one of the two quantities

$$[\mu/2]_{11}, \quad [(\mu/2) + 11]_{11} \quad (4)$$

is odd. We define the mass label of the point to be this odd quantity. When $\mu = 0$ we define the mass label to be ± 11 , without specifying the sign. We denote this unsigned quantity by $[11]$.

Figure 2.1 shows the capacity and mass labelings of the first block.

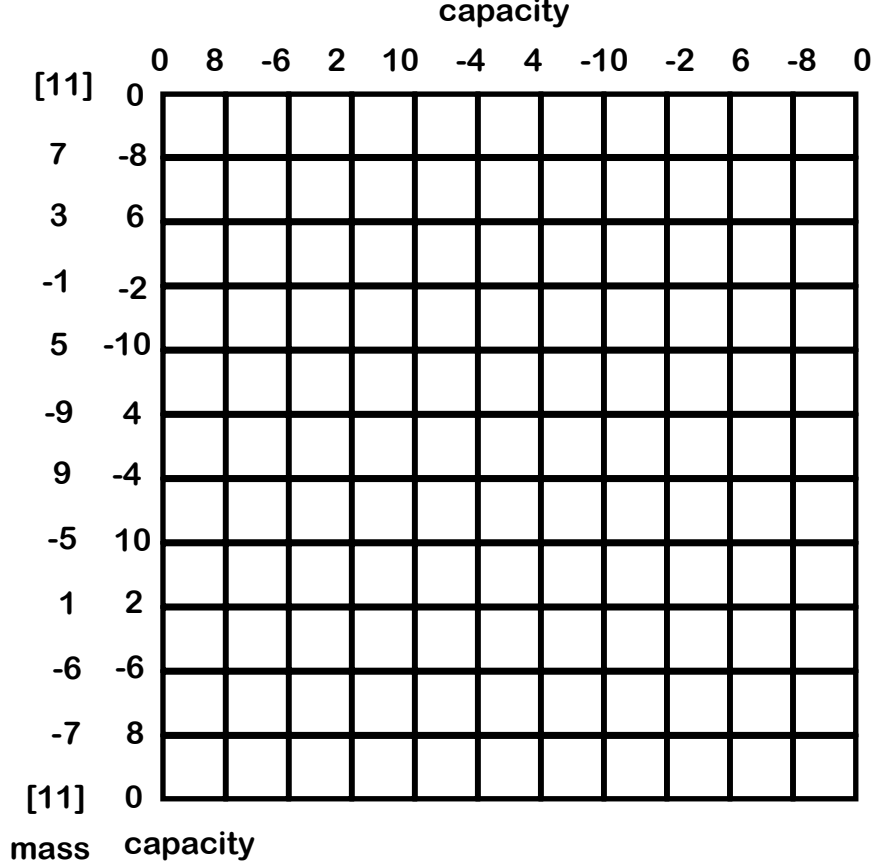


Figure 2.1: The mass and capacity labelings for the first block.

2.2 Definition of the Model

We define 6 families of lines

- \mathcal{H} : Horizontal lines intersecting the y -axis at integer points.
- \mathcal{V} : Vertical lines intersecting the x -axis at integer points.
- \mathcal{P}_- : Lines of slope $-4/11$ intersecting the y -axis at integer points.
- \mathcal{Q}_- : Lines of slope $-18/11$ intersecting the y -axis at integer points.
- \mathcal{P}_+ : Lines of slope $+4/11$ intersecting the y -axis at integer points.
- \mathcal{Q}_+ : Lines of slope $+18/11$ intersecting the y -axis at integer points.

We call the \mathcal{H} and \mathcal{V} lines *grid lines*. We call the lines from the latter 4 families the *slanting lines*. The grid lines divide \mathbf{R}^2 into the usual grid of unit squares. We call the edges of these equares *unit grid segments*. When we want to be more specific, we will speak of *unit horizontal segments* and *unit vertical segments*.

Say that an *intersection point* is a point on a unit grid segment which is also contained on a slanting line. Every intersection point is actually contained on two slanting lines, one of positive slope and one of negative slope. With the correct multiplicity convention, every unit grid segment contains 2 intersection points. The multiplicity convention is that the horizontal unit segments which cross the lines $x = (11/2) + 11k$ for $k \in \mathbf{Z}$ are declared to contain 2 intersection points. What is going on is that these segments contain a single point which lies on 4 slanting lines. we call these intersection points *light* and *dark* according to the following rules:

Vertical Rule Suppose that z is an intersection point contained in a vertical unit line segment. We call z a *light point* if and only if the 3 lines through z all have the same sign, and the common sign is usual.

Horizontal Rule: If z happens to lie on the special segments mentioned in the section on the hexagrid – i.e. if z is an intersection point of multiplicity two – then z is not a light point. Otherwise, z is a light point if and only if the signs of the three lines are usual, and the sign of the horizontal line matches the sign of the line of negative slope and is opposite from the sign of the line of positive slope.

Remark: It might happen that the point z is a vertex of one of the unit squares. In this case, we apply each rule separately. It turns out that this situation happens only when z lies on a vertical line of the form $x = n\omega$ for $n \in \mathbf{Z}$. In this case, only the horizontal rule can make z a light point because the vertical line just mentioned has an unusual sign.

Now we define the plaid model. We say that a unit grid segment is *on* if it contains exactly 1 light point. We proved in [S1] that each unit square has either 0 or 2 edges which are on. (This result takes up the bulk of [S1].) We form the *plaid model* as follows: In each square which has 2 on edges, we connect the centers of these edges by a segment. By construction, the union of all these connector segments is a countable union of embedded polygons. This union of polygons is the plaid model for the given parameter.

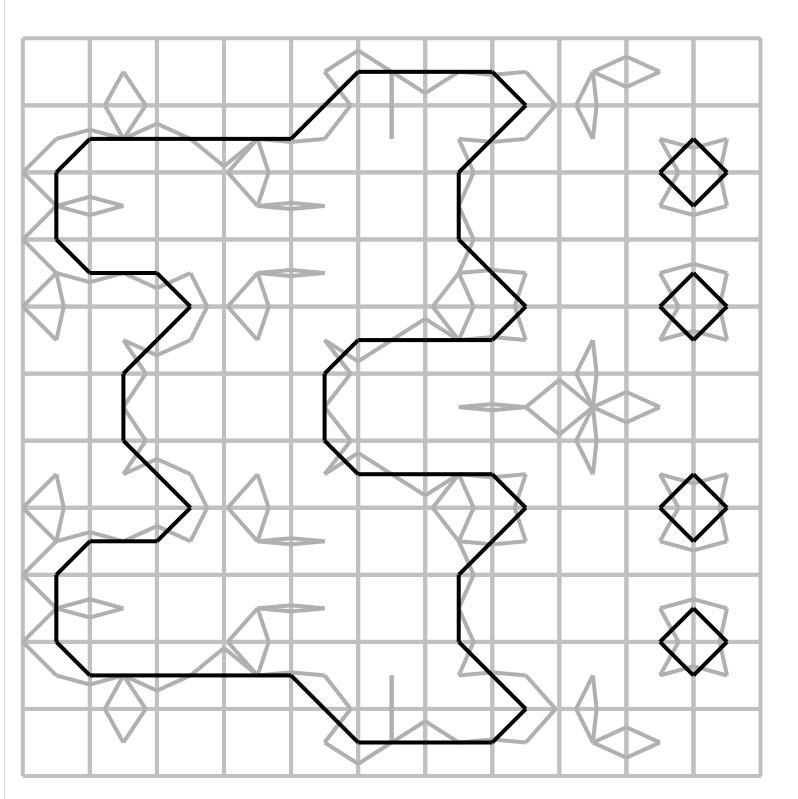


Figure 2.2: The first block of the plaid model for $p/q = 2/9$. first block.

Figure 2.2 needs some explanation. The black polygons are the plaid polygons. We have illustrated the light points in each unit square by drawing a grey arc from the center of the square to the corresponding light points. Notice that none of the black arcs touch edges which have two grey arcs incident to them.

It is worth pointing out that the picture looks different in different blocks. Figure 2.3 shows the picture in the block

$$[0, 11]^2 + (55, 0).$$

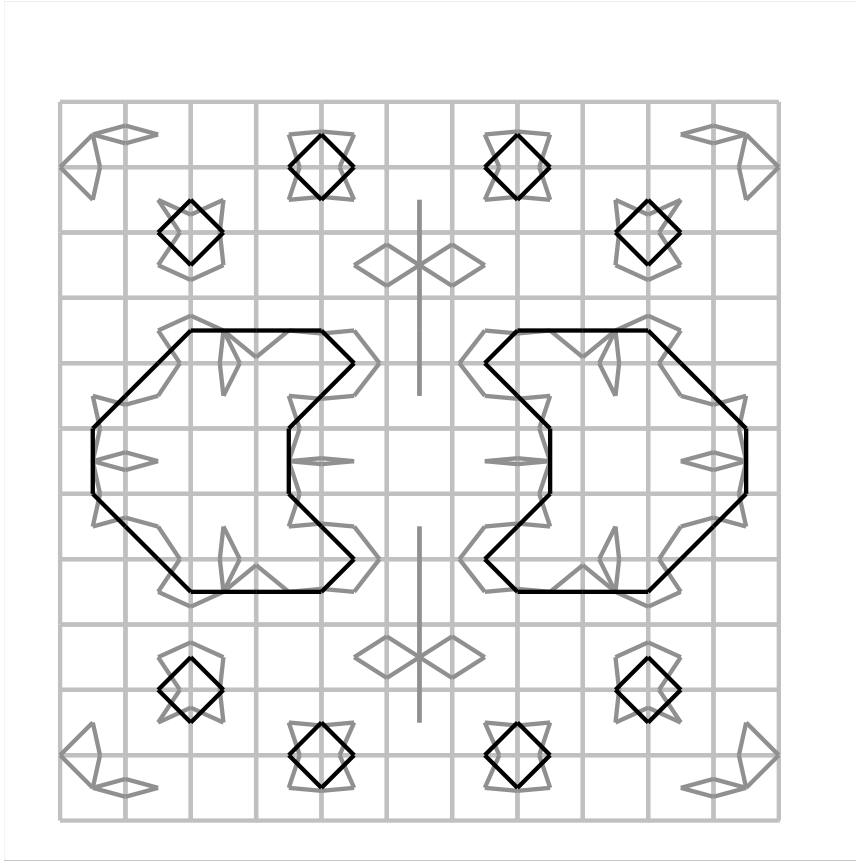


Figure 2.2: The plaid model for for $p/q = 2/9$ in $[55, 66] \times [0, 11]$.

The center of rotational symmetry is $(11^2/2, 11/2)$.

The plaid model for this parameter is invariant under the reflections in the lines $y = 11/2$ and $x = 11^2/2$. In particular, the point $(11^2/2, 11/2)$ is a center of rotational symmetry. All this is proved, for the general parameter, in [S1, §2].

2.3 Alternate Definition

There is a second definition which just uses the lines in the families \mathcal{V} , \mathcal{H} , \mathcal{P}_- and \mathcal{Q}_- . In this definition, an intersection point is light if and only if it is the intersection point of a grid line and a negative slanting line such that the mass of the slanting line is less than the capacity of the grid line and the signs of the two lines are the same.

This second definition points out the hierarchical nature of the plaid model. The plaid model has 4 grid lines of capacity $2k$, two horizontal and two vertical, and each of them carries at most $2k$ light points. This hierarchical structure is exploited in [S1] and [S2] to get control over the geometry of the components of the plaid model.

It is not at all clear from either definition that the number of light points on sides of an integer unit square is either 0 or 2. However, we proved this in [S1]. It is a consequence of the Isomorphism Theorem.

3 The Arithmetic Graph

3.1 Special Orbits and the First Return Map

We will describe the picture when $p/q \in (0, 1)$ is rational. We need not take pq even. Let $A = p/q$. We consider outer billiards on the kite K_A , described in Equation 1 and shown in Figure 3.1. Recall from the introduction that the *special orbits* are the orbits which lie on the set S of horizontal lines having odd integer y -intercepts.

Let ψ_A denote the second iterate of the outer billiards map. This map is a piecewise translation. Let Ψ_A denote the first return map of ψ_A to the union Ξ of 2 rays shown in Figure 3.1 below Here

$$\Xi = \mathbf{R}_+ \times \{-1, 1\} \subset S \quad (5)$$

Lemma 3.1 *Every special orbit is combinatorially identical to the orbit of a point of the form*

$$\left(2mA + 2n + \frac{1}{q}, \pm 1\right). \quad (6)$$

Here $m, n \in \mathbf{Z}$ and the left hand side of the equation is meant to be positive.

Proof: This is proved in [S1]. Here is a sketch of the proof. What is going on is that ψ_A permutes the intervals of a certain partition of S into intervals of length $2/q$, namely

$$S = \bigcup_{m, n \in \mathbf{Z}^2} \left(\frac{2m}{q}, n\right)$$

and so every orbit is combinatorially identical to the orbit of a center point of one of these intervals. Moreover, all such orbits intersect the set Ξ . When the orbit of a center point of an interval in the partition intersects Ξ , it does so in a point of the form given in Equation 6. The left hand side of Equation 6 is an alternate way of writing the set

$$\left(\bigcup_{m \in \mathbf{Z}} \frac{2m}{q}\right) \cap \mathbf{R}_+.$$

♠

Remark: The same result holds if $1/q$ in Equation 6 is replaced by any $\iota \in (0, 2/q)$. We will take $\iota = 1/q$ when we state the Master Picture Theorem.

3.2 The Arithmetic Graph

Suppose that m_0, n_0 are integers such that $2m_0A + 2n_0 \geq 0$. Then, by definition, there are integers m_1, n_1 , with $2m_1A + 2n_1 \geq 0$ such that

$$\Psi_A\left(2m_0A + 2n_0 + \frac{1}{q}, 1\right) = \left(2m_1A + 2n_1 + \frac{1}{q}, \epsilon\right), \quad (7)$$

where $\epsilon \in \{-1, 1\}$ is given by

$$\epsilon = (-1)^{m_0+m_1+n_0+n_1}. \quad (8)$$

Reflection in the x -axis conjugates Ψ_A to Ψ_A^{-1} , so we also have

$$\Psi_A^{-1}\left(2m_0A + 2n_0 + \frac{1}{q}, -1\right) = \left(2m_1A + 2n_1 + \frac{1}{q}, -\epsilon\right), \quad (9)$$

Actually, we won't end up caring about ϵ .

Figure 3.1 shows an cartoon of what Equation 7 looks like geometrically when $\epsilon = -1$.

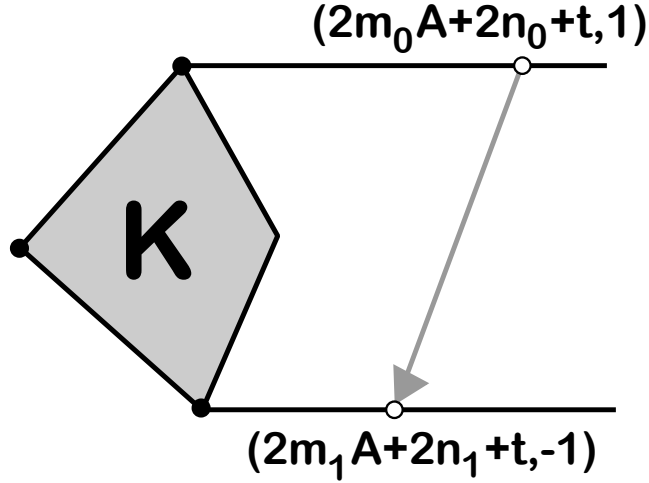


Figure 3.1: The arithmetic graph construction.

We form a graph Γ_A whose vertices are \mathbf{Z}^2 by joining (m_0, n_0) to (m_1, n_1) by an edge if and only if these points are related as in Equation 7. We proved in [S1] that all the edges of Γ_A have length at most $\sqrt{2}$. That is, there are just 8 kinds of edges. We also proved that Γ_A is a union of pairwise disjoint embedded polygonal paths. All these paths are closed when pq is even.

The nontrivial components of Γ all lie in the half plane above the line L of slope $-A$ through the origin. The map

$$f(m, n) = \left(2Am + 2n + \frac{1}{q}, (-1)^{m+n} \right) \quad (10)$$

carries each component of Γ_A to a different special orbit. The image of this map is “half” the special special orbits, in the sense that every special orbit, or its mirror, is represented. The *mirror* of a special orbit is its reflection in the x -axis. If we wanted to get the other half of the special orbits, we would use the map $\rho \circ f$, where ρ is reflection in the x -axis.

It is possible to extend Γ_A in a canonical way so that it fills the entire plane, and not just the half plane. We want to do this so that the Quasi-Isomorphism Theorem is true as stated. There are two ways to do this, and they give the same answer.

1. Dynamically, we can consider the first return map to the negative-pointing rays $-\Xi$ and make the same construction.
2. Using the classifying space picture described below, we can simply take the domain to be all of \mathbf{Z}^2 rather than just the portion of \mathbf{Z}^2 above L .

We will take the second approach below. We call this extended version of Γ_A the *arithmetic graph* at the parameter A .

3.3 The Canonical Affine Transformation

The Quasi-Isomorphism Theorem compares the plaid model with a certain affine image of the arithmetic graph. In this section we describe the affine map. Recall that $A = p/q$ and $\omega = p + q$. The affine map from the Quasi-Isomorphism Theorem is given by

$$T \begin{pmatrix} x \\ y \end{pmatrix} = \frac{1}{A+1} \begin{pmatrix} A^2 + A & A+1 \\ -A^2 + 2A + 1 & -2A \end{pmatrix} \begin{pmatrix} x \\ y \end{pmatrix} + \begin{pmatrix} \frac{1}{2q} \\ -\frac{-1}{2q} + \frac{1}{p+q} + \tau \end{pmatrix}. \quad (11)$$

Here τ is the solution in $(0, \omega)$ to the equation $2p\tau \equiv 1 \pmod{\omega}$. The linear part of the map T is defined for irrational parameters as well as rational parameters, but the map itself is only defined when p/q is an even rational.

Normalized Arithmetic Graph: The canonical affine transformation T is the implied affine map in the Quasi-Isomorphism Theorem. We define the *normalized arithmetic graph* to be the T -image of the arithmetic graph. The Quasi-Isomorphism Theorem says that the plaid model and the normalized arithmetic graph are 2-quasi-isometric at each parameter.

The inverse of the canonical affine transformation is

$$T^{-1} \begin{pmatrix} x \\ y \end{pmatrix} = \frac{1}{(A+1)^2} \begin{pmatrix} 2A & A+1 \\ -A^2+2A+1 & -A^2-A \end{pmatrix} \begin{pmatrix} x \\ y \end{pmatrix} + \frac{1}{2p+2q} \begin{pmatrix} -1-2q\tau \\ -1+2p\tau \end{pmatrix}. \quad (12)$$

Again, the linear part is defined even for irrational parameters. However, the entire map is only defined for even rationals.

The Graph Grid: We define the *graph grid* to be the grid $T(\mathbf{Z}^2)$. The vertices of the normalized arithmetic graph lie in the graph grid. A calculation shows that $\det(dT) = 1 + A$, so the graph grid has co-area $1 + A$, as mentioned in the introduction. What makes T canonical is that $T(\mathbf{Z}^2)$ has rotational symmetry about the origin.

The Anchor Point: Let

$$\zeta = \left(\frac{1+A}{2}, \frac{1-A}{2} \right). \quad (13)$$

We compute

$$T^{-1}(\zeta) = \left(\frac{1}{2}, \frac{1}{2} \right) + \left(\frac{-1-2q\tau}{2\omega}, \frac{-1+2p\tau}{2\omega} \right).$$

The second summand is a vector having half-integer coordinates. Hence, $T^{-1}(\zeta) \in \mathbf{Z}^2$. Hence $\zeta \in T(\mathbf{Z}^2)$. We call ζ the *anchor point*. Given the existence of ζ , we can redefine the graph grid to be the translate of $dT(\mathbf{Z}^2)$ which contains ζ . This allows us to define the graph grid even at irrational parameters, even though the canonical affine transformation is only defined for even rational parameters. As A varies from 0 to 1, the grid $T(\mathbf{Z}^2)$ interpolates between the grid of half integers and the grid of integers whose coordinates have odd sum, and each individual point travels along a hyperbola or straight line.

Distinguished Edges and Line: Say that a *distinguished edge* in the grid graph is one connecting distinct points of the form

$$T(\zeta), \quad T(\zeta + (i, j)), \quad i, j \in \{-1, 0, 1\}. \quad (14)$$

Let $\mathcal{F}(i, j)$ denote the family of distinguished edges corresponding to the pair (i, j) . In [S0] we proved that the arithmetic graph is embedded, and each edge is one of the 8 shortest vectors in \mathbf{Z}^2 . Thus, the edges of the normalized arithmetic graph are all distinguished.

Say that a *distinguished line* is a line that contains a distinguished edge of the grid graph. If these lines are parallel to edges in $\mathcal{F}(i, j)$ we say that the lines have *type* (i, j) .

3.4 Geometry of the Graph Grid

In this section we prove a number of statements about the geometry of the graph grid. The word *square* always means integer unit square, as in the plaid model.

Lemma 3.2 (Grid Geometry) *The following is true at each parameter.*

1. *No point of the grid graph lies on the boundary of a square.*
2. *Two points of the grid graph cannot lie in the same square.*
3. *A union of 3 horizontally consecutive squares intersects the grid graph.*
4. *A union of 2 vertically consecutive squares intersects the grid graph.*
5. *Two graph grid points in consecutive squares are always connected by a distinguished edge.*
6. *If two parallel distinguished lines intersect the interior of the same edge e of a square, then the lines have type $(-1, 1)$ and e is horizontal.*
7. *The slopes of the distinguished edges are never in $\{-1, 1, 0, \infty\}$.*

Proof of Statement 1: We just need to prove, for each $(x, y) \in \mathbf{Z}^2$, that neither coordinate of $T(x, y)$ is an integer. The two coordinates of $T(x, y)$ are

$$\frac{1}{2q} + \frac{px}{q} + y, \quad \tau - \frac{q-p}{2q(p+q)} + \frac{-2p^2x + 4pqx + 2q^2x - 4pqy}{2q(p+q)}$$

The first number is always $k/(2q)$ where K is an odd integer. The second number is always $n/(2q(p+q))$, where n is odd. ♠

Lemma 3.3 Suppose v is a vector with $\|v\| < \sqrt{2}$. Then $\|dT^{-1}(v)\| < 2$.

Proof: For any matrix M , we have $\|M(v)\| \leq \|M\|_2 \|v\|$. Here $\|M\|_2$ is the L_2 norm of M . Setting $M = dT^{-1}$ we get

$$\|M\|_2^2 = \sum_{ij} M_{ij}^2 = \frac{2(1 + 3A + 4A^2 - A^3 + A^4)}{(1 + A)^4} \leq 2$$

The inequality on the right, which holds for all $A \in [0, 1]$, is an exercise in calculus: We check that the derivative of this expression does not vanish in $[0, 1]$, and then we evaluate at $A = 0$ and $A = 1$ to get the bound on the right. The final result is that $\|M\|_2 \leq \sqrt{2}$. ♠

Proof of Statement 2: Call a vector in $dT(\mathbf{Z}^2)$ *bad* if both its coordinates are less than 1 in absolute value. Thanks to the previous result, if this lemma is false then there is some bad vector in $dT(\mathbf{Z}^2)$. A bad vector has length less than $\sqrt{2}$. Hence, by the previous result, a bad vector must have the form $dT(\zeta)$, where ζ is one of the 8 shortest nonzero vectors in \mathbf{Z}^2 . By symmetry we just have to check 4 out of the 8, namely:

- $dT(1, 0) = \left(A, \frac{1+2A-A^2}{1+A}\right)$.
- $dT(0, 1) = \left(1, \frac{-2A}{1+A}\right)$.
- $dT(1, 1) = (1 + A, 1 - A)$.
- $dT(1, -1) = \left(-1 + A, \frac{1+4A-A^2}{1+A}\right)$.

Here we have set $A = p/q \in (0, 1)$. In all cases, we can see that least one coordinate is at least 1 in absolute value. ♠

Proof of Statement 3: It suffices to prove that every translate of $T^{-1}(R)$ intersects \mathbf{Z}^2 . The vertices of $T^{-1}(R)$ are

$$R_0 = (0, 0), \quad R_1 = \left(1, -\frac{2A}{1+A}\right), \quad R_2 = \left(3A, \frac{3+6A-3A^2}{1+A}\right), \quad R_3 = R_1 + R_2.$$

Clearly R_1 lies below the line $y = 0$. A bit of calculus shows that R_2 and R_3 both lie above the line $y = 2$. Furthermore, any line of the form $y = h$ with $h \in [0, 2]$ intersects $T^{-1}(R)$ in a segment of width

$$\frac{1+2A+A^2}{1+2A-A^2} > 1.$$

This is sufficient to see that every translate of $T^{-1}(\mathbf{R})$ intersects \mathbf{Z}^2 . ♠

Proof of Statement 4: Let R be a union of two vertically consecutive squares. Let C_R denote the infinite column of integer unit squares containing R . Note that $T(0, 1) = (1, -P)$. Say that a *distinguished array* is an infinite set of points of the form $T(m_0, n)$, where m_0 is held fixed and $n \in \mathbf{Z}$. Because the first coordinate of $T(0, 1)$ is 1, we see that every row intersects C_R in one point.

Let ρ_m denote the m th row of points. Let y_m denote the y -coordinate of the point v_m where ρ_m intersects C_R . Looking at the formulas above, observe that the difference in the x coordinates of $dT(1, 0)$ and $dT(1, -1)$ is 1 and that both y coordinates are in $[1, 2]$. For this reason, one of the two points $v_m + dT(1, 0)$ or $v_m + dT(1, -1)$ lies on a row above v_m and moreover the vertical distance between these points is less than 2. Hence $|h_{m+1} - h_m| < 2$ for all m . But then R contains some v_m . ♠

Proof of Statement 5: Let

$$f = v_1 - v_2 = (f_1, f_2) = dT(i, j).$$

When the squares are stacked on top of each other, we have the constraints $|f_1| < 1$ and $|f_2| = 2$. When the squares are stacked on top of each other, we have the constraints $|f_1| < 2$ and $|f_2| = 1$. Both cases give $\|f\| < \sqrt{5}$. This combines with $\|dT^{-1}\|_2 < \sqrt{2}$ to show that $i^2 + j^2 < 10$. An explicit case-by-case rules everything out but

- $(i, j) \in \{\pm(1, 0), \pm(1, -1)\}$ in the first case.
- $(i, j) \in \{\pm(0, 1), \pm(1, 1)\}$ in second case.

These cases do actually occur. ♠

Proof of Statement 6: Let us first consider in detail the case when L_1 and L_2 have type $(1, 0)$ and the edge e is vertical. To rule out this case, we just need to intersect two adjacent lines with the y -axis and see that the distance between the intersection points is at least 1 unit. Let dT be the linear part of T . Two consecutive lines are given by

$$(1 - s)dT(0, 0) + sdT(1, 0), \quad (1 - s)dT(0, 1) + sdT(1, 1).$$

The first line contains $(0, 0)$. To see where the second line intersects the y -axis, we set the first coordinate equal to 0 and solve for t . This gives $t = -1/A$. Plugging this into the equation, we see that the y intercept is $-1 - 1/A$. Hence, the vertical distance is $1 + 1/A$, a quantity that always exceeds 1. We record this information by writing $d(1, 0, V) = 1 + 1/A$. Following the same method, we do the other 7 cases. Here is the result:

$$\begin{aligned} d(1, 0, V) &= 1 + \frac{1}{A}, & d(1, 0, H) &= \frac{1 + 2A + A^2}{1 + 2A - A^2}. \\ d(0, 1, V) &= 1 + A, & d(0, 1, H) &= \frac{1 + 2A + A^2}{2A}. \\ d(1, 1, V) &= 1, & d(1, 1, H) &= \frac{1 + A}{1 - A}. \\ d(-1, 1, V) &= \frac{1 + A}{1 - A}, & d(-1, 1, H) &= \frac{1 + 2A + A^2}{1 + 4A - A^2}. \end{aligned}$$

Only the last quantity can drop below 1. ♠

Proof of Statement 7: We compute that the possible slopes for the distinguished edges are

$$\frac{1 + 2A - A^2}{A + A^2}, \quad \frac{-2A}{1 + A}, \quad \frac{1 - A}{1 + A}, \quad \frac{1 + 4A - A^2}{A^2 - 1}.$$

It is an easy exercise in algebra to show that these quantities avoid the set $\{-1, 0, 1, \infty\}$ for all $A \in (0, 1)$. ♠

4 The Proof in Broad Strokes

4.1 Pixellated Squares

We fix some even rational parameter $A = p/q$ for the entire chapter. All the definitions are made with respect to this parameter. Also, to save words, *square* will always denote a unit integer square. Finally, by *arithmetic graph*, we mean the image of the arithmetic graph under the canonical affine transformation.

Plaid Nontriviality: We say that a square Σ is *plaid nontrivial* if the plaid tile at Σ is nontrivial. Otherwise we call Σ *plaid trivial*. When Σ is plaid nontrivial, we define the *plaid edge set* of Σ to be the two edges of Σ crossed by the plaid polygon that enters Σ .

Grid Fullness: We say that Σ is *grid full* if Σ contains a point of the graph grid. Otherwise we call Σ *grid empty*. When Σ is grid full, there is a unique point of the graph grid contained in Σ , and this point lies in the interior of Σ . See the Grid Geometry Lemma.

Graph Nontriviality: This definition only applies when Σ is grid full. We say that Σ is *graph trivial* if the point σ of the graph grid contained in Σ is isolated in the arithmetic graph. Otherwise we call Σ *graph nontrivial*. When Σ is graph nontrivial, we call the two edges of the arithmetic graph incident to σ the *graph edges associated to Σ* .

Pixellation: This definition only applies to squares Σ which are graph full. We call Σ *pixellated* if the following is true:

- Σ is graph trivial if and only if Σ is plaid trivial.
- If Σ is plaid nontrivial then the graph edges associated to Σ cross Σ in the interiors of the edges in the plaid edge set of Σ .

When Σ is pixellated, the plaid model at Σ determines the local picture of the graph model in Σ in the cleanest possible way.

We can see that all the grid full squares in Figure 1 are pixellated. Indeed, for the parameter $3/8$ and many others, every grid full square is pixellated. However, this perfect situation fails for some parameters.

4.2 Bad Squares

Bad Squares We keep the notation and terminology from the previous section. We call the square Σ *bad* if Σ is graph full but not pixellated. It turns out that this only happens when Σ is both plaid nontrivial and graph nontrivial. (See the Pixellation Theorem below.)

Offending Edges: We say that an *offending edge* is a graph edge associated to Σ which does not cross the boundary of Σ in the interior of one of the edges of the edge set.

Unused Sides: We say that an *unused side* is an edge in the plaid edge set of Σ which is not crossed by a graph edge associated to Σ . The existence of an unused side implies the existence of an offending edge, and *vice versa*.

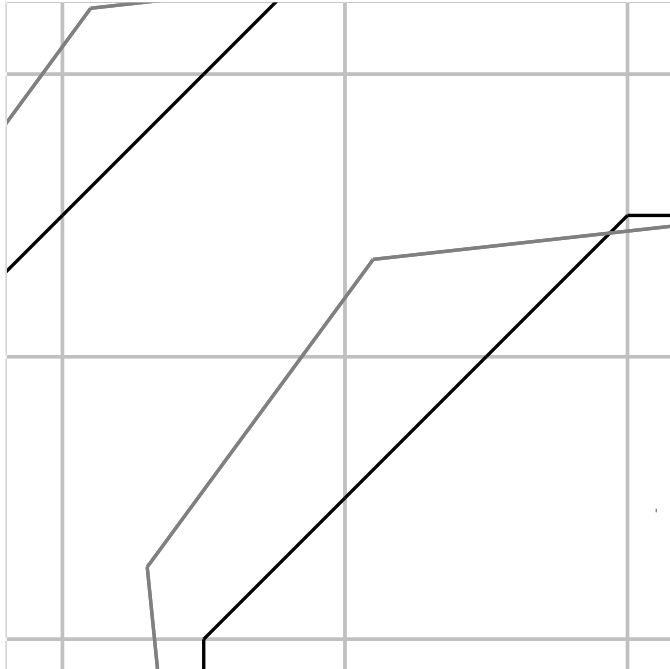


Figure 4.1: Some bad squares for the parameter $p/q = 4/5$.

Figure 4.1 shows a closeup of the picture when $p/q = 4/5$. The plaid polygons are in black and the arithmetic graph polygons are in grey. The top right and bottom left squares are bad. The top left and bottom right squares are grid empty.

Catches: Figure 4.2 shows a picture of two possible patterns of squares which involve a bad square, an offending edge and an unused side. In both cases, the bad square is meant to be the top right one. The plaid segment in the top right square either connects the south edge to the north edge or to the east edge. The shaded squares are meant to be grid empty. The offending edge is drawn as a curved grey segment. We mean to consider now just these patterns, but also the ones which arise by applying a symmetry of the square grid to these. In other words, we don't want to fix the orientation of the pattern in the plane.

In both cases, the portion of the plaid model in the bottom two squares makes a straight diagonal segment, and the sign of the slope of the offending edge is the same as the sign of the portion of the diagonal segment. In these pictures, we say that the unused side and the offending edge are *associated*. We call these two patterns (and their isometric images) *catches* for the offending edge.

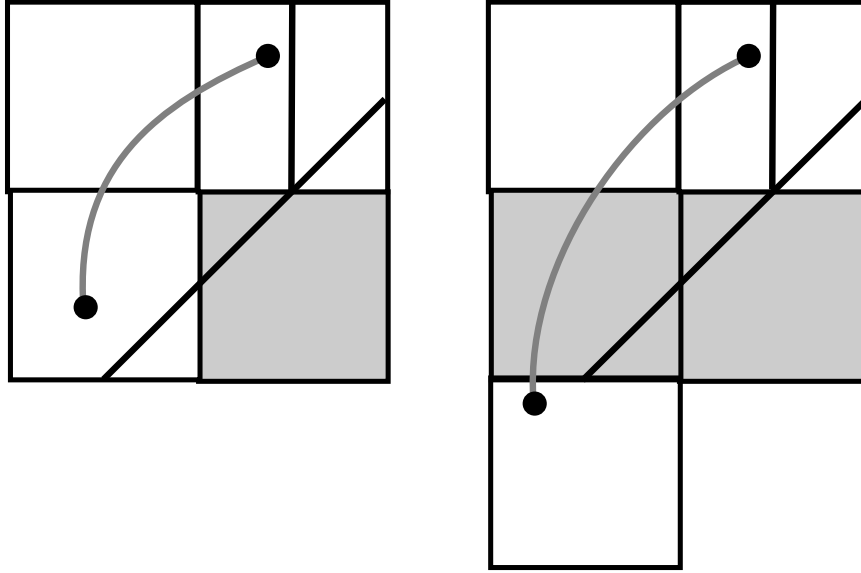


Figure 4.2: The two catches for an offending edge in a bad square.

The Pixellation Theorem, stated below, says that the pictures in Figure 4.2 and their rotated/reflected images are always present when there is an unused side and an offending edge. We defer the statement of the Pixellation Theorem for a while, because we want to bundle some other minor results into it.

4.3 Errand Edges and Double Crossings

Errand Edges: Say that an *errand edge* is an edge of the arithmetic graph with sits with respect to the plaid model as in Figure 4.3. The grey arc is the arithmetic graph edge. We have drawn it curved because here and below a curved picture will look nicer. Of course, we are representing a straight line segment. The numbers 1 and 2 denote squares Σ_1 and Σ_2 . The edge $\Sigma_1 \cap \Sigma_2$ is in the plaid edge set of Σ_1 (and of Σ_2) and hence the arithmetic graph edge is not an offending edge with respect to Σ_1 . However, it rises up at least one unit above the top of Σ_1 and Σ_2 while the plaid polygon in Σ_2 either goes straight across Σ_2 or else moves downward. As usual, we mean to consider all possible orientations of these configurations.

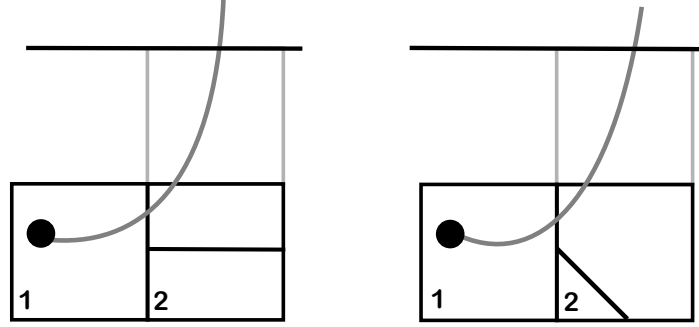


Figure 4.3: errand edges

Double Crossings: We say that a *double crossing* is a union of two disjoint distinguished edges e_1 and e_2 which have endpoints v_1 and v_2 in adjacent unit integer squares Σ_1 and Σ_2 and both cross $\Sigma_1 \cap \Sigma_2$ at interior points. The two squares may either be stacked on top of each other, as in Figure 4.4, or stacked side by side.

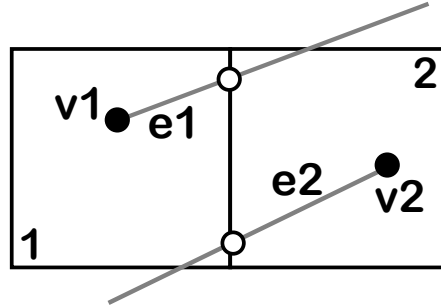


Figure 4.4: A double crossing

4.4 The Pixellation Theorem

Here is our main result.

Theorem 4.1 (Pixellation) *The following is true for any even rational parameter.*

1. *There are no double crosses in the arithmetic graph.*
2. *A square is plaid nontrivial if and only if it is grid nontrivial.*
3. *There are no errant edges in the arithmetic graph.*
4. *When a square is graph nontrivial, the two associated graph edges must cross distinct sides of the square.*
5. *In a bad square, there is a bijection between unused sides and offending edges, and each matched pair of objects is involved in a catch.*

The Pixellation Theorem says that the vast majority of grid full squares are pixellated, and it precisely characterizes the local picture around the ones which are not. To deduce the Quasi-Isomorphism Theorem from the Pixellation Theorem, we need to see that the various local pictures implied by the Pixellation Theorem piece together correctly. The next section contains the result we need, the Bound Chain Lemma. Here are some remarks on the wording in the Pixellation Theorem.

Statement 5 has a complicated phrasing which we want to explain. Logically, the existence of an unused side implies the existence of an offending edge, but we want to make sure that there is an offending edge that specifically is associated to the unused side of interest to us. Likewise, the existence of an offending edge implies the existence of an unused side, but we want to make sure that there is an unused side that specifically is associated to the offending edge of interest to us.

Statements 1 and 3 will not be used directly in our deduction of the Quasi-Isomorphism Theorem. However, they will be used, in the next chapter, for the deduction of the Bound Chain Lemma.

4.5 The Bound Chain Lemma

The main weakness in the Pixellation Theorem is that it only deals with grid full squares. Here we deal with the grid empty squares.

We say that a finite union of squares $\Sigma_1, \dots, \Sigma_m$ is *linked* if

- Σ_1 and Σ_m are grid fill, and the remaining squares are grid empty.
- $\Sigma_k \cap \Sigma_{k+1}$ is an edge, for each $k = 1, \dots, (m - 1)$.
- A single plaid polygon intersects Σ_k for all k .

To avoid trivialities, we take $m \geq 2$. It follows from Statements 3 and 4 of the Grid Geometry Lemma that a linked chain has length at most 4.

We say that our linked sequence is *bound* if a single edge in the arithmetic graph joins the graph grid point in Σ_1 to the graph grid point in Σ_m .

Figure 4.5 shows a linked and bound chain of length 4. We have drawn the arithmetic graph edge as curved, to get a nicer picture.

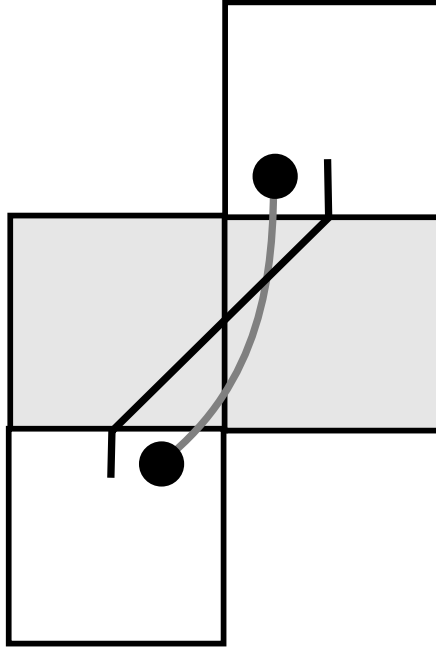


Figure 4.5: A Linked and Bound Chain of Length 4

In the next chapter, we will prove the following result, essentially using the Pixellation Theorem and a case-by-case analysis.

Lemma 4.2 (Bound Chain) *Every linked chain is bound.*

4.6 Proof of the Quasi-Isomorphism Theorem

The Quasi-Isomorphism Theorem is a fairly immediate consequence of the Pixellation Theorem and the Bound Chain Lemma. Here we produce an explicit homeomorphism between the union of polygons in the plaid model and the union of polygons in the arithmetic graph. The homeomorphism moves no point more than 2 units. The homeomorphism is defined in several pieces, depending on the type of square we have.

Let Σ be a pixellated square. Let v be the graph grid point in Σ and let e_1 and e_2 be the two edges incident to v . Let v' be the midpoint of the plaid segment contained in Σ and let e'_1 and e'_2 be the halves of the plaid segment on either side of v' . We map $e_k \cap \Sigma$ linearly to e'_k for $k = 1, 2$. We choose the labeling so that e_k and e'_k both intersect the same side of Σ . Figure 4.6 shows this simple map in action.

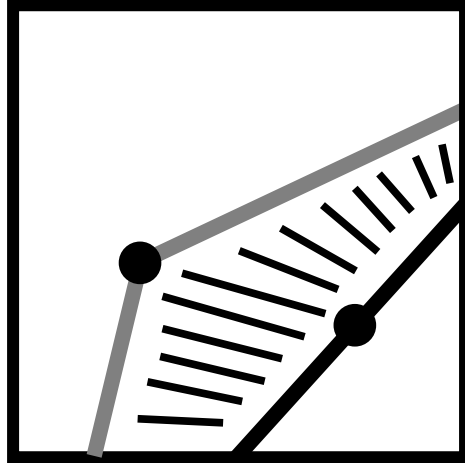


Figure 4.6: The Map on Pixellated Squares

We use the same notation for discussing bad squares. If Σ is a bad square and e_1 is not an offending edge of Σ then we do the same map as for pixellated squares. If e_1 is an offending edge, we map e_1 to the union of squares in the catch as shown in Figure 4.7 for each of the two kinds of catches. The white dots in Figure 4.7 are just extra guides for the map. On the right hand side of Figure 4.7, we have drawn one particular way that the plaid segment could look. The black dot the bottom square is meant to be the midpoint of the plaid segment, whatever it looks like.

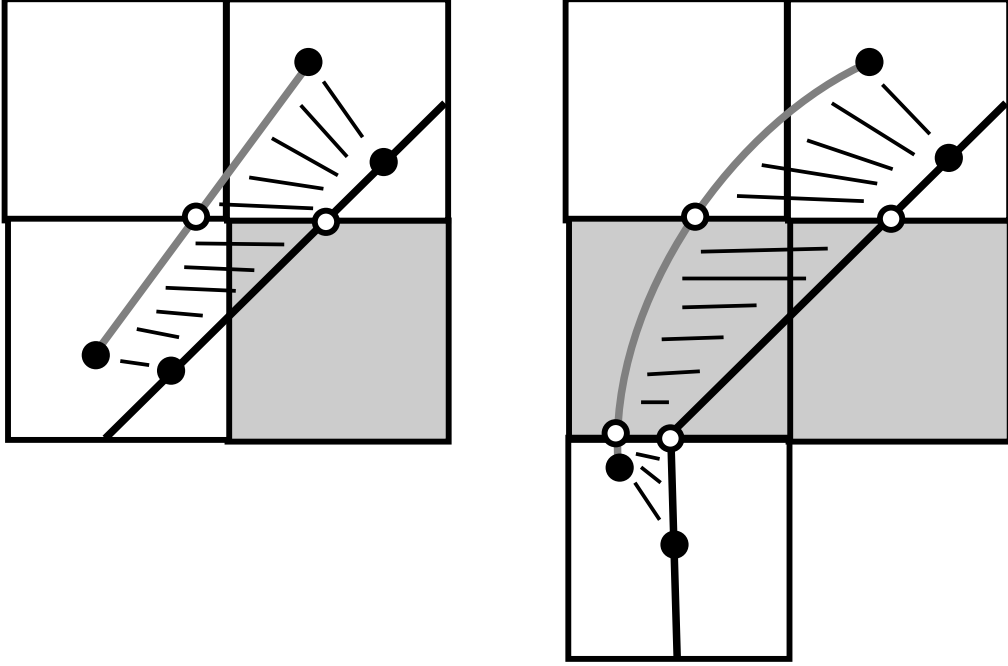


Figure 4.7: The Map on Bad Squares

Say that a *clean linked chain* is a chain $\Sigma_1, \dots, \Sigma_m$ such that the arithmetic graph edge e connecting v_1 to v_m crosses $\Sigma_1 \cap \Sigma_2$ and $\Sigma_{m-1} \cap \Sigma_m$. We say that the *graph core* associated to the clean linked chain is the segment

$$\hat{e} = e - (\Sigma_1 \cap \Sigma_m). \quad (15)$$

The segment \hat{e} has endpoints on $\Sigma_1 \cap \Sigma_2$ and $\Sigma_{m-1} \cap \Sigma_m$. Corresponding to the \hat{e} is the portion of the plaid model connecting these same two edges. We call this the *plaid core* associated the clean linked chain.

Our map is defined everywhere on the arithmetic graph polygons except on the graph cores. These comprise a disjoint set of segments. The image of our map so far is exactly the complement of the plaid cores. We finish the proof by mapping the graph cores to the plaid cores according to the scheme in Figure 4.8.

Figure 4.8 doesn't show every possibility, but these examples should be sufficient to show what we do in every case. In every case, the Pixellation Theorem and the Bound Chain Theorem imply that the map is well defined and only moves points by at most 2 units. We call our map Θ . By construction, Θ maps each arithmetic graph polygon homeomorphically to some plaid polygon.

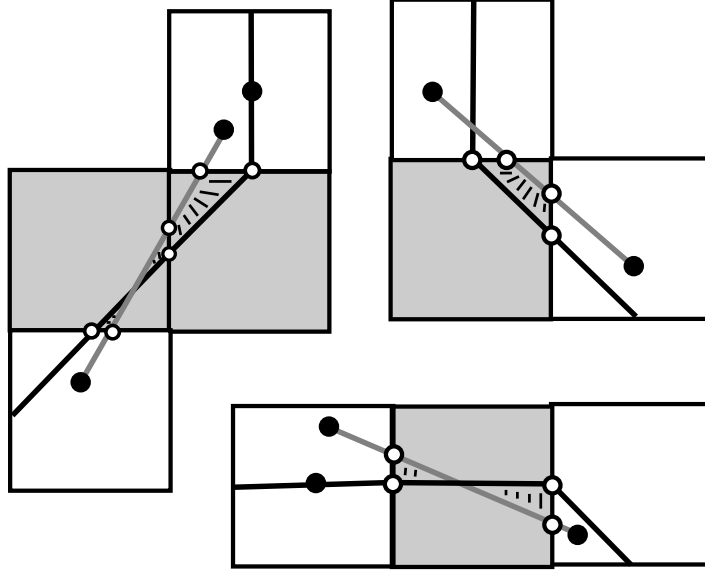


Figure 4.8: The Map on Bad Squares

Lemma 4.3 Θ is injective.

Proof: Suppose γ_1 and γ_2 are graph polygons which both map to the plaid polygon π . Suppose π never enters a square with a non-offending edge. Then, according to the Pixellation Lemma, π travels in a straight diagonal line. Since π is closed, this situation is impossible. Hence, π must enter at least one square Σ which has at least one non-offending edge e . The only way γ_1 and γ_2 are both mapped on to $e \cap \Sigma$ is if both these polygons contain the grid point in Σ . But then $\gamma_1 = \gamma_2$. ♠

Lemma 4.4 Θ is surjective.

Proof: Each plaid polygon π has length at least 4. Hence, by Statements 3 and 4 of the Grid Geometry Lemma the polygon π intersects at least one grid full square Σ . But then Φ maps the arithmetic graph polygon which contains the graph grid point in Σ to π . ♠

In short, Θ is a bijection between the components and a homeomorphism on each one, and Θ moves points by at most 2 units. This completes the proof of the Quasi-Isomorphism Theorem.

5 Proof of the Bound Chain Lemma

5.1 Length Two Chains

Let Σ_1, Σ_2 be a linked chain of length 2. This means that both Σ_1 and Σ_2 are plaid nontrivial and grid full, and a single plaid polygon runs through both. By the Pixellation Theorem, Σ_1 and Σ_2 are graph full as well.

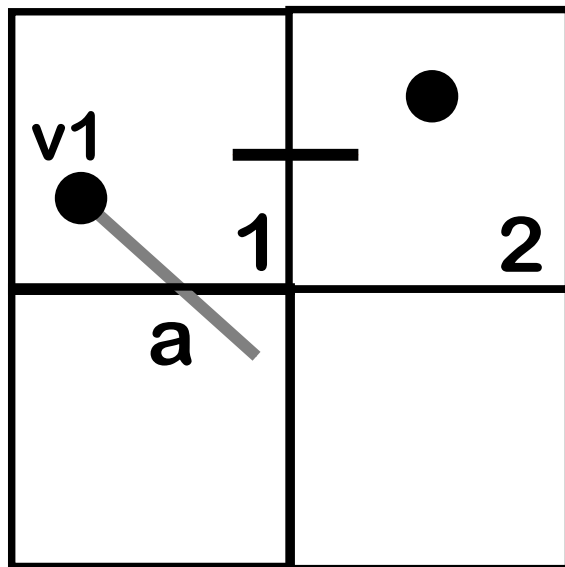


Figure 5.1: Σ_1 and Σ_2 , and an uncaught offending edge.

Let v_j be the graph grid point in Σ_j . Suppose that no graph edge incident to v_1 crosses $\Sigma_1 \cap \Sigma_2$. Then there must be an offending edge a incident to v_1 and associated to $\Sigma_1 \cap \Sigma_2$. This edge must cross either the bottom or the top of Σ_1 , and we have shown it crossing the bottom. But the picture contradicts Statement 5 of the Pixellation Theorem, because the catch for a would involve Σ_2 , and Σ_2 would be grid empty in the catch.

The argument in the preceding paragraph shows that there is some graph edge e_1 incident to v_1 which crosses $\Sigma_1 \cap \Sigma_2$. Likewise, there is some graph edge e_2 incident to $v_2 \in \Sigma_2$ which crosses $\Sigma_1 \cap \Sigma_2$. If e_1 and e_2 are disjoint, then we have a bad configuration. The Bad Configuration Lemma rules this out. Since the arithmetic graph is embedded, one of our two edges connects v_1 to v_2 , and in fact these two edges must coincide. (Otherwise we contradict the Pixellation Theorem.) In short, Σ_1, Σ_2 is a bound chain.

5.2 Length Three Chains: Case A

Here we consider a length 3 chain in which the three squares are the same horizontal row.

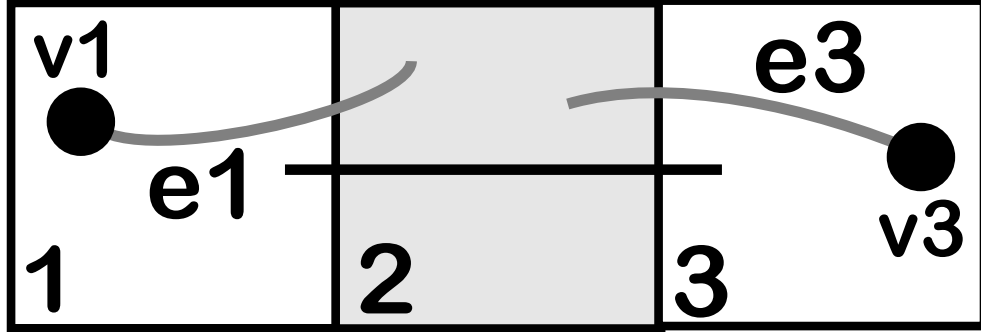


Figure 5.2 A horizontal chain

Lemma 5.1 *There is an edge of the arithmetic graph connecting v_1 and v_3 .*

Because the plaid polygon in Σ_2 is not a diagonal segment, there is no way to involve Σ_2 in a catch for an offending edge incident to v_1 and associated to $\Sigma_1 \cap \Sigma_2$. Hence, $\Sigma_1 \cap \Sigma_2$ is not an unused edge of Σ_1 . Hence there is some graph edge e_1 incident to v_1 and crossing $\Sigma_1 \cap \Sigma_2$. The same argument shows that there is an arithmetic graph edge e_3 associated to Σ_3 which crosses $\Sigma_2 \cap \Sigma_3$.

If the other endpoint e_1 of e_1 lies in Σ_3 then this other endpoint must be v_3 , because there is at most one graph grid point in Σ_3 . So, to finish the proof, we just have to rule out the other possible squares which could potentially contain the endpoint of e_1 .

The edge e_1 has length less than 2 because $\|dT\|_2 < \sqrt{2}$ and e_1 is the image of a vector in \mathbf{Z}^2 of length at most $\sqrt{2}$. This bound on the length cuts down on the possibilities where e_1 could end up. For one thing, e_1 cannot end up in any square to the right of Σ_3 . Also, e_1 cannot cross the line one unit above the top of Σ_2 , by Statement 3 of the Pixellation Theorem: no errant edges. Hence, the other endpoint of e_1 lies in the row of squares above Σ_2 . We will consider the 3 cases when e_1 ends in a square in the row above Σ_3 . The “below” case has the same treatment.

Case 1: Suppose first e_1 ends in Σ_4 , as shown on the left in Figure 5.3. In this case, e_1 connects v_1 with the graph grid point v_4 in Σ_4 . The plaid edge set of Σ_4 cannot contain $\Sigma_2 \cap \Sigma_4$ because the $\Sigma_2 \cap \Sigma_4$ is not in the plaid edge set of Σ_2 . Hence e_1 is an offending edge for Σ_4 . But then, by the Pixellation Theorem, the portion of the plaid model inside Σ_1 must look as drawn. This is impossible, because it forces the plaid edge set of Σ_1 to have 3 edges in it.

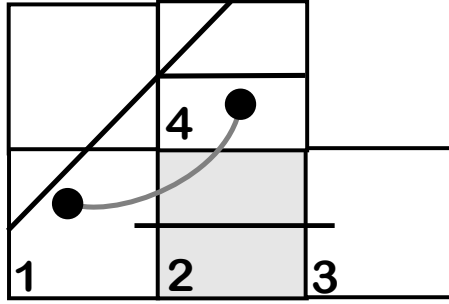


Figure 5.3: Case 1.

Case 2: Suppose e_1 crosses $\Sigma_3 \cap \Sigma_5$ and ends in Σ_5 . Note that e_1 cannot be an offending edge for Σ_5 because Σ_2 does not have the right form to be part of a catch for e_1 . Hence $\Sigma_3 \cap \Sigma_5$ is in the plaid edge set for Σ_5 . But then the result for length 2 chains says that some graph edge joins v_3 to v_5 . But then both graph edges incident to v_5 cross the same edge of Σ_5 . This contradicts Statement 4 of the Pixellation Lemma.

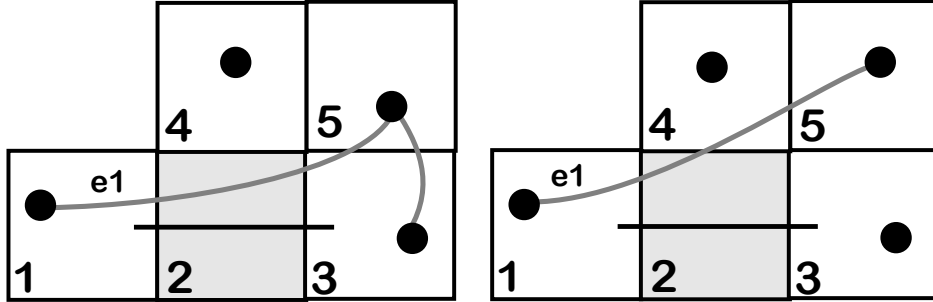


Figure 5.4: Cases 2 and 3

Case 3: Suppose that $w_1 \in \Sigma_5$ and e_1 crosses $\Sigma_4 \cap \Sigma_5$. By Statement 4 of the Grid Geometry Lemma, the square Σ_4 is grid full, just like Σ_3 is. The same argument as in Case 2, with Σ_4 replacing Σ_3 , takes care of this case. ♠

5.3 Length Three Chains: Case B

Here we consider a length 3 chain in which the three squares are the same vertical column. Our proof refers to Figure 5.5

This situation is not quite the same as in Case A because we can have 2 horizontally consecutive grid empty squares. If neither Σ_4 nor Σ_5 , shown in Figure 5.5, is grid empty, then the same argument as in Case A applies here. We just have to worry about the case when one of Σ_4 or Σ_5 is grid empty. We will consider the case when Σ_5 is grid empty. The other case has the same treatment.

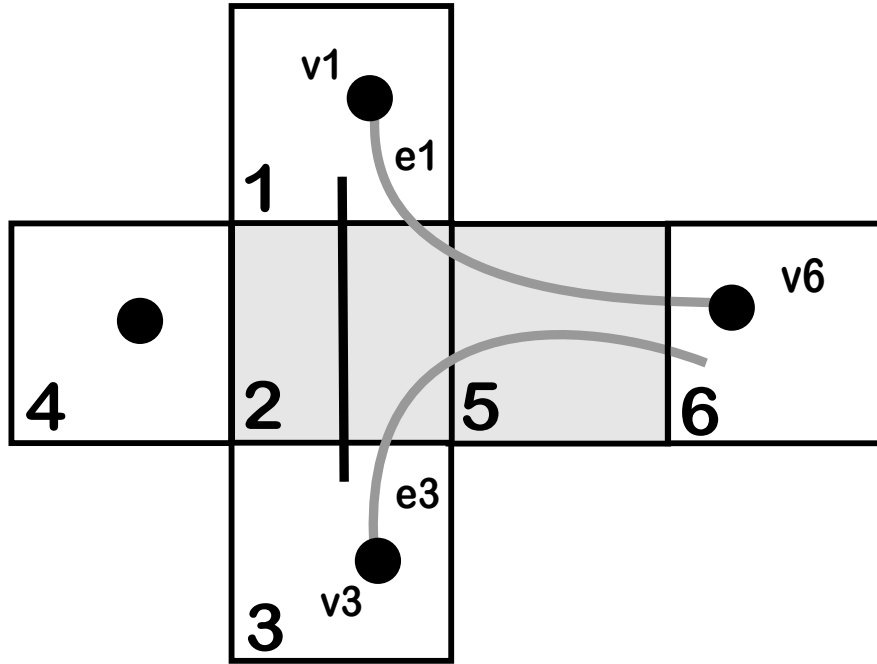


Figure 5.5: A vertical chain

In order to avoid finishing the proof as in Lemma 5.1 both edges e_1 and e_3 must cross $\Sigma_2 \cap \Sigma_5$. Neither edge can end in Σ_5 because Σ_5 is grid empty. If e_1 crosses the bottom edge of Σ_5 then e_1 blocks e_3 from exiting Σ_5 , which is a contradiction. Hence e_1 does not exit the bottom edge of Σ_5 . Similarly, e_3 cannot cross the top edge of Σ_5 . Hence, both e_1 and e_3 cross $\Sigma_5 \cap \Sigma_6$. But then e_1 and e_3 are errant edges, and this contradicts Statement 3 of the Pixellation Theorem.

5.4 Length Three Chains: Case C

Now we consider the remaining kind of length 3 chain, shown in Figure 5.6. As usual, let v_j be the graph grid point in Σ_j for $j = 1, 3$. We want to prove that an arithmetic graph edge connects v_1 to v_3 . This case is rather painful.

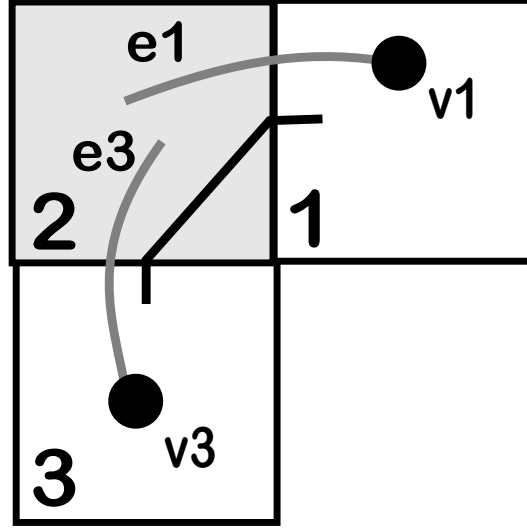


Figure 5.6

By Statement 5 of the Pixellation Theorem, $\Sigma_1 \cap \Sigma_2$ cannot be an unused edge with respect to Σ_1 , for the following reasons.

- If the associated offending edge were to cross through the top of Σ_1 , then the plaid segment in Σ_2 (which is part of the catch) would have the wrong position.
- If the associated offending edge were to cross through the bottom of Σ_1 , then the plaid segment in Σ_3 (which is part of the catch) would have the wrong position.

Hence some graph edge e_1 incident to v_1 crosses $\Sigma_1 \cap \Sigma_2$. The same argument applies to Σ_3 . So, we can assume that the edges e_1 and e_3 are as in Figure 5.6. We will show that e_1 has its other endpoint in Σ_3 . Since there is only one graph grid point in Σ_3 , the other endpoint of e_1 must be v_3 . In short, e_1 is the desired arithmetic graph edge connecting v_1 and v_3 . There are 6 situations we must rule out, and we deal with them in turn.

Case 1: Suppose e_1 ends in Σ_4 . Since $\Sigma_2 \cap \Sigma_4$ is not in the edge set of Σ_4 , the edge e_1 is offending with respect to Σ_4 . Given the negative slope of e_1 , the associated unused edge must be the right edge of Σ_4 and the catch must involve $\Sigma_1, \Sigma_2, \Sigma_4$. But then the plaid segment in Σ_1 is in the wrong position. This is a contradiction. The long Y-shaped graph in Figure 5.7 shows the shape of the plaid arc implied by the existence of the catch, and this contradicts the fact that the plaid arc in Σ_1 also crosses into Σ_2 .

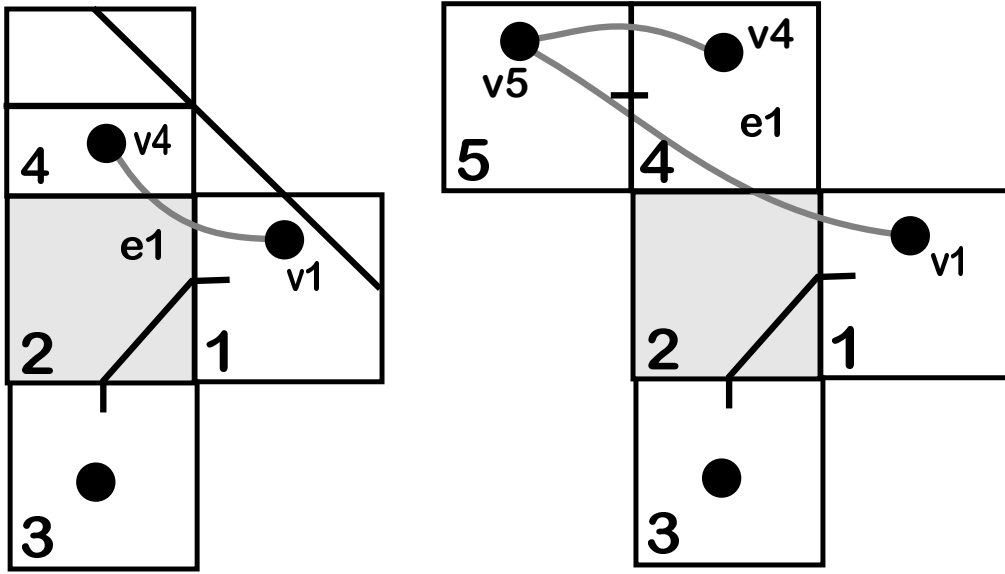


Figure 5.7: Cases 1 and 2

Case 2: Suppose e_1 ends in Σ_5 and that e_1 crosses $\Sigma_4 \cap \Sigma_5$. By Statement 4 of the Grid Geometry Lemma, the square Σ_4 is grid full. So, Σ_4 and Σ_5 are both grid full. If e_1 is an offending edge with respect to Σ_5 , then the associated unused edge is the bottom edge of Σ_5 . But then the catch for e_1 must involve $\Sigma_2, \Sigma_4, \Sigma_5$, and the plaid segment in Σ_2 is in the wrong position. Hence $\Sigma_4 \cap \Sigma_5$ is in the edge set for Σ_5 . Hence Σ_4, Σ_5 form a linked chain and some arithmetic graph edge joins v_4 and v_5 . This contradicts the Statement 4 of the Pixellation Theorem.

Case 3: Suppose that e_1 ends in Σ_5 and crosses $\Sigma_5 \cap \Sigma_6$, as shown on the left in Figure 5.8. If Σ_6 is not grid empty, then the same argument in Case 2 finishes the job. So, we may assume that Σ_6 is grid empty.

Now, e_1 cannot be an offending edge with respect to Σ_5 for the same reason as in Case 2. Thus, $\Sigma_5 \cap \Sigma_6$ is in the plaid edge set for Σ_6 . The left edge of Σ_6 cannot be in the plaid edge set for Σ_6 because this would make e_1 an errant edge for Σ_5 . Hence, the segment of the plaid model in Σ_6 connects $\Sigma_5 \cap \Sigma_6$ to $\Sigma_6 \cap \Sigma_7$. But then, by Case B in the previous section, some arithmetic graph edge connects Σ_5 to Σ_7 , as shown in Figure 5.10. But then two arithmetic graph edges cross $\Sigma_5 \cap \Sigma_6$, contradicting Statement 4 of the Pixellation Theorem.

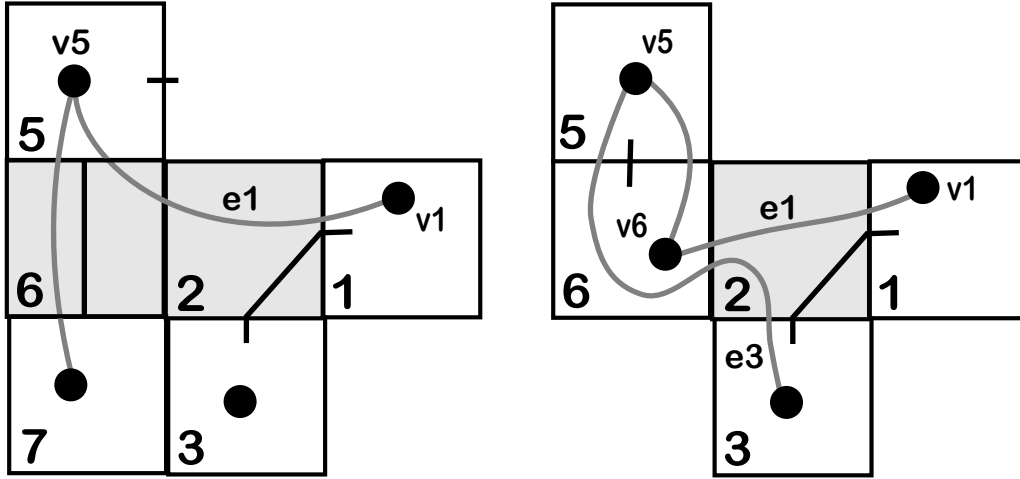


Figure 5.8: Cases 3 and 4

Case 4: Suppose that e_1 ends in Σ_6 and e_3 crosses $\Sigma_2 \cap \Sigma_6$. If e_3 ends at v_6 , then both e_1 and e_3 cross the same edge of Σ_6 and we contradict Statement 4 of the Pixellation Theorem. Since e_3 has length less than 2 and is not an errant edge for Σ_3 , the only possibility is that e_3 ends at v_5 . But the same argument as in Case 3 shows that e_3 is not an offending edge for Σ_5 . Hence Σ_6, Σ_5 is a linked chain. But then some other edge of the arithmetic graph connects v_6 to v_5 . This contradicts Statement 4 of the Pixellation Theorem.

Case 5: Suppose that e_1 ends in Σ_6 and e_3 does not cross $\Sigma_6 \cap \Sigma_2$. Note that e_1 blocks e_3 from crossing the top of Σ_2 , so e_2 crosses $\Sigma_1 \cap \Sigma_2$.

Note that e_1 is an offending edge for Σ_6 , because Σ_2 does not have $\Sigma_6 \cap \Sigma_1$ in its plaid edge set. The plaid segment in Σ_2 is not in the correct position for Σ_2 to be part of a catch for e_1 , as would happen if e_1 had negative slope. Hence e_1 has positive slope. Note that e_3 also has positive slope, because it rises up to cross $\Sigma_3 \cap \Sigma_2$. So, both e_1 and e_2 have the same slope. (In the reflected case, both would have negative slope.)

There are two kinds of distinguished edges having positive slope, and only one of them has a horizontal projection of length greater than 1. (The same goes in the negative slope case, which arises in the reflected case.) We know that the horizontal projection of e_1 is greater than 1. If the horizontal projection of e_3 is greater than 1, then e_1 and e_3 must be parallel. However, then we contradict Statement 6 of the Grid Geometry Lemma. We have found two parallel distinguished lines which intersect the same vertical edge of a square. In short e_3 has horizontal projection at most 1. Hence the endpoint of e_3 is either in Σ_1 or in Σ_7 .

If the endpoint of e_3 lies in Σ_1 , we are done. So, consider the case when the endpoint of e_3 lies in Σ_7 , as shown in Figure 5.9. In this case, we get the same contradiction as in Case 4.

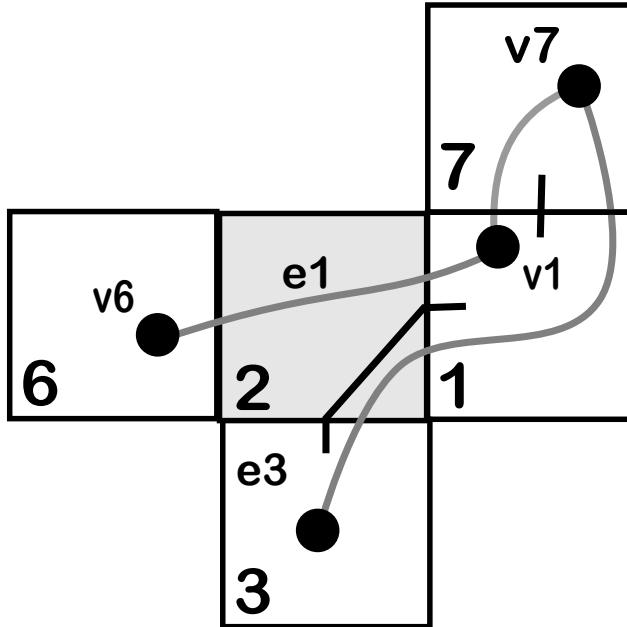


Figure 5.9: Case 5

Case 6: Suppose that $w_1 \in \Sigma_8$ or $w_1 \in \Sigma_9$. Then e_1 has positive slope and horizontal projection at least 1. If e_3 does not cross $\Sigma_2 \cap \Sigma_6$ then we get the same contradiction as in Case 5. So, we can assume that e_3 crosses $\Sigma_2 \cap \Sigma_6$, as shown in Figure 5.10. But then, as Figure 5.10 indicates, e_3 cannot be an offending edge for Σ_6 because the plaid segment in Σ_3 is not in the right position. Hence, $\Sigma_2 \cap \Sigma_6$ is in the edge set for Σ_6 . But this would make the edge set of Σ_2 have 3 members, which is a contradiction.

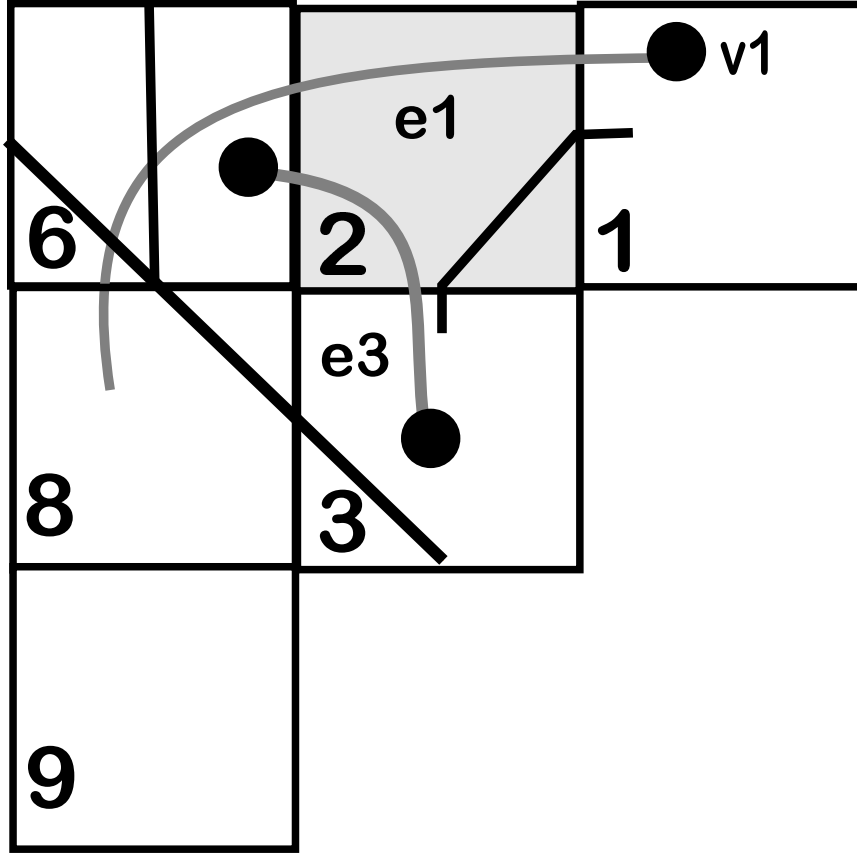


Figure 5.10: Case 6

This completes the analysis of Case C. At this point we have proved the Bound Chain Lemma for all linked chains, except those of length 4.

5.5 Length Four Chains: Case A

Suppose that $\Sigma_1, \Sigma_2, \Sigma_3, \Sigma_4$ is a length 4 linked chain, and all four of these squares are on the same row. The same argument as in Case 3A above shows that there must be some graph edge e_1 , incident to v_1 , which crosses $\Sigma_1 \cap \Sigma_2$. Figure 5.11 shows a tree of possibilities. We will show that, actually, this case cannot occur. Without loss of generality, we will consider the case when e_1 does not end up in a row of squares below our chain. Since e_1 has length less than 2, and e_1 is not an errant edge, e_1 must end either in Σ_5 or Σ_6 .

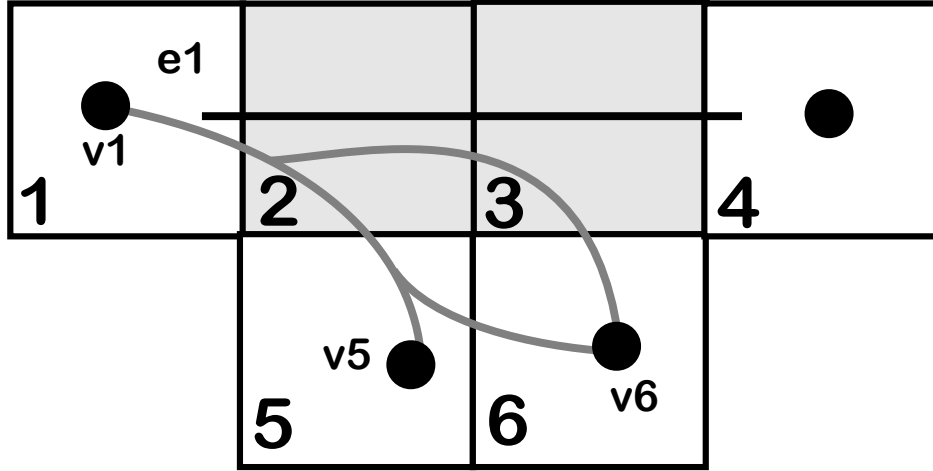


Figure 5.11: Four-in-a-row case

Case 1: Suppose e_1 lands in Σ_5 . Since $\Sigma_2 \cap \Sigma_5$ is an unused edge for Σ_5 and e_1 crosses this edge, e_1 must be an offending edge associated to the left edge of Σ_5 . But then $\Sigma_1, \Sigma_2, \Sigma_5$ are part of the catch for this edge. The plaid segment in Σ_1 is in the wrong position for this.

Case 2: Suppose e_1 lands in Σ_6 and crosses $\Sigma_5 \cap \Sigma_6$. Then e_1 cannot be an offending edge for Σ_6 because the plaid segment in Σ_3 is in the wrong position for it to participate in the required catch. Hence, some other arithmetic graph edge joins v_5 and v_6 . But then two graph edges are incident to v_6 and cross $\Sigma_5 \cap \Sigma_6$. This contradicts Statement 4 of the Pixellation Theorem.

Case 3: Suppose e_1 lands in Σ_6 and crosses $\Sigma_3 \cap \Sigma_6$. The same kind of argument as in Case 1 works here.

5.6 Length Four Chains: Case B

Suppose that $\Sigma_1, \Sigma_2, \Sigma_3, \Sigma_4$ is a length 4 linked chain, and exactly 3 of these squares are on the same row. Without loss of generality, we consider the case shown in Figure 5.12. The same argument as in Case A above shows that there must be some graph edge e_1 , incident to v_1 , which crosses $\Sigma_1 \cap \Sigma_2$.

Since e_1 has length less than 2 and cannot be an errant edge, e_1 must end in one of the squares $\Sigma_4, \Sigma_5, \Sigma_6, \Sigma_7$. Moreover, all these squares are grid full, by Statement 4 of the Grid Geometry Lemma. We want to show that e_1 ends in Σ_4 . There are 4 cases to rule out. All 4 cases are handled by arguments just like those in Cases 4A1 and 4A2 above.

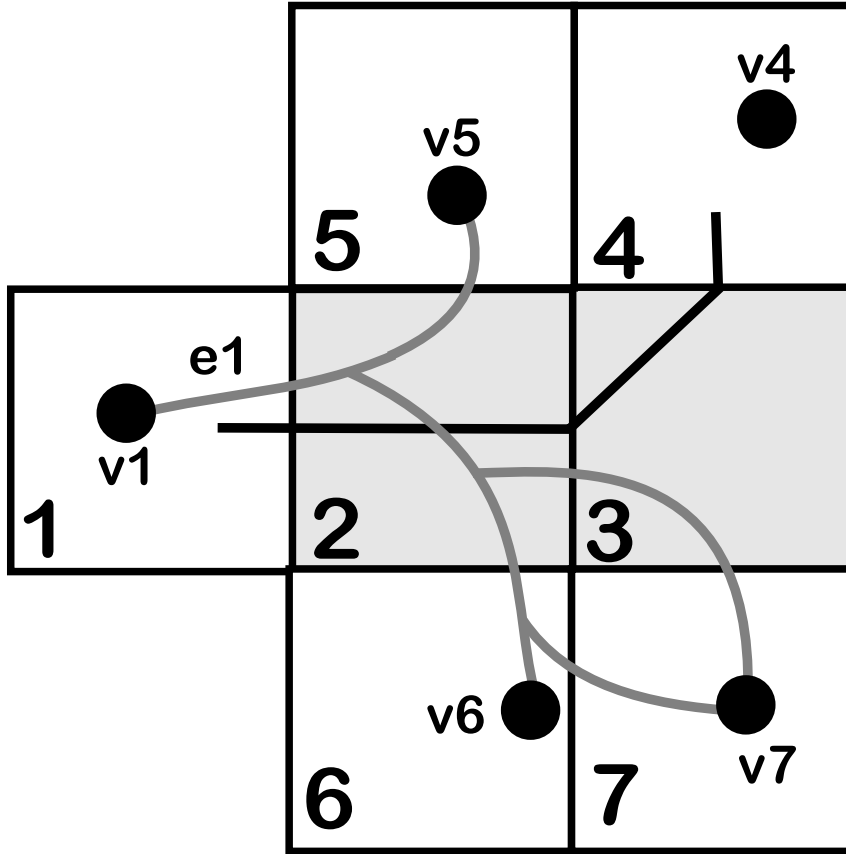


Figure 5.12: Three-in-a-row case.

Remark: We have stopped short of ruling out the existence of chains like this, but we think that they never actually occur.

5.7 Length Four Chains: Case C

Suppose that $\Sigma_1, \Sigma_2, \Sigma_3, \Sigma_4$ is a length 4 linked chain, making a 2×2 block as shown in Figure 5.13.

The same argument as in previous cases shows that there is some graph edge e_1 incident to v_1 which crosses $\Sigma_1 \cap \Sigma_2$. We want to show that e_1 connects v_1 to v_4 . Actually, this situation is impossible, given that we already know that e_1 crosses $\Sigma_1 \cap \Sigma_2$. So, our argument will really show that this kind of linked chain is impossible.

Before we start our analysis, we make special mention of the squares Σ_6 and Σ_9 . We do not know in general whether these squares are grid full or grid empty. However, these squares are irrelevant for all our arguments unless e_1 actually ends in them. In those cases, the relevant square is grid full, by definition. So, in all relevant cases, Σ_6 and Σ_9 are grid full, as drawn.

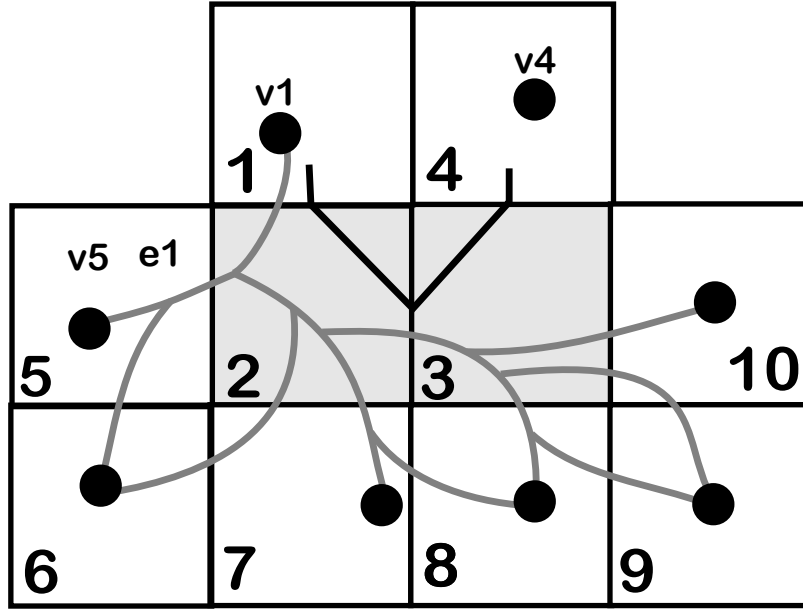


Figure 5.13: Block case

Case 1: Suppose e_1 ends in Σ_5 or Σ_{10} . This is the same as Case 4A1.

Case 2: Suppose e_1 lands in Σ_6 , Σ_8 , or Σ_9 . In all these cases, the argument is the same as in Case 4A2.

Case 3: Suppose that e_1 lands in Σ_7 . Here we redraw the picture to focus more particularly on this case. Since $\Sigma_7 \cap \Sigma_2$ is not in the edge set for Σ_2 , the edge e_1 must be an offending edge in Σ_7 associated to $\Sigma_7 \cap \Sigma_2$.

If e_1 has negative slope, then $\Sigma_2, \Sigma_5, \Sigma_6, \Sigma_7$ form the catch for e_1 . But the catch must be of the first kind, and e_1 must connect v_7 to v_5 . This is a contradiction. If e_1 has positive slope, then a similar argument shows that actually e_1 connects v_7 to v_4 , another contradiction.

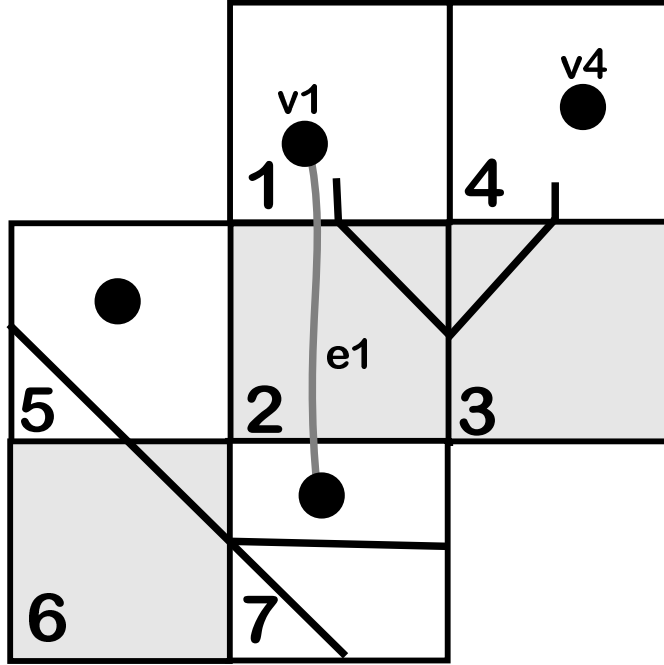


Figure 5.14: Case 3

5.8 Length Four Chains: Case D

There is only one remaining case, and this case actually occurs. Suppose that $\Sigma_1, \Sigma_2, \Sigma_3, \Sigma_4$ is a length 4 linked chain, making a zig-zag pattern as in Figure 5.15 below.

As in Case 3C, it could happen that the edge $\Sigma_1 \cap \Sigma_2$ is an unused side for Σ_1 . In this case, there is an offending edge e associated to $\Sigma_1 \cap \Sigma_2$. The catch for e must be of the second kind because Σ_3 is grid empty. The catch involves $\Sigma_1, \Sigma_2, \Sigma_3, \Sigma_4, \Sigma_{10}$, and by definition e must end in Σ_4 as desired. So, we just have to worry about the case when some graph edge e_1 is incident to v_1 and crosses $\Sigma_1 \cap \Sigma_2$.

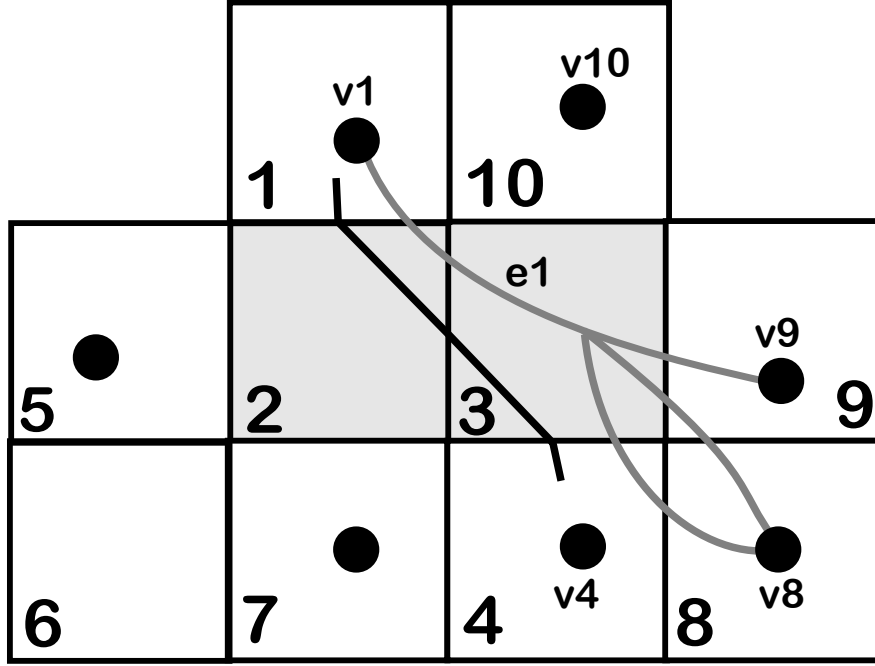


Figure 5.15: zig-zag case

The same reasons as in Case 4C rule out the possibility that e_1 ends in Σ_5 , Σ_6 , or Σ_7 . We just have to rule out e_1 ending in Σ_8 or Σ_9 . The same remarks as in Case 4C apply to the drawing of the square Σ_8 : This square could be either grid full or grid empty, but in the case relative to the argument it is grid full.

Case 1: Suppose e_1 ends in Σ_8 and crosses $\Sigma_4 \cap \Sigma_8$. The argument in Case 4B2 rules this out: Two graph edges would be incident to Σ_8 and would cross $\Sigma_4 \cap \Sigma_8$.

Case 2: Suppose e_1 ends in Σ_8 and crosses $\Sigma_9 \cap \Sigma_8$. If e_1 is not an offending edge for Σ_8 then we get the same contradiction as in Case 1. But if e_1 is an offending edge for Σ_8 then, inspecting the nature of the catches, we see that e_1 must connect v_8 to v_{10} .

Case 3: Suppose e_1 ends in Σ_9 . Looking at the portion of the plaid segment in Σ_3 , we see that $\Sigma_3 \cap \Sigma_9$ is not in the plaid edge set for Σ_9 . Hence e_1 is an offending edge for Σ_9 . The catch for e_1 must be of the first kind, because Σ_{10} is grid full. But then e_1 connects v_9 to v_{10} , a contradiction.

6 The Plaid Master Picture Theorem

6.1 The Spaces

Define

$$\widehat{X} = \mathbf{R}^3 \times [0, 1]. \quad (16)$$

The coordinates on \widehat{X} are given by (x, z, y, P) . We think of

$$P = \frac{2A}{1+A}, \quad A = p/q, \quad (17)$$

but P is allowed to take on any real value in $[0, 1]$. Define the following affine transformations of \widehat{X} .

- $T_X(x, y, z, P) = (x + 2, y + P, z + P, P)$.
- $T_Y(x, y, z, P) = (x, y + 2, z, P)$;
- $T_Z(x, y, z, P) = (x, y, z + 2, P)$;

Define two abelian groups of affine transformations:

$$\widehat{\Lambda}_1 = \langle T_X, T_Y, T_Z \rangle, \quad \widehat{\Lambda}_2 = \langle T_X^2, T_Y, T_Z \rangle. \quad (18)$$

Finally define

$$X_k = \widehat{X} / \Lambda_k, \quad k = 1, 2. \quad (19)$$

The space X_2 is a double cover of X_1 . Both spaces should be considered flat affine manifolds - i.e. manifolds whose overlap functions are restrictions of affine transformations. All the affine transformations in sight preserve the slices $\mathbf{R}^3 \times \{P\}$ and act as translations on these slices. This X_1 and X_2 are fibered by 3-dimensional Euclidean tori.

Remark: The reason why we keep track of two spaces is that a suitable partition of X_1 into polytopes determines the unoriented polygons in the plaid model whereas a suitable partition of X_2 determines the oriented polygons in the plaid model. What we will do is describe a partition of X_2 that is invariant under the action of T_X . To get a partition of X_1 we simply take the quotient and forget some auxiliary information about the labelings. The partition of X_2 has more information but we sometimes consider the picture in X_1 because it makes some formulas simpler and cuts down on the computations.

6.2 The Plaid Master Picture Theorem

Here we will describe the Isomorphism Theorem from [S1]. (Again, I am rechristening this result the Plaid Master Picture Theorem.) The *plaid grid* is defined to be the set G_Π of centered of integer unit squares. When we know that we are taking about the plaid grid, as opposed to the graph grid, we will set $G = G_\Pi$. For each parameter $A \in (0, 1)$, there is a linear map $\Phi_A : G \rightarrow \widehat{X}$, given by

$$\Phi_{A,k}(x, y) = (2Px + 2y, 2Px, 2Px + 2Py, P), \quad P = \frac{2A}{1 + A}. \quad (20)$$

At the same time \widehat{X} has a Λ_1 -invariant tiling by 4 dimensional convex integral polytopes. Modulo the action of Λ_1 there are 26 such polytopes. We list the coordinates of 26 representatives of the orbit equivalence classes below. We call these representatives the *fundamental polytopes*. Their union is a fundamental domain for the action of Λ_1 . By taking the Λ_1 -orbit of the fundamental polytopes, we get a partition of \widehat{X} into infinitely many convex integral polytopes.

The polytopes in the partition have an auxiliary labeling. Either the labeling is by the empty set, or it is by an unordered pair of letters in $\{S, W, N, E\}$. Here is a precise statement of the Plaid Master Picture Theorem.

Theorem 6.1 *For any even rational parameter $A = p/q$ the following is true. At the point $c \in G$ the plaid tile is determined by the labeling of the polytope which contains $\Phi_A(c)$ in its interior.*

In case the labeling is $(0, 0)$ the tile centered at c is the empty tile. Otherwise, the tile is determined by the correspondence above. For instance, if $\Phi_A(c)$ lies in a polytope labeled $\{1, 2\}$, then the tile at c has the connector joining the South edge to the West edge. Implicit in the statement of the theorem is that $\Phi(c)$ does always lie in the interior of one of the Polytopes.

In [S1] we proved an enhancement of Theorem 6.1. The labeling of the polytopes by unordered pairs can be enhanced to a labeling by *ordered pairs* provided that we only require that the labeling has Λ_2 symmetry and moreover that the action of the affine map T_X reverses the ordering of the labels. Thus the union of the 26 polytopes below and their images under T_X , with the labels reversed, gives a fundamental domain for the action of Λ_2 on \widehat{X} . The enhanced version of Theorem 6.1 is as follows:

Theorem 6.2 *For any even rational parameter $A = p/q$ the following is true. At the point $c \in G$ the oriented plaid tile is determined by the enhanced labeling of the polytope which contains $\Phi_A(c)$ in its interior.*

We explain what we mean by way of example. Suppose that $\Phi_A(c)$ lies in a polytope labeled $\{1, 2\}$, then the tile at c has the connector joining the South edge to the West edge and pointing from South to West.

We can think of the classifying map Φ_A as having its range in X_1 . In this case, the tiling of \widehat{X} descends to a tiling of X_1 by 26 convex polytopes, each of which is labeled by an unordered pair of integers, as above. Likewise, we can think of the classifying map Φ_A as having its range in X_2 . In this case, the tiling of \widehat{X} descends to a tiling of X_2 by 56 convex polytopes, each of which is labeled by an ordered pair of integers.

Note that Theorem 6.2 is stronger than Theorem 6.1, but for our proof of the Quasi-Isomorphism Theorem it is useful sometimes to keep Theorem 6.1 in mind. The calculations are simpler. On the other hand, the advantage to working with X_2 is that this space has a natural interpretation as an affine PET. We will explain this interpretation below. Thus, for the Quasi-Isomorphism Theorem, it is best to keep track of both spaces and partitions.

6.3 The Partition

In §6.6 we list the vertices and oriented labels of 10 polytopes. All the polytopes in the partition of \widehat{X} can be obtained from these using the group generated by Λ_1 and the following two additional elements:

- **Negation:** The map $(x, y, z, A) \rightarrow (-x, -y, -z, A)$ preserves the partition and changes the labels as follows: N and S are swapped and E and W are swapped.
- **Flipping:** The map $(x, y, z, A) \rightarrow (x, z, y, A)$ preserves the partition and changes the labels as follows: N and S are swapped, and the order of the label is reversed.

Our listing of polytopes, together with the explicit formulas above, gives a complete account of Theorem 6.1 and Theorem 6.2. However, this description is not very satisfying from a geometric point of view. The partition is actually quite beautiful.

In [S1] we gave a careful geometric description of the partition. Rather than repeat *verbatim* what we said in [S1], here we describe enough of the partition so that the very motivated reader could reconstruct it from scratch. In our computer program, we have an interface which allows the reader to navigate through the partition and instantly see the features we discuss here. We describe the partition of X_1 . The partition of X_2 is obtained using the action of Λ_1 , as described above.

The rectangular solid

$$[-1, 1]^3 \times [0, 1]. \quad (21)$$

serves as a fundamental domain for the action of Λ_1 on \hat{X} . We think of this space as a fiber bundle over the (x, A) plane. The base space B is the rectangle $[-1, 1] \times [0, 1]$. The space B has a partition into 3 triangles, as shown in Figure 6.1.

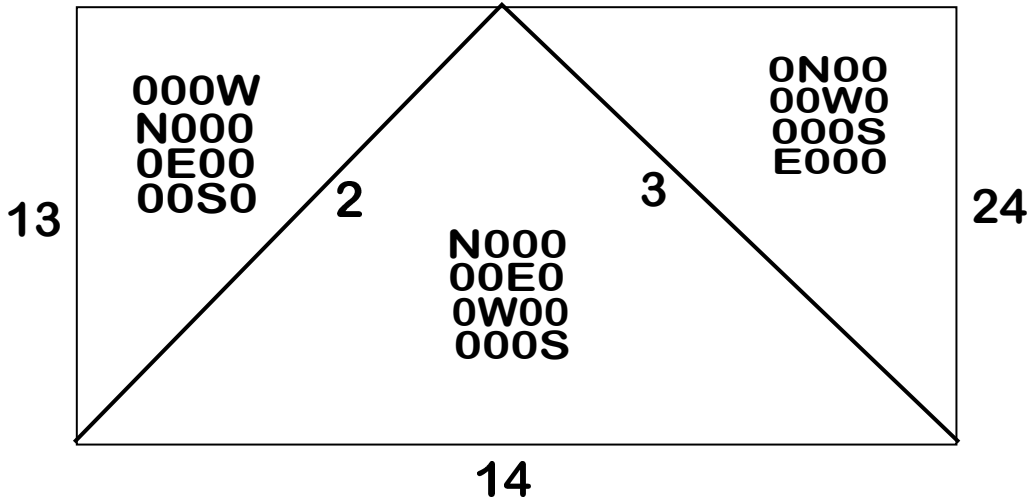


Figure 6.1: The (x, A) base space.

Each triangular region has been assigned a 4×4 matrix which we will explain momentarily. The slices above each open triangle in the partition of B consists of a 4×4 grid of rectangles. For of the rectangles, corresponding to the polytopes labeled by the emptyset are squares. (In Figure 6.2 we replace the emptyset by the symbols $\{S, W, N, E\}$ because this makes the rest of the labeling pattern more clear. The pattern of the squares is indicated by the nonzero entries in the matrices. For instance, the grid shown in Figure 6.2 corresponds to a fiber over the left triangle. We have also indicated the labels in the picture.

WN	WE	WS	W
N	NE	NS	NW
EN	E	ES	EW
SN	SE	S	SW

Figure 6.2: The checkerboard partition

The labels can be derived from the matrices in Figure 6.1. Every non-square rectangle in a column has the same first label and every rectangle in a row has the same second label.

The edge labels in Figure 6.1 encode degenerations in the fibers. Away from the singular edges of the base space, each polytope is a rectangle bundle over an open triangle. As one approaches the edges of the triangles in the base, the partition degenerates in that some of the rectangles shrink to line segments or points. The numbers on the edges in Figure 6.1 indicate which rows and columns degenerate. For instance, as we approach the edge labeled 2, the thickness of second column from the left tends to 0 and at the same time the thickness of the second row from the bottom tends to 0. The whole (unlabeled) picture is symmetric with respect to reflection in the line $y = x$.

From the description of these degenerations and from the fact that we know we are looking at slices of convex integral polytopes, one can actually reconstruct the entire partition from the labelings in Figure 6.1.

6.4 Curve Following Dynamics

Recall that $P = 2A/(1+A)$. Recall also that \mathcal{C} is the set of centers of integer unit squares in the plane. We fix a parameter $A = p/q$ and consider the map $f_A : G \rightarrow G$ that comes from simply following the arrows on the tiles. Given $c_0 \in G$, the new point $C_1 = f_A(c_0)$ is defined to be the center of the tile into which the tile at c_0 points. For instance, the tile centered at c_0 is NE, then $c_1 = c_0 + (1, 0)$. In case the tile centered at c_0 is empty, we have $c_1 = c_0$.

In view of Theorem 6.2 there is a corresponding map $F : \widehat{X} \rightarrow \widehat{X}$ such that

$$F \circ \Phi_A = \Phi_A \circ f_A. \quad (22)$$

Looking at Equation 20 we see that F has the following description.

- F is the identity on tiles labeled by the empty set.
- On all polytopes whose labels end in N , we have

$$F(x, y, z, P) = (x, y, z, P) + (2, 0, 2P, 0).$$

- On all polytopes whose labels end in S , we have

$$F(x, y, z, P) = (x, y, z, P) - (2, 0, 2P, 0).$$

- On all polytopes whose labels end in E , we have

$$F(x, y, z, P) = (x, y, z, P) + (2P, 2P, 2P, 0).$$

- On all polytopes whose labels end in N , we have

$$F(x, y, z, P) = (x, y, z, P) - (2P, 2P, 2P, 0).$$

We can also interpret F as a map $F_2 : X_2 \rightarrow X_2$, because everything in sight is Λ_2 invariant. With this interpretation, (X_2, F_2) is the fibered integral affine PET. What we mean is the 4 dimensional system is piecewise affine, and that the PET preserves the P -slices and acts as an ordinary piecewise translation in each fiber. The 4 dimensional system is integral in the sense that all the polytopes in the partition have integer vertices.

6.5 The Triple Partition

Suppose that \mathcal{P}_1 and \mathcal{P}_2 are two partitions of \widehat{X} into polytopes, say

$$\mathcal{P}_k = \bigcup_i P_{i,k}. \quad (23)$$

We define the *common refinement* to be

$$\mathcal{P}_1 \bowtie \mathcal{P}_2 = \bigcup_{i,j} P_{i,1} \cap P_{j,2}. \quad (24)$$

This is the usual definition. In case the polytopes in the two partitions have rational vertices, the polytopes, in the common refinement will also have rational vertices. This construction may be iterated, so that we can take the n -fold common refinement of n partitions.

Let \mathcal{P}_0 be the partition of \widehat{X} that we have described above. We define

$$\mathcal{P}_k = F^k(\mathcal{P}_0). \quad (25)$$

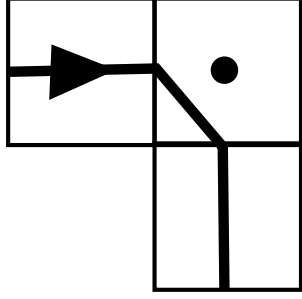
In other words, we take the original partition and apply a power of the PET dynamics. We define the *triple partition* to be the common refinement

$$\mathcal{TP} = \mathcal{P}_{-1} \bowtie \mathcal{P}_0 \bowtie \mathcal{P}_1. \quad (26)$$

We will prove that every vertex of every polytope in \mathcal{TP} has a coordinates which are divisors of 60. That is, if Q is a polytope of \mathcal{TP} , then $60Q$ is an integer polytope.

Each polytope in \mathcal{TP} has a 6 letter label. We simply concatenate the labels for each of the 3 polytopes involved in the intersection, starting with the label for the polytope in \mathcal{P}_{-1} and ending with the label for the polytope in \mathcal{P}_1 . This 6 letter label has the following meaning. We look at the label of the polytope containing $\Phi_A(c)$ and the label determines the shape of the length 3 arc of the oriented plaid component that is centered at c . Figure 6.3 illustrates this principle with two examples. In Figure 6.3 we show the label and the corresponding path. We hope that these examples suffice to convey the general idea.

WEWSNS



EWEEWE

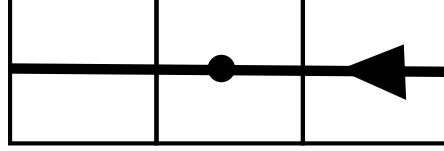


Figure 6.3: The meaning of the 6 letter labels

We define the *reduced triple partition* to be partition

$$\mathcal{RTP} = \mathcal{TP} \bowtie ([-1, 1]^3 \times [0, 1]). \quad (27)$$

Essentially we are taking the pieces of \mathcal{TP} which lie inside our favorite fundamental domain for Λ_1 , but in case any of the pieces slop over the boundary of this fundamental domain, we chop them off. Once again, for every $Q \in \mathcal{RTP}$, the scaled polytope $60Q$ is integral.

We think of the polytopes in \mathcal{RTP} as being labeled by the same 6-letter labels, modulo reversal of the labeling. With this interpretation, we can interpret that map $\Phi_A G \rightarrow \widehat{X}$ as a classifying map for unoriented arcs of the plaid model having combinatorial length 3. We just use the action of Λ_1 to move $\Phi_A(c)$ into \mathcal{RTP} and then we read off the label.

There is one minor issue that we need to address. It follows from Theorem 6.2 that $\Phi_A(c)$ always lies in the interior of a polytope of \mathcal{TP} , but it might happen that there are several images of $\Phi_A(c)$ on the boundary of the fundamental domain. This is the usual problem with fundamental domains. However, in this situation, all the images will lie in polytopes having the same labels. So, even when there is some ambiguity in interpreting Φ_A as a map from G into \mathcal{RTP} , the ambiguity is harmless.

Even though it is somewhat less natural than \mathcal{TP} , we will use \mathcal{RTP} for the proof of the Quasi-Isomorphism. The formula for the projective intertwiner discussed in the introduction is simpler when we restrict our attention to X_1 . The projective intertwiner is the most important ingredient in the proof, and so we wanted to make it as nice as possible.

6.6 The Fundamental Polytopes

Here is the list of the 10 labeled polytopes. The label X denotes that the label is the empty set. Also, the last polytope listed has 12 vertices, and the listing is spread over 2 lines.

$$\begin{array}{cccccc}
 \begin{bmatrix} -1 \\ -1 \\ -1 \\ 0 \end{bmatrix} & \begin{bmatrix} -1 \\ +1 \\ -1 \\ 0 \end{bmatrix} & \begin{bmatrix} +1 \\ +1 \\ -1 \\ 0 \end{bmatrix} & \begin{bmatrix} +1 \\ +1 \\ +1 \\ 0 \end{bmatrix} & \begin{bmatrix} 0 \\ 0 \\ 0 \\ +1 \end{bmatrix} & (W, E) \\
 \\
 \begin{bmatrix} +1 \\ +1 \\ -1 \\ 0 \end{bmatrix} & \begin{bmatrix} +1 \\ +1 \\ 0 \\ +1 \end{bmatrix} & \begin{bmatrix} +1 \\ +1 \\ -1 \\ +1 \end{bmatrix} & \begin{bmatrix} 0 \\ +1 \\ -1 \\ +1 \end{bmatrix} & \begin{bmatrix} 0 \\ 0 \\ -1 \\ +1 \end{bmatrix} & (E, S) \\
 \\
 \begin{bmatrix} +1 \\ -1 \\ -1 \\ 0 \end{bmatrix} & \begin{bmatrix} +1 \\ 0 \\ 0 \\ +1 \end{bmatrix} & \begin{bmatrix} +1 \\ 0 \\ -1 \\ +1 \end{bmatrix} & \begin{bmatrix} 0 \\ 0 \\ -1 \\ +1 \end{bmatrix} & \begin{bmatrix} 0 \\ -1 \\ -1 \\ +1 \end{bmatrix} & (E, N) \\
 \\
 \begin{bmatrix} -1 \\ +1 \\ -1 \\ 0 \end{bmatrix} & \begin{bmatrix} +1 \\ +1 \\ -1 \\ 0 \end{bmatrix} & \begin{bmatrix} +1 \\ +1 \\ +1 \\ 0 \end{bmatrix} & \begin{bmatrix} 0 \\ 0 \\ 0 \\ +1 \end{bmatrix} & \begin{bmatrix} 0 \\ +1 \\ 0 \\ +1 \end{bmatrix} & \begin{bmatrix} +1 \\ +1 \\ 0 \\ +1 \end{bmatrix} & \begin{bmatrix} +1 \\ +1 \\ +1 \\ +1 \end{bmatrix} & (W, S) \\
 \\
 \begin{bmatrix} -1 \\ -1 \\ -1 \\ 0 \end{bmatrix} & \begin{bmatrix} +1 \\ -1 \\ -1 \\ 0 \end{bmatrix} & \begin{bmatrix} +1 \\ +1 \\ -1 \\ 0 \end{bmatrix} & \begin{bmatrix} 0 \\ 0 \\ -1 \\ +1 \end{bmatrix} & \begin{bmatrix} 0 \\ 0 \\ 0 \\ +1 \end{bmatrix} & \begin{bmatrix} +1 \\ 0 \\ 0 \\ +1 \end{bmatrix} & \begin{bmatrix} +1 \\ +1 \\ 0 \\ +1 \end{bmatrix} & (S, W) \\
 \\
 \begin{bmatrix} -1 \\ +1 \\ +1 \\ 0 \end{bmatrix} & \begin{bmatrix} -1 \\ 0 \\ 0 \\ +1 \end{bmatrix} & \begin{bmatrix} -1 \\ 0 \\ +1 \\ +1 \end{bmatrix} & \begin{bmatrix} -1 \\ +1 \\ 0 \\ +1 \end{bmatrix} & \begin{bmatrix} -1 \\ +1 \\ +1 \\ +1 \end{bmatrix} & \begin{bmatrix} 0 \\ +1 \\ +1 \\ +1 \end{bmatrix} & \begin{bmatrix} -2 \\ 0 \\ 0 \\ +1 \end{bmatrix} & X
 \end{array}$$

$$\begin{array}{cccccccc}
\begin{bmatrix} -1 \\ -1 \\ -1 \\ 0 \end{bmatrix} & \begin{bmatrix} +1 \\ -1 \\ -1 \\ 0 \end{bmatrix} & \begin{bmatrix} -1 \\ -1 \\ -1 \\ +1 \end{bmatrix} & \begin{bmatrix} 0 \\ 0 \\ 0 \\ +1 \end{bmatrix} & \begin{bmatrix} 0 \\ 0 \\ -1 \\ +1 \end{bmatrix} & \begin{bmatrix} 0 \\ -1 \\ 0 \\ +1 \end{bmatrix} & \begin{bmatrix} 0 \\ -1 \\ -1 \\ +1 \end{bmatrix} & \begin{bmatrix} +1 \\ 0 \\ 0 \\ +1 \end{bmatrix} & (S, N) \\
\begin{bmatrix} +1 \\ +1 \\ -1 \\ 0 \end{bmatrix} & \begin{bmatrix} +1 \\ -1 \\ -1 \\ 0 \end{bmatrix} & \begin{bmatrix} +1 \\ +1 \\ 0 \\ +1 \end{bmatrix} & \begin{bmatrix} +1 \\ 0 \\ 0 \\ +1 \end{bmatrix} & \begin{bmatrix} +1 \\ +1 \\ -1 \\ +1 \end{bmatrix} & \begin{bmatrix} +1 \\ 0 \\ -1 \\ +1 \end{bmatrix} & \begin{bmatrix} 0 \\ 0 \\ -1 \\ +1 \end{bmatrix} & \begin{bmatrix} 2 \\ +1 \\ 0 \\ +1 \end{bmatrix} & (E, W) \\
\begin{bmatrix} -1 \\ -1 \\ +1 \\ 0 \end{bmatrix} & \begin{bmatrix} -1 \\ -1 \\ 0 \\ +1 \end{bmatrix} & \begin{bmatrix} 0 \\ -1 \\ 0 \\ +1 \end{bmatrix} & \begin{bmatrix} 0 \\ 0 \\ 0 \\ +1 \end{bmatrix} & \begin{bmatrix} 0 \\ -1 \\ +1 \\ +1 \end{bmatrix} & \begin{bmatrix} 0 \\ 0 \\ +1 \\ +1 \end{bmatrix} & \begin{bmatrix} +1 \\ 0 \\ +1 \\ +1 \end{bmatrix} & \begin{bmatrix} +1 \\ -1 \\ +1 \\ 0 \end{bmatrix} & X \\
\begin{bmatrix} -1 \\ -1 \\ -1 \\ 0 \end{bmatrix} & \begin{bmatrix} -1 \\ +1 \\ +1 \\ 0 \end{bmatrix} & \begin{bmatrix} -1 \\ -1 \\ +1 \\ 0 \end{bmatrix} & \begin{bmatrix} -1 \\ +1 \\ -1 \\ 0 \end{bmatrix} & \begin{bmatrix} +1 \\ +1 \\ +1 \\ 0 \end{bmatrix} & \begin{bmatrix} -1 \\ -1 \\ -1 \\ +1 \end{bmatrix} & & & \\
\begin{bmatrix} -1 \\ 0 \\ -1 \\ +1 \end{bmatrix} & \begin{bmatrix} -1 \\ -1 \\ 0 \\ +1 \end{bmatrix} & \begin{bmatrix} -1 \\ 0 \\ 0 \\ +1 \end{bmatrix} & \begin{bmatrix} 0 \\ 0 \\ 0 \\ +1 \end{bmatrix} & \begin{bmatrix} -3 \\ -1 \\ -1 \\ 0 \end{bmatrix} & \begin{bmatrix} -2 \\ -1 \\ -1 \\ +1 \end{bmatrix} & & & X
\end{array}$$

7 The Graph Master Picture Theorem

7.1 Heuristic Discussion

The Master Picture Theorem from [S0] says that the arithmetic graph has a classifying map and space much like the plaid model does. Following this section, we will give an account of the Master Picture Theorem. Here, with a view towards making this paper more self-contained, I'd like to give some idea why the Master Picture Theorem is true.

Let $K = K_A$ be the kite (implicitly) involved in the Quasi-Isomorphism Theorem. Given an edge e of K , we form a strip Σ_e as follows: One boundary line of Σ_e is L_e , the line containing e . The other boundary line L'_e is parallel to L_e and such that the point of P farthest from L_e lies halfway between L_e and L'_e . These 4 strips $\Sigma_1, \dots, \Sigma_4$ are ordered cyclically, according to their slopes. Figure 7.1 shows the picture. The big disk in the middle covers up the mess in the middle of the picture.

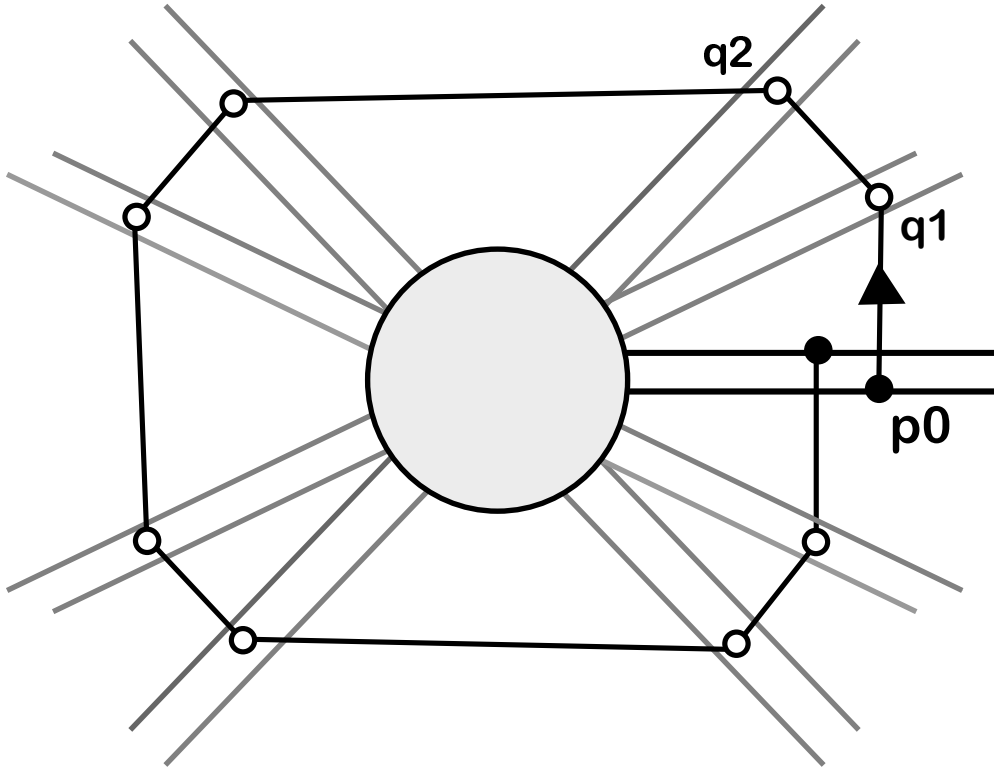


Figure 7.1: The strips defined by the kite

Let ψ denote the second iterate of the outer billiards map. Let Ξ denote the distinguished pair of rays involved in the construction of the arithmetic graph. Let $\Psi : \Xi \rightarrow \Xi$ denote the first return of ψ to Ξ . A general feature of ψ is the orbit $p_0, \psi(p_0), \psi^2(p_0), \dots$ moves along a straight line, in evenly spaced points, until it lands in one of the strips. We call the points where the orbit lands in the strips the *turning points*. It seems plausible (and in fact is true) that the way the orbit returns to Ξ is determined by the relative positions of the turning points inside the strips – i.e., how they sit with respect to the boundaries of the strips.

To formalize this idea, we define a map

$$\Phi' : \Xi \rightarrow [0, 1]^8,$$

as follows. Starting with the point p_0 , we let q_1, \dots, q_8 denote the successive points where the ψ -orbit of p_0 intersects a strip. We let $t_k \in [0, 1]$ the position of q_k in the strip relative to the boundary components. Thus, $t_k \approx 0$ if q_k lies near one boundary component of the strip, $t_k \approx 1$ if q_k lies near the other boundary component, and $t_k \approx 1/2$ if q_k lies near the midline of the strip. The map is then

$$\Phi'(p_0) = (t_1, \dots, t_8).$$

Thanks to some relations between the slopes of the strips, the image $\Phi'(\Xi)$ is contained in a 3-dimensional slice of $[0, 1]^8$. The image $\Phi'(p_0)$ classifies the *first return vector* $\Psi(p_0) - p_0$ in the following sense. There is a partition of the 3 dimensional slice into polyhedra such that p_0 and p'_0 have the same first return vector provided that $\Phi'(p_0)$ and $\Phi'(p'_0)$ lie in the same polyhedron.

In [S0] we make this construction carefully, then introduce a suitable affine change coordinates, and then finally interpret the result directly in terms of the arithmetic graph. (The arithmetic graph encodes the first return vectors.) When all this is done, we get the Master Picture Theorem.

It is worth pointing out that the existence of this compactification works in much more generality. In my paper [S3], I give a similar result for any convex polygon with no parallel sides. Rather than consider the return map to some distinguished pair of rays – a construction which doesn't even make sense in general – I consider a return map to one of the strips. This first return map has a compactification whose dimension is comparable to the number of sides of the polygon. One could probably deduce the Master Picture Theorem from the general compactification theorem in [S3], but I haven't tried.

7.2 The Master Picture Theorem

We will give a simplified presentation of what is contained in [S0, §6], because some of the fine points there are irrelevant to us. Also, in order to line up the picture better with the plaid model, we switch the x and z coordinates.

We fix $A = p/q$ as above. As in the case of the plaid PET, we work in the space $\widehat{X} = \mathbf{R}^3 \times [0, 1]$. This time, we use the coordinates (x, y, z, A) on \widehat{X} .

Let Λ denote the abelian group of generated by the following affine transformations.

- $T_X(x, y, z, A) = (x + 1, y - 1, z - 1, A)$.
- $T_Y(x, y, z, A) = (x, y + 1 + A, z + 1 - A, A)$.
- $T_Z(x, y, z, A) = (x, y, z + 1 + A, A)$.

For each parameter A , the rectangular solid

$$R_A = [0, 1] \times [0, 1 + A] \times [0, 1 + A] \times \{A\} \quad (28)$$

serves as a fundamental domain for the action of Λ on $\mathbf{R}^3 \times \{A\}$. The quotient is some flat 3-torus which depends on A . The union

$$R = \bigcup_{A \in [0, 1]} R_A, \quad (29)$$

is a convex integer polytope.

We introduce a map $\Phi'_A : \mathbf{Z}^2 \rightarrow \widehat{X}$, as follows.

$$\phi_A(m, n) = (t, t, t, A), \quad t = Am + n + \frac{1}{2q}. \quad (30)$$

There are two Λ -invariant partitions of \widehat{X} into convex integral polytopes. Each polytope in each partition is labeled by a pair of integers $(i, j) \in \{-1, 0, 1\}$. The labeling has the property that the local structure of the arithmetic graph at the point $c \in \mathbf{Z}^2$ is determined by the labels of the polytopes in each partition which contain the image $\Phi'(c)$. Implicit in this statement is the fact that $\Phi'(c)$ lies in the interior of a polytope in each partition.

Here is what we mean more precisely. Suppose that $\Phi'(c)$ lies in a polytope in the first partition with label (i_1, j_1) and a polytope in the second partition with labels (i_2, j_2) . Then the arithmetic graph has the edge connecting c to $c + (1_1, j_1)$ and the edge connecting c to $c + (i_2, j_2)$. We have $(i_1, j_1) = (0, 0)$ if and only if $(i_2, j_2) = (0, 0)$. In this case, c is an isolated point in the graph.

For each partition, a certain union of 14 polytopes forms a fundamental domain for the action of Λ . In both cases, the fundamental domain is an integral translate of the polytope R from Equation 29. The polytopes in the two partitions are related as follows. Define

$$I(x, y, z, A) = (1, A, 2 + A, A) - (x, y, z, 0). \quad (31)$$

Then

- $Q_j = I(P_j)$ for all $j = 1, \dots, 14$.
- The label of Q_j is the negative of the label of P_j .

The map I is an involution, so we have $I(Q_j) = P_j$ as well.

We call these two partitions the $(+)$ graph partition and the $(-)$ graph partition. We denote these partitions by \mathcal{G}_+ and \mathcal{G}_- . The *double partition* is $\mathcal{G}_+ \bowtie \mathcal{G}_-$, the common refinement of the two partitions. Each polytope Z in the double partition is labeled by a quadruple (i_+, j_+, i_-, j_-) , where (i_\pm, j_\pm) is the label of the polytope in \mathcal{P}_\pm containing Z . The polytope of the double partition which contains $\Phi'_A(c)$ determines the two unoriented edges of the arithmetic graph incident to c . The polytopes in the double partition have rational coordinates. We did not work out the double partition explicitly, because we don't need to know it explicitly.

In [S0, §6] we give a detailed geometric description of (translates of) the partitions \mathcal{G}_+ and \mathcal{G}_- . The geometric description is more intricate than what we did for the plaid PET. We will not repeat the description here. The reader can get a very clear picture of the partitions using our computer program.

In §7.5 we list the 14 fundamental polytopes of \mathcal{G}_+ , together with their labels. This listing combines with the information above to give a complete account of the statement of the Master Picture Theorem. My computer program allows the user to navigate through both partitions. Using the program, one can get a good visual sense of the partitions.

7.3 Pulling Back the Maps

Let T be the canonical affine transformation from §3. This map is given in Equation 11 and the inverse map is given in Equation 11. We can interpret the Master Picture Theorem as a statement about the structure of the affine image $T(\Gamma)$, where Γ is the arithmetic graph as defined in previous chapters. After this section, we will save words by using the term *arithmetic graph* to denote $T(\Gamma)$ rather than Γ . The vertices of $T(\Gamma)$ are contained in the graph grid $T(\mathbb{Z}^2)$.

To convert the Master Picture Theorem into a statement about the desired affine image, we simply pull back the classifying map. We define

$$\Phi = \Phi' \circ T^{-1}. \quad (32)$$

The domain for Φ is the graph grid G . A calculation shows that

$$\Phi(x, y) = (x, x, x, A). \quad (33)$$

This nice equation suggests that there is something canonical about the affine map that appears in the Quasi-Isomorphism Theorem.

7.4 Further Discussion

There are three small differences between our presentation of the Master Picture Theorem here and the one given in [S0]. For the reader who is interested in comparing what we say here to what we say in [S0], we discuss those differences.

First, here we have one classifying map and two partitions, whereas in [S0] we have two classifying maps, differing from each other by translations, and two slightly different partitions. The two partitions in [S0] are translates of the ones here respectively by the vectors $(0, 1, 0, 0)$ and $(-1, 0, 0, 0)$. When these changes are made, the involution I simply becomes reflection in the midpoint of the fundamental domain R , and the union of the 14 fundamental polytopes, in either partition, is precisely R . In short, the partitions in [S0] are obtained from the ones here by translating so that everything lies in R . This picture is geometrically more appealing, but it serves our purposes here to have one map rather than two.

Second, even after we take into account the translations we just discussed, the map we have here is not quite the same as the map in [S0]. Were we

to strictly translate the map from [S0] the small term $1/2q$ in Equation 30 would be replaced by an infinitesimally small positive number $\iota = 0_+$. (If you like, you can interpret 0_+ as an infinitesimally small positive number in a nonstandard field containing \mathbf{R} .) Put another way, we set $\iota = 0$, and then in those rare cases when $p = \Phi'_A(m, n)$ lies in the boundary of one of the polytopes, we select the polytope which contains $p + (\epsilon, \epsilon, \epsilon, 0)$ for all sufficiently small ϵ . In fact, any choice of ι in $(0, 1/q)$ would give exactly the same result. Setting $\iota = 0$ and then stipulating the rules for handling boundary cases seemed at the time to simplify the picture. In hindsight, the choice $\iota = 1/2q$, as we make here, is more canonical. Also, it is better suited to our present purposes. See Equation 33 in the next chapter.

Third, as we mentioned above, we have switched the first and third coordinates. Thus, the vertex (x, y, z, A) of a polytope here corresponds to the vertex (z, y, x, A) in [S0]. Again, this change makes the Master Picture Theorem line up more gracefully with the Isomorphism Theorem for the plaid model. This switch also effects the definition of the lattice Λ .

There is one more point we'd like to discuss. Since the arithmetic graph comes from following the dynamics of the first return map, it is possible to orient the paths in the arithmetic graph. It is also possible to determine when the first partition determines the edge pointing to c or the edge pointing away to c . This fine point is not needed for the proof of the Quasi-Isomorphism Theorem, but it would be needed if we wanted to have a well-defined affine PET associated to the arithmetic graph, as we constructed for the plaid model.

Here is the recipe for determining the orientations from the classifying map. We introduce the integer function

$$\rho_A(m, n) = \text{floor}(s), \quad s = (1 + A)m + \frac{1}{2q}. \quad (34)$$

Then \mathcal{G}_+ determines the outward pointing edge at (m, n) if and only if $\rho_A(m, n)$ is even. This result is implicit in the development given in [S0].

7.5 The Fundamental Polytopes

Here are the 14 fundamental polytopes for the $(+)$ partition. Note that the listing for the last one is spread over two lines.

$$\begin{bmatrix} 0 \\ -1 \\ 0 \\ 0 \end{bmatrix} \begin{bmatrix} 0 \\ 0 \\ 0 \\ +1 \end{bmatrix} \begin{bmatrix} 0 \\ -1 \\ +1 \\ +1 \end{bmatrix} \begin{bmatrix} 0 \\ 0 \\ +1 \\ +1 \end{bmatrix} \begin{bmatrix} +1 \\ 0 \\ +1 \\ +1 \end{bmatrix} (0, +1)$$

$$\begin{bmatrix} 0 \\ -1 \\ 0 \\ +1 \end{bmatrix} \begin{bmatrix} +1 \\ -1 \\ 0 \\ 0 \end{bmatrix} \begin{bmatrix} +1 \\ -1 \\ 0 \\ +1 \end{bmatrix} \begin{bmatrix} +1 \\ 0 \\ 0 \\ +1 \end{bmatrix} \begin{bmatrix} +1 \\ -1 \\ +1 \\ +1 \end{bmatrix} (0, +1)$$

$$\begin{bmatrix} 0 \\ 0 \\ +1 \\ 0 \end{bmatrix} \begin{bmatrix} 0 \\ +1 \\ +1 \\ +1 \end{bmatrix} \begin{bmatrix} 0 \\ 0 \\ 2 \\ +1 \end{bmatrix} \begin{bmatrix} 0 \\ +1 \\ 2 \\ +1 \end{bmatrix} \begin{bmatrix} +1 \\ +1 \\ 2 \\ +1 \end{bmatrix} (-1, 0)$$

$$\begin{bmatrix} 0 \\ 0 \\ 0 \\ 0 \end{bmatrix} \begin{bmatrix} 0 \\ 0 \\ +1 \\ +1 \end{bmatrix} \begin{bmatrix} +1 \\ 0 \\ +1 \\ +1 \end{bmatrix} \begin{bmatrix} +1 \\ +1 \\ +1 \\ +1 \end{bmatrix} \begin{bmatrix} +1 \\ 0 \\ 2 \\ +1 \end{bmatrix} (-1, 0)$$

$$\begin{bmatrix} 0 \\ -1 \\ +1 \\ +1 \end{bmatrix} \begin{bmatrix} +1 \\ -1 \\ +1 \\ 0 \end{bmatrix} \begin{bmatrix} +1 \\ -1 \\ +1 \\ +1 \end{bmatrix} \begin{bmatrix} +1 \\ 0 \\ +1 \\ +1 \end{bmatrix} \begin{bmatrix} +1 \\ -1 \\ 2 \\ +1 \end{bmatrix} (+1, 0)$$

$$\begin{bmatrix} 0 \\ 0 \\ 0 \\ 0 \end{bmatrix} \begin{bmatrix} +1 \\ 0 \\ 0 \\ 0 \end{bmatrix} \begin{bmatrix} +1 \\ 0 \\ +1 \\ 0 \end{bmatrix} \begin{bmatrix} +1 \\ 0 \\ +1 \\ +1 \end{bmatrix} \begin{bmatrix} +1 \\ +1 \\ +1 \\ +1 \end{bmatrix} \begin{bmatrix} +1 \\ 0 \\ 2 \\ +1 \end{bmatrix} (-1, -1)$$

$$\begin{bmatrix} 0 \\ -1 \\ 0 \\ 0 \end{bmatrix} \begin{bmatrix} 0 \\ 0 \\ 0 \\ 0 \end{bmatrix} \begin{bmatrix} +1 \\ 0 \\ 0 \\ 0 \end{bmatrix} \begin{bmatrix} +1 \\ +1 \\ 0 \\ +1 \end{bmatrix} \begin{bmatrix} +1 \\ 0 \\ +1 \\ +1 \end{bmatrix} \begin{bmatrix} +1 \\ +1 \\ +1 \\ +1 \end{bmatrix} (-1, 0)$$

$$\begin{bmatrix} 0 \\ -1 \\ +1 \\ 0 \end{bmatrix} \begin{bmatrix} 0 \\ 0 \\ +1 \\ 0 \end{bmatrix} \begin{bmatrix} 0 \\ 0 \\ +1 \\ +1 \end{bmatrix} \begin{bmatrix} +1 \\ 0 \\ +1 \\ 0 \end{bmatrix} \begin{bmatrix} 0 \\ -1 \\ 2 \\ +1 \end{bmatrix} \begin{bmatrix} 0 \\ 0 \\ 2 \\ +1 \end{bmatrix} \begin{bmatrix} +1 \\ 0 \\ 2 \\ +1 \end{bmatrix} (+1, 0)$$

8 The Graph Reconstruction Formula

The purpose of this chapter is to present a formula which we call the *Reconstruction formula*, which relates the geometry of the graph grid to the graph PET classifying map. Combining this formula with the Master Picture Theorem, we will prove Statement 1 of the Pixellation Theorem.

8.1 Main Result

Recall that $\widehat{X} = \mathbf{R}^3 \times [0, 1]$. For each parameter A , the affine group acting on \widehat{X} in connection with the graph PET acts as an abelian group of translations. Precisely, this group is $\Lambda(\mathbf{Z}^3)$, where

$$\Lambda = \begin{bmatrix} 1 & 0 & 0 \\ -1 & 1+A & 0 \\ -1 & 1-A & 1+A \end{bmatrix} \mathbf{Z}^3 \quad (35)$$

Given a point $\xi \in G$, let $[\xi] \in \mathbf{R}^2/\mathbf{Z}^2$ denote the equivalence class of ξ . We now explain how we can use the map Φ to determine $[\xi]$.

We introduce linear maps $\Theta_1, \Theta_2 : \mathbf{R}^3 \rightarrow \mathbf{R}$:

$$\Theta_1(x, y, z) = x, \quad \Theta_2(x, y, z) = \frac{y - Ax}{1 + A}. \quad (36)$$

Checking on the obvious basis for Λ , we see that $\Theta_j(\Lambda) \subset \mathbf{Z}$. Therefore Θ_1 and Θ_2 both give well defined maps from \mathbf{R}^3/Λ , the domain for the graph compactification at A , to the torus \mathbf{R}/\mathbf{Z} . Hence, we have a locally affine map

$$\Theta : \mathbf{R}^3/\Lambda \rightarrow \mathbf{R}^2/\mathbf{Z}^2, \quad L = [(\Theta_1, \Theta_2)]. \quad (37)$$

The goal of this section is to establish the following result.

Lemma 8.1 (Reconstruction)

$$[\xi] = \Theta \circ \Phi(\xi). \quad (38)$$

We call this equation the Reconstruction Formula. Equation 38 allows us to get control over how the arithmetic graph sits with respect to \mathbf{Z}^2 . We've already proven that no point of G lies on the boundary of an integer unit square. So, we can interpret both sides of Equation 38 as referring to points in the open integer unit square $(0, 1)^2$. We fix a parameter A throughout the proof.

Lemma 8.2 *Equation 38 holds at $\xi = T(0, 0)$.*

Proof: A direct calculation shows that

$$[\xi] = \left(\frac{1}{2q}, \frac{q-p}{2q(q+p)} \right).$$

Next, we compute

$$\Phi(\xi) = \left(\frac{1}{2q}, \frac{1}{2q}, \frac{1}{2q}, A \right).$$

A direct calculation then shows that

$$\Theta_2(\Phi(\xi)) = \frac{(p/q)(1/2q) - (1/2q)}{1 + (p/q)} = \frac{q-p}{2q(q+p)}.$$

Hence, the two sides of the equation agree. ♠

Lemma 8.3 *If Equation 38 holds at ξ , it also holds at $\xi \pm dT(0, 1)$.*

Proof: We do the (+) case. The (−) case has the same proof. Let $\xi' = \xi + dT(0, 1) = \xi + (1, -P)$. Here $P = 2A/(1 + A)$. We compute

$$\Theta \circ \Phi(\xi') - \Theta \circ \Psi(\xi) = \Theta(1, 1, 1) = \left(1, \frac{1-A}{1+A} \right) = (1, -P + 1).$$

The last expression is congruent to $\zeta' - \zeta = (1, -P) \bmod \mathbf{Z}^2$. ♠

Lemma 8.4 *If Equation 38 holds at ξ , it also holds at $\xi \pm dT(1, 1)$.*

Proof: We do the (+) case. The (−) case has the same proof. We have $dT(1, 1) = (1 + A, 1 + A)$. Using the same notation as in the previous argument, we have

$$\Theta \circ \Phi(\xi') - \Theta \circ \Psi(\xi) = \Theta(1 + A, 1 + A, 1 + A) = (1 + A, 1 - A) = \zeta' - \zeta.$$

This completes the proof ♠

These three lemmas together show that Equation 38 holds on all of $dT(\mathbf{Z}^2)$, as desired.

8.2 Eliminating Most Double Crossings

In this section we eliminate most of the double crossings mentioned in §4.3. This section does not use either the Reconstruction Formula or the Master Picture Theorem.

Let T be the canonical affine transform. See §3.3. Recall that a *distinguished edge* is an edge having vertices $v_1, v_2 \in T(\mathbf{Z})$ such that $v_1 - v_2 = T(\zeta)$, where ζ is one of the 8 shortest nonzero vectors in \mathbf{Z}^2 . We say that the edge belongs to the family $\mathcal{F}(i, j)$ is $\zeta = \pm(i, j)$.

A *double crossing* is a configuration of the kind shown in Figure 4.4 or in Figure 8.1 below. The configuration consists of two adjacent unit integer squares Σ_1 and Σ_2 , graph grid points $v_1 \in \Sigma_1$ and $v_2 \in \Sigma_2$, and disjoint distinguished edges e_1 and e_2 incident to v_1 and v_2 respectively which both cross $\Sigma_1 \cap \Sigma_2$.

Lemma 8.5 *A bad configuration must have the following structure.*

- $\Sigma_1 \cap \Sigma_2$ is horizontal.
- The edge connecting v_1 to v_2 belongs $\mathcal{F}(1, 0)$.
- At least one of the two edges e_1 or e_2 belongs to $\mathcal{F}(-1, 1)$.

Proof: Let $f = v_2 - v_1$. By Statement 5 of the Grid Geometry Lemma, f must be a distinguished edge.

We define S_1 to be the set of 8 distinguished edges incident to v_1 . We think of these edges as vectors pointing out of v_1 . This set has a natural cyclic order on it. Likewise we define S_2 .

Let $\Sigma_{12} = \Sigma_1 \cap \Sigma_2$. The edges of S_1 which intersect Σ_{12} closest to $f \cap \Sigma_{12}$ are obtained by turning f one click in S_1 , either clockwise or counterclockwise. Likewise, the edges of S_2 which intersect Σ_{12} closest to $f \cap \Sigma_{12}$ are obtained by turning $(-f)$ one click in S_2 , counter clockwise or counterclockwise. The two turnings must be in the same direction, because otherwise the resulting edges would intersect.

So, the shortest possible distance between the two intersection points occurs when e_1 and e_2 are parallel. Statement 6 of the Grid Geometry Lemma now says that Σ_{12} is horizontal and the parallel lines are of type $(-1, 1)$. Looking at the proof of Statement 6 of the Grid Geometry Theorem given in §3.4, we see that this forced $f \in \mathcal{F}(1, 0)$. ♠

8.3 Eliminating the last Double Crossing

Now we will use the Reconstruction Formula and the Master Picture Theorem to rule out the last kind of double crossing. This proves Statement 1 of the Pixellation Lemma. We will suppose that the arithmetic graph has a double crossing for some parameter A and derive a contradiction. The reader is warned in advance that our proof, at the end, is just a computer assisted calculation.

We will consider the case when the edge e_1 shown on the left side of Figure 8.1 is in the family $\mathcal{F}(-1, 1)$. The other case, when $e_2 \in \mathcal{F}(-1, 1)$, has a similar proof. Indeed, the second case follows from the first case and from the rotational symmetry of the arithmetic graph.

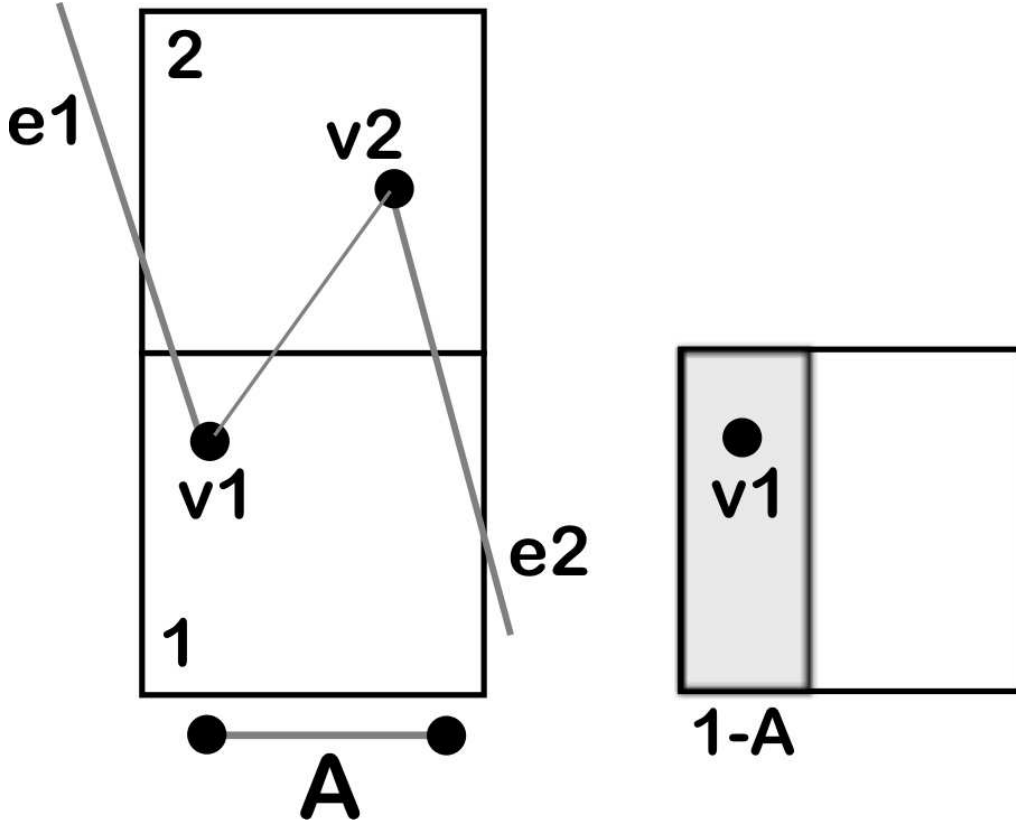


Figure 8.1: A double crossing.

Let G denote the graph grid and let $\Phi : G \rightarrow \hat{X}$ be the graph classifying map.

Lemma 8.6 $\Phi(v_1)$ lies in the region of $\widehat{X} \cap H$, where H is the half space given by the equation $x < 1 - A$.

We know that the edge joining v_1 to v_2 is in the family $\mathcal{F}(1, 0)$. The first coordinate of $T(1, 0)$ is A , so the horizontal distance from v_1 to v_2 is A . That means that v_1 is within $1 - A$ units of the left edge of Σ_1 , as shown on the right half of Figure 8.1.

By the Reconstruction Formula, $\Phi(v_1)$ lies in the region

$$R_A = X_A \cap \{x \mid x < 1 - A\}. \quad (39)$$

R_A lies in the region

$$H \cap \widehat{X}, \quad (40)$$

where H is the halfspace given by the equation $x < 1 - A$. Recall that the coordinates on this space are (x, y, z, A) , so H is defined by integer equations. Also, H is invariant under the action of the graph lattice Λ defined in §7.2. ♠

Recall that we parametrize $\widehat{X} \subset \mathbf{R}^4$ with coordinates (x, y, z, A) . So, H is a halfspace defined by integer equations. Moreover, H is invariant under the action of the graph lattice defined in §7.2.

The way the graph classifying map works is that we look at $\Phi(v_1)$ and record the labels of the polytope in each partition which contains this point.

Lemma 8.7 *Assuming that a bad configuration exists, one of the polytopes in one of the partitions has the label $(1, -1)$ and intersects H .*

Proof: There are two polytopes of interest to us: the one in each partition which contains $\Phi(v_1)$. These polytopes both intersect H . One of these polytopes is responsible for the assignment of the vector e_1 to v_1 . Call this the *magic polytope*. Since e_1 is in the family $\mathcal{F}(-1, 1)$, the label of the magic polytope is either $(-1, 1)$ or $(1, -1)$. We check that $T(1, -1)$ is the one with positive y coordinate. Hence, the label of the magic polytope is $(1, -1)$. ♠

Now for the computer assisted part of the proof. We check that no polytope at all in the $(+)$ partition has the label $(1, -1)$, and the only polytopes in the $(-)$ partition intersect H . This is obvious from the pictures on my computer program, and I will describe in the last chapter the short linear algebra computation which checks it. This completes the proof.

9 The Hitset and the Intertwiner

9.1 The Hitset

We fix a parameter A . Recall that a unit integer square is *grid full* if it contains a graph grid point, and otherwise grid empty. Recall that Φ_Π is the plaid classifying map. Let G_Π denote the plaid grid - i.e., the centers of the unit integer squares. Let $G_\Pi^* \subset G_\Pi$ denote the set of centers of grid full squares. In this section we state a result which characterizes the image

$$\bigcup_{\zeta \in G_\Pi^*} \Phi_\Pi(\zeta). \quad (41)$$

The domain of Φ_Π is the unit cube

$$X_\Pi = [-1, 1]^3. \quad (42)$$

We define the *hitset* to be the subset of X_Π having the form

$$X_\Pi^* = H \times [-1, 1], \quad (43)$$

where H is the octagon with vertices

$$\begin{aligned} &(-1, 1), (-1 + P, -1 + P), (1 - P, -1), (1, -1 + P) \\ &(1, 1), (1 - P, 1 - P), (-1 + P, 1), (-1, 1 - P). \end{aligned} \quad (44)$$

The vertices are listed in cyclic order. The octagon H has a kind of zig-zag shape. Figure 9.1 shows the picture for several parameters.

In this chapter we will prove the following theorem.

Theorem 9.1 (Hitset) *For any parameter A , we have*

$$\bigcup_{\zeta \in G_\Pi^*} \Phi_\Pi(\zeta) \subset X_\Pi^*. \quad (45)$$

The Hitset Theorem is sharp in the following sense. All the objects make sense at irrational parameters as well as rational parameters, and for irrational parameters, the set on the left is dense in the set on the right. We will not prove this, because we do not need the result, but a proof would not be so difficult given everything else we prove in this chapter.

In Figure 9.1 below we show the polygon H for the parameters $k/5$ for $k = 1, 2, 3, 4$. (The picture makes sense for all parameters, and not just even rational ones.) Actually, we show not just H but also the image of H under the action of the lattice Λ_Π . We think of this lattice as acting on the xy plane just by forgetting about the third coordinate. The lattice is generated by the vectors $(2, P)$ and $(0, 2)$.

Thanks to the product structure of X_Π and X_Π^* , the planar pictures we show capture all the information. The various images of H fit together to form infinite bands which look like zigzags. As $A \rightarrow 0$ the zigzags come together and fill up the plane.

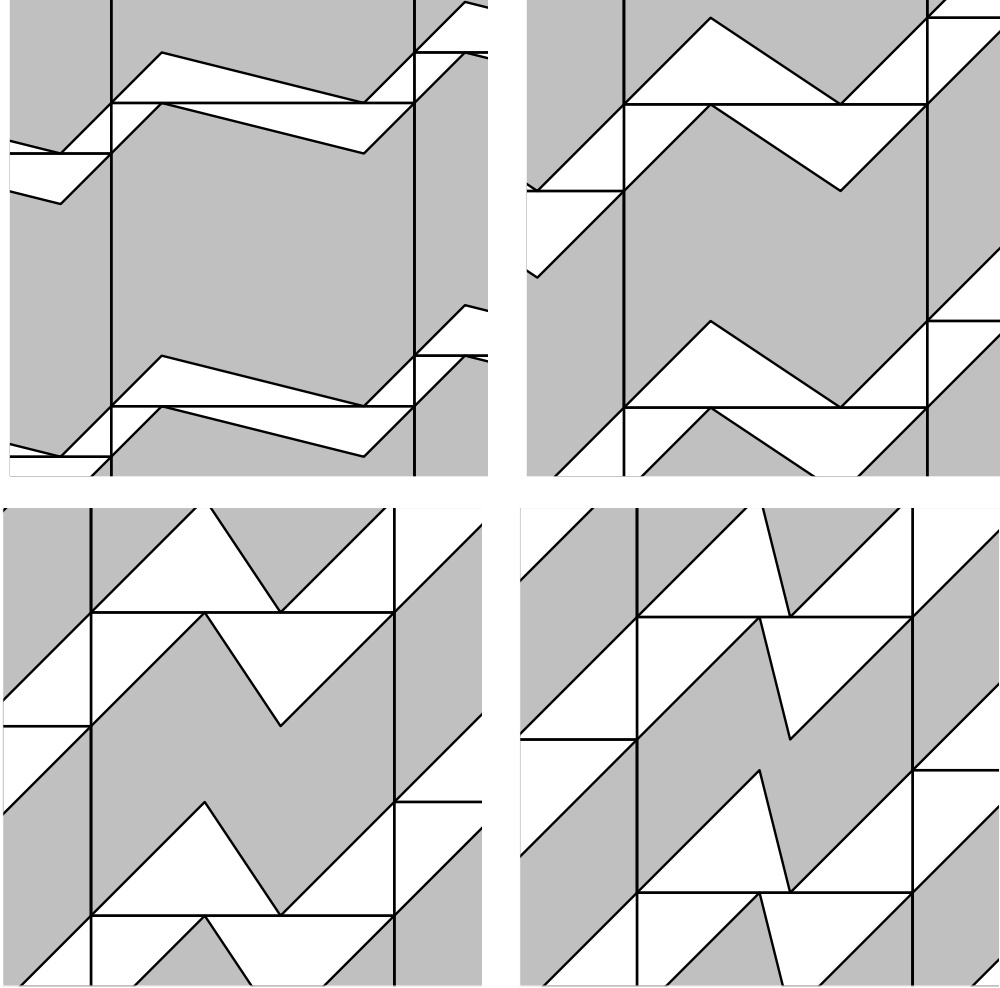


Figure 9.1: The orbit $\Lambda_\Pi(H)$ for parameters $A = k/5$, $k = 1, 2, 3, 4$.

9.2 The Projective Intertwiner

The symbol Ψ will denote the map which we call *the projective intertwiner*. We will define Ψ after we specify its domain and range. Recall that our total space is $\widehat{X} = \mathbf{R}^3 \times [0, 1]$.

Domain: The domain of Ψ is X_Π , though our theorem really only concerns the image of Ψ on the hitset X_Π^* . The set X_Π is the fundamental domain for the lattice Λ_1 acting on \widehat{X} . See §6.1.

We write

$$X_\Pi = X_{\Pi,-} \cup X_{\Pi,+}, \quad (46)$$

Where $X_{\Pi,+}$ consists of those points (x, y, z, P) where $x \leq y$ and $X_{\Pi,-}$ consists of those points there $y \leq x$. This is a partition of X_Π into two isometric halves.

Range: The range of Ψ is

$$X_\Gamma = \widehat{X}/\Lambda, \quad (47)$$

where Λ is the graph lattice defined in §7.2.

The Map: Now we define the map

$$\Psi : X_\Pi \rightarrow X_\Gamma.$$

For $(x, y, z, P) \in X_{\Pi,\pm}$, we define

$$\Psi(x, y, z, P) = \left[\frac{1}{2-P} \left(x-y, -y-1, z+P+1, P \right) \pm (1, 0, 0, 0) \right]_\Lambda \quad (48)$$

That is, we add or subtract 1 depending on which half of the partition our point lies in, and we take the result mod Λ . In the next section we check that Ψ is well defined even in boundary cases. The map Ψ is a piecewise defined integral projective transformation. If we hold P fixed and restrict Ψ to a slice, then Ψ is an affine transformation. We call Ψ the *projective intertwiner*.

The Main Result: Let G_Γ denote the graph grid. Let G_Π denote the plaid grid. Each point $\zeta_\Gamma \in G_\Gamma$ lies in the interior of a unique integer square. We let $\zeta_\Pi \in G_\Pi$ denote the center of this square.

Let $\Phi_{\Pi} : G_{\Pi} \rightarrow X_1$ denote the plaid classifying map. Recall that, at the parameter A , the range of Φ_{Π} is contained in the slice $\mathbf{R}^3 \times \{P\}$, where $P = 2A/(1 + A)$. Let $\Phi_{\Gamma} : G_{\Gamma} \rightarrow \widehat{X}/\Lambda$ be the graph classifying map.

Theorem 9.2 (Intertwining) *The following holds for every even rational parameter:*

$$\Phi_{\Gamma}(\zeta_{\Gamma}) = \Psi \circ \Phi_{\Pi}(\zeta_{\Pi}) \quad \forall \zeta_{\Gamma} \in G_{\Gamma}. \quad (49)$$

Remarks:

(i) I checked Equation 49 computationally for all relevant points and all parameter p/q with $q < 30$. This check is not meant as a substitute for a rigorous proof, but it is nice to know. I didn't check the Hitset Theorem as systematically, but my computer program plots the left and right hand sides of Equation 45, and one can see that it always works.

(ii) Notice in Equation 48 that the fourth coordinate on the right hand side is A , because $A = P/(2 - P)$. Thus, Ψ maps the relevant slices to each other.

(iii) It might be nicer if there were a global projective transformation from \widehat{X} to itself which works in place of our piecewise projective map Ψ . However, we have $\Psi(T_X(V) - V) = (2, 0, 0, 0)$. The vector on the right does not have for them $\lambda(W) - W$ for any transformation $\lambda \in \Lambda_1$, the plaid lattice. This situation makes the existence of a global projective intertwiner impossible. On the other hand, below in §9.8 we will modify the domain of Ψ so that Ψ is projective throughout the interior of the new domain. When we look at the action of Ψ on the new domain, we will see the canonical nature of Ψ . See Lemma 9.4 for instance.

(iv) When it comes time to prove the Pixellation Theorem, we shall be interested in the action of Ψ on the polytopes of the plaid triple partition. At first, it looks like we might have trouble, due to the piecewise nature of Ψ . However, it turns out that every plaid triple polytope is contained in one of the two pieces of the partition of X_{Π} .

(v) Our proof will show that a suitable formulation of the Intertwining Theorem holds for all parameters, and not just even rational ones. Indeed, it basically follows from continuity.

(vi) The reader who is keen to see how the proof of the Pixellation Theorem works might want to take the Hitset Theorem and the Intertwining Theorem for granted on the first reading. Our proof of the Pixellation Theorem only uses the truth of these statements, and not any theory developed during their proof. §10.2 gives a good illustration of how we use the Intertwining Theorem.

9.3 Well Definedness

Since Ψ is only piecewise defined, we have to worry about the cases when there are two competing definitions for Ψ . In our discussion of this matter, the symbol $(*)$ stands for a coordinate value that we don't care about. We fix some even rational parameter for the discussion.

There are three issues. One issue is that perhaps

$$\Phi_{\Pi}(\zeta) = (-1, *, *).$$

In this case, the two points

$$\phi_+ = \Phi_{\Pi}(\zeta), \quad \phi_- = \Phi_{\Pi}(\zeta) + (2, P, P)$$

are equally good representatives. Here $\phi_{\pm} \in X_{\Pi, \pm}$. An easy calculation shows that

$$\begin{aligned} \Psi(\phi_-) - \Psi(\phi_+) &= \frac{1}{2-P} \left(2-P, -P, PP, -P, 2-P \right) - (2, 0, 0) = \\ &= (-1, -A, A) \in \Lambda_1. \end{aligned} \tag{50}$$

Hence, either representative gives rise to the same point in the range.

The second issue seems more serious, in view of Remark (v) above. It might happen that

$$\phi = \Phi_{\Pi}(\zeta) = (v, v, *).$$

That is, ϕ lies on the boundary of both pieces of the partition of X_{Π} . Let's check that this situation cannot arise for the images of points of G_{Π} . Such points have the form (x, y) where x and y are half integers. We compute that

$$\Phi_{\Pi}(x, y) = (2Px + 2y, 2Px, *) + (2m, Pm, *), \tag{51}$$

for a suitable integer m . We also observe that $2y$ is odd. Equation 51 leads to

$$P = \frac{2m + 2y}{m}.$$

This is impossible, because $P = 2p/(p+q)$, and $2m + 2y$ is an odd integer.

The third issue is that $\Phi_{\Pi}(\zeta) = (*, u, v)$ with either $u = \pm 1$ or $v = \pm 1$ or both. The case $u = \pm 1$ is impossible for similar reasons that we have just discussed. When $v = \pm 1$ it has replacing v by $v \mp 2$ has no effect on the Intertwining formula.

9.4 Strategy of the Proof

The rest of the chapter is devoted to proving the Hitset Theorem and the Intertwining Theorem. We prove these two results at the same time because they are closely related to each other. Here are the steps of the proof. We fix a parameter $A = p/q$.

- We prove the Intertwining Theorem for points of the form

$$\zeta_n = (n + 1/2)(1 + A, 1 - A), \quad n = 0, 1, 2, \dots \quad (52)$$

These points all belong to G_Γ because ζ_0 is the anchor point and $\zeta_n - \zeta_0 = ndT(1, 1)$. Here T is the canonical affine transformation. We call the points in Equation 52 the *diagonal points*.

- We prove the Hitset Theorem for the points in Equation 52.
- We prove the following induction step: Suppose that the Hitset Theorem is true for some graph grid point ζ . Then it is also true for $\zeta + dT(0, 1)$. We call this *Hitset Induction*.
- We prove the following induction step: Suppose that the Intertwining Theorem is true for some graph grid point ζ . Then it is also true for $\zeta + dT(0, 1)$. We call this *Intertwiner Induction*.

Let L denote the lattice of symmetries generated by the vectors $(\omega^2, 0)$ and $(0, \omega)$. Here $\omega = p + q$, as usual. We have already shown that both the plaid model and the arithmetic graph are invariant under L . We say that an *L-orbit* is an orbit of L acting on the graph grid. By symmetry, it suffices to prove our two theorems on a set which contains at least one point of every L -orbit.

The four steps above combine to to prove that the two theorems hold true on sets of the form $dT(B)$ where B is a ball in \mathbf{Z}^n of arbitrarily large radius. For sufficiently large B , the set $dT(B)$ intersects every L orbit.

Remark: It would have been nice if the set of points $\{\zeta_n\}$ intersected every L -orbit. If this was true, we would not need the induction part of the proof. Likewise, it would have been nice if, starting from a single point (such as the anchor), we could reach every L -orbit just by repeatedly adding $dT(0, 1)$. If this was true, we would not need the first two steps of our proof. Alas, neither of these step-saving situations is true.

9.5 The Intertwining Theorem on the Diagonal

In this section we prove the Intertwining Theorem for points of the form

$$\zeta_n = \left(n + \frac{1}{2}\right)(1 + A, 1 - A), \quad n = 0, 1, 2, \dots \quad (53)$$

These points all belong to G_Γ , because $\zeta_n = \zeta_0 + dT(n, n)$ and ζ_0 is the anchor point.

We fix the value of n . It is convenient to consider the sub-intervals

$$R_{n,k} = \left(\frac{2k}{2n+1}, \frac{2k+1}{2n+1}\right), \quad k = 0, \dots, (n-1). \quad (54)$$

$$L_{n,k} = \left(\frac{2k-1}{2n+1}, \frac{2k}{2n+1}\right), \quad k = 1, \dots, (n-1). \quad (55)$$

We ignore the endpoints of these intervals; the boundary cases, when relevant, follow from continuity.

Let $I = (A_0, A_1)$ be one of the intervals of interest. We will sometimes use the following trick to bound certain numerical quantities that depend on $A \in I$. When the quantity is monotone, we get the bounds by evaluating the expression on the boundary values $A = A_0$ and $A = A_1$. We call this method *the boundary trick*.

When $A \in L_{n,k}$ (respectively $R \in L_{n,k}$, the point ζ_n lies in the left (respectively right) half of the square with center

$$\zeta_{n,k} = \left(n + \frac{1}{2}, n + \frac{1}{2}\right) + (k, -k). \quad (56)$$

First we consider the case when $A \in L_{n,k}$. We have

$$\Phi_\Pi(\zeta_{n,k}) \equiv (P(2n+2k+1) + (2n-2k+1), P(2n+2k+1), 2P(2n+1)). \quad (57)$$

The symbol \equiv means that we still need to reduce mod Λ_1 to get a vector in the fundamental domain.

The boundary trick tells us that the first coordinate in Equation 57 lies in

$$\left(1 + 2k + 2n - \frac{1+2n}{k+n}, 1 + 2k + 2n\right) \quad (58)$$

So, we subtract off the lattice vector $(n+k)(2, P, P)$. This gives

$$\Phi_\Pi(\zeta_{n,k}) \equiv (P(2n+2k+1) - 4k + 1, P(1+k+n), 2P(2-k+3n)). \quad (59)$$

The boundary trick tells us that the second coordinate in Equation 59 lies in the interval $(-1, 1) + 2k$. Subtracting $(0, 2k, 0)$ from Equation 59, we get a point in the fundamental domain:

$$\Phi_{\Pi}(\zeta_{n,k}) = (P(2n+2k+1)-4k+1, P(1+k+n)-2k, P(2-k+3n)+2\beta). \quad (60)$$

Here β is some integer whose value we don't care about.

The interval check shows that the first coordinate in Equation 60 is larger than the second coordinate. (We apply the trick to the difference of the coordinates.) Hence the point in Equation 60 lies in $X_{\Pi,-}$. We also have

$$\Phi_{\Gamma}(\zeta) \equiv \left(n + \frac{1}{2}\right)(1+A, 1+A, 1+A) \bmod \Lambda. \quad (61)$$

Here Λ is the graph lattice. (In all these equations we are leaving off the fourth coordinate; we know this works out already.)

A calculation, which we do in Mathematica, shows that

$$\begin{aligned} \Psi(\Phi_{\Pi}(\zeta_{n,k}) - \Phi_{\Gamma}(\zeta) = & \\ & (-1-k-n)(1, -1, -1) + \\ & (-2-2n)(0, 1+A, 1-A) + \\ & (1-k+\beta)(0, 0, 1+A). \end{aligned}$$

In other words, we have written the difference between the quantities as an integer combination of vectors in the graph lattice Λ . Hence, the two quantities are equal, as desired.

When $A \in R_{n,k}$ the calculation is very similar and we will just describe the differences. This time the interval trick tells us to subtract off the vector $(n+k+1)(2, P, P)$ from the point in Equation 57. Then, as in the other case, we subtract off $(0, -2k, 0)$. The result is

$$\Phi_{\Pi}(\zeta_{n,k}) = (P(2k+2n+1)-4k-1, P(k+n)-2k, P(1-k+3n)+\beta) \quad (62)$$

The interval trick shows that this point lies in $X_{\Pi,+}$. Now we compute

$$\begin{aligned} \Psi(\Phi_{\Pi}(\zeta_{n,k}) - \Phi_{\Gamma}(\zeta) = & \\ & (-k-n)(1, -1, -1) + \\ & (-1-2n)(0, 1+A, 1-A) + \\ & (1-k+\beta)(0, 0, 1+A). \end{aligned}$$

This gives us the same desired conclusion as in the first case.

9.6 The Hitset Theorem on the Diagonal

Now we prove the Hitset Theorem for the points we considered in Step 1. We first consider the case when $A \in L_{n,k}$. The triangle Δ_L with vertices

$$(-1 + P, -1 + P), \quad (1, -1 + P), \quad (1, 1) \quad (63)$$

is the convex hull of 3 of the vertices and is contained in the polygon defining the hitset.

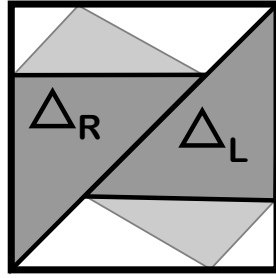


Figure 9.2: The triangles Δ_L and Δ_R .

Let ξ denote the point in the plane obtained by taking the first two coordinates of the point in Equation 60. That is:

$$\xi = (P(2n + 2k + 1) - 4k + 1, P(1 + k + n) - 2k). \quad (64)$$

It suffices to prove that $\xi \in \Delta_L$ for all $A \in L_{n,k}$. One of the sides of Δ_L is the line $x = 1$, and certainly ξ does not cross this line; it corresponds to one of the sides of the fundamental domain. Another side of Δ_L is the line $y = -1 + P$. The interval trick shows that ξ stays above this line. Finally, the other side of Δ_L is the line $y = x$. We already know that $\Phi_{\Pi}(\zeta) \in X_{\Pi,-}$, and this is the equivalent to the statement that ξ lies to the right of this line. These three conditions together imply that $\xi \in \Delta_L$. My computer program allows you to see a plot of ξ and Δ_L for all the relevant parameters.

Now consider the case when $A \in R_{n,k}$. This time we use the triangle $\Delta_R = -\Delta_L$, obtained by negating all the coordinates of the vertices of Δ . This time we want to show that the point

$$(P(2k + 2n + 1) - 4k - 1, P(k + n) - 2k) \quad (65)$$

lies in Δ_R . The same arguments as above shows that this point lies to the right of the line $x = -1$, below the line $y = 1 - P$, and to the left of the line $y = x$. This does the job for us.

9.7 Hitset Induction

Here we will prove Hitset Induction modulo what we call *the geometric claim*. We will prove the geometric claim at the end of the chapter.

We set $\zeta_\Gamma = \zeta$ and $\zeta'_\Gamma = \zeta + dT(0, 1)$. Similarly, we define ζ_Π and ζ'_Π . Here ζ_Π is the center of the unit integer square that contains ζ_Γ . Since we will be mentioning both the plaid lattice and the graph lattice, we let Λ_Π denote the plaid lattice and Λ_Γ denote the graph lattice.

We have

$$dT(0, 1) = (1, -P). \quad (66)$$

From this equation, we see that we have one of two possibilities for $\zeta_{\Pi'} - \zeta_\Pi$. This difference either equals $(1, 0)$ or $(1, -1)$. To be more precise, let G_Γ^{hi} denote the union of those choices of $\zeta_\Gamma = (x, y)$ such that $x - \text{floor}(x) > P$. Define ζ_Π^{lo} to be the complementary set. For even rational parameters, it never happens that $y = \text{floor}(y) = P$, because then ζ'_Γ would lie on the boundary of a unit integer square.

Let H^{lo} denote the parallelogram with vertices

$$(1 - 3P, 1 - 3P), \quad (1 - P, 1 - P), \quad (-1 + P, 1) \quad (-1 - P, 1 - 2P). \quad (67)$$

Let H^{hi} denote the polygon with vertices

$$(-1 + P, -1 + P), \quad (1 - P, -1), \quad (3 - 3P, 1 - 2P) \quad (1 - P, 1 - P). \quad (68)$$

These polygons are not subsets of H . However, the orbits $\Lambda_\Pi(H^{\text{hi}})$ and $\Lambda_\Pi(H^{\text{lo}})$ together give a partition of $\Lambda_\Pi(H)$. The dark region is the *lo orbit* and the light region is the *hi orbit*.

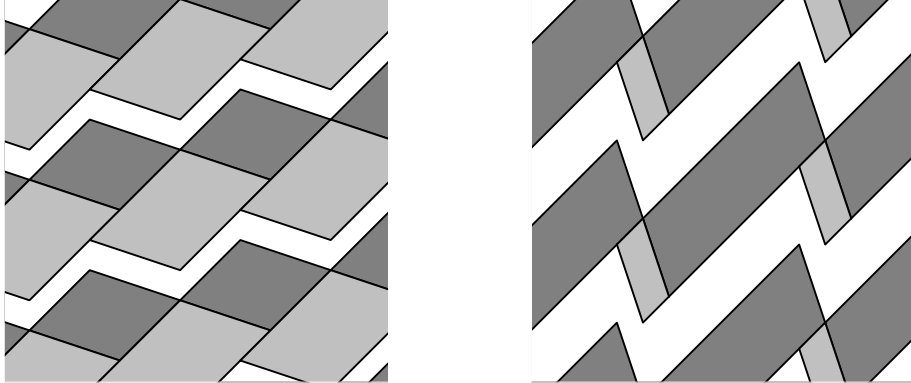


Figure 9.4: The orbits $\Lambda_\Pi H^{\text{lo}}$ and $\Lambda_\Pi H^{\text{hi}}$ for $A = 1/4$ and $A = 3/4$.

Geometric Claim:

- $\zeta_\Gamma \in G_\Gamma^{\text{hi}}$ implies $\Phi_\Pi(\zeta_\Pi) \in \Lambda_\Pi(H^{\text{hi}} \times [-1, 1])$
- $\zeta_\Gamma \in G_\Gamma^{\text{lo}}$ implies $\Phi_\Pi(\zeta_\Pi) \in \Lambda_\Pi(H^{\text{lo}} \times [-1, 1])$

We call this claim the *geometric claim*.

We introduce the new sets

$$(H^{\text{hi}})' = H^{\text{hi}} + (2P, 2P), \quad (H^{\text{lo}})' = H^{\text{lo}} + (2P - 2, 2P - 2). \quad (69)$$

If $\zeta_\Gamma \in G_\Gamma^{\text{hi}}$ and the geometric claim is true, then

$$\Phi_\Pi(\zeta'_\Pi) \in \Lambda_\Pi((H^{\text{hi}})' \times [-1, 1]).$$

The same goes when we replace *hi* with *lo*. In the low case, we are using the fact that $(2P - 2, 2P - 2)$ and $(2P - 2, 2P)$ are equal up to a vector in Λ_Π .

Now for the punchline. $\Lambda_\Pi((H^{\text{lo}})')$ and $\Lambda_\Pi((H^{\text{hi}})')$ give a second partition of $\Lambda_\Pi(H)$. Figure 9.5 shows the picture for the parameters $A = 1/4$ and $A = 3/4$.

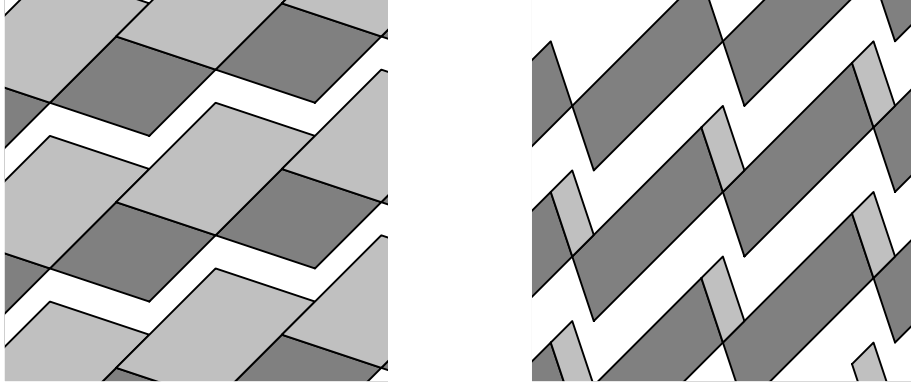


Figure 9.5: The orbits $\Lambda_\Pi(H^{\text{lo}})'$ and $\Lambda_\Pi(H^{\text{hi}})'$ for $A = 1/4$ and $A = 3/4$.

We get exactly the same picture as in Figure 9.4 except that the pieces have each been translated.

What we are really saying is that there is an infinite polygon exchange transformation on $\Lambda_\Pi(H)$ which corresponds to the operation of adding the vector $dT(0, 1)$ in G_Γ . The orbit $\Lambda_\Pi(H)$ decomposes into a countable union of parallelograms, each partitioned into a light parallelogram and a dark one. Our map simply exchanges the light and dark pieces within each component. On each component, our map is essentially a rotation of a flat torus.

Figure 9.6 shows the two partitions side by side, for the parameter $A = 1/4$. The “components” we are talking about are parallelograms which are bounded on opposite sides by lines of slope 1. For later reference, we call these parallelograms *dipoles*. So, again, each dipole is partitioned into a light and dark parallelogram, and our polygon exchange simply exchanges the two pieces within each dipole.

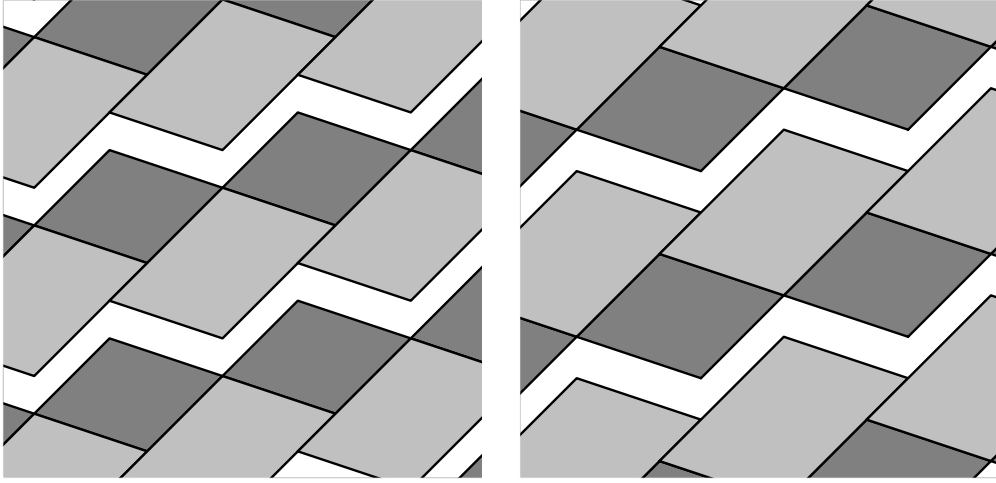


Figure 9.6: The two partitions of $\Lambda_{\Pi}(H)$ for the parameter $A = 1/4$.

The Geometric Claim immediately implies Hitset Induction. Hence, the Geometric Claim implies the Hitset Theorem.

9.8 Changing the Fundamental Domain

Observe that the orbit $\Lambda_{\Pi}(H)$ is simply a union of dipoles. Rather than consider $X_{\Pi} = [-1, 1]^3$ as our fundamental domain for the action of Λ_{Π} , we instead consider the fundamental domain to be

$$\Upsilon \times [-1, 1] \tag{70}$$

where Υ is the dipole that intersects $[-1, 1]^2$ to the right of the diagonal line $y = x$. Figure 9.7 shows Υ and how it sits with respect to $[-1, 1]$.

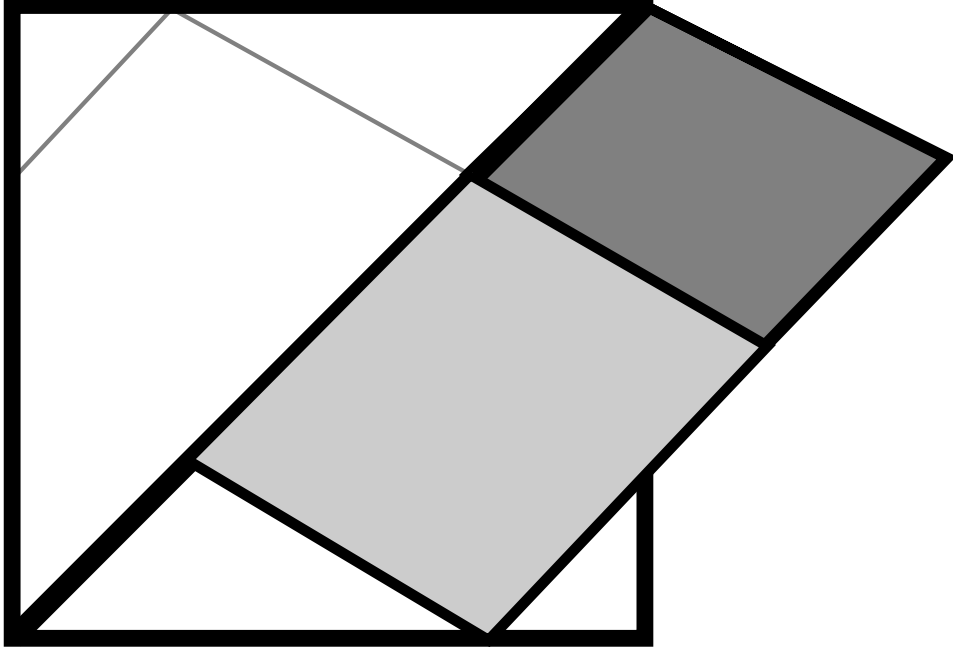


Figure 9.7: The fundamental dipole.

We get an easier calculation if we use $\Upsilon \times [-1, 1]$ as the domain for the projective intertwiner Ψ . To do this, we need to define Ψ on the whole fundamental domain, and check that the new definition agrees with the original in the appropriate sense.

The points of $\Upsilon - [-1, 1]^2$ all lie to the right of $[-1, 1]^2$, and one simply subtracts off $(-2, -P)$ to get them back into $[-1, 1]^2$. For any

$$\phi \in \left(\Upsilon - [-1, 1]^2 \right) \times [-1, 1], \quad (71)$$

We define $\Psi(\phi)$ using the branch of Φ which is defined for $X_{\Pi,-}$. Let $\phi^* = \phi - (2, P, P) \in X_{\Pi,+}$. Using the fact that $\phi \in X_{\Pi,-}$ and $\phi^* \in X_{\Pi,+}$, we compute

$$\Psi(\phi) - \Psi(\phi^*) = (-1, -A, A) = (-1, 1, 1) - (0, 1 + A, 1 - A) \in \Lambda_{\Gamma}. \quad (72)$$

So, our redefinition does not change anything. We can prove Induction Statement 2 using the new fundamental domain. Moreover, the restriction of Ψ to the new domain is projective throughout.

9.9 Intertwiner Induction

Since $\Phi_\Gamma(x, y) = (x, x, x) \bmod \Lambda_\Gamma$, we have

$$\Phi_\Gamma(\zeta'_\Gamma) - \Phi_\Gamma(\zeta_\Gamma) = (1, 1, 1) \bmod \Lambda_\Gamma. \quad (73)$$

Let

$$\phi = \Phi_\Pi(\zeta_\Pi), \quad \phi' = \Phi_\Pi(\zeta'_\Pi). \quad (74)$$

To establish Intertwiner Induction, we just have to prove

$$\Psi(\phi') - \Psi(\phi) - (1, 1, 1) \in \Lambda_\Gamma. \quad (75)$$

Using our new fundamental domain, and also the action of the map Φ_Π , we have one of

$$\phi - \phi' = (2P, 2P, 2P + 2\beta), \quad \phi' - \phi = (2P - 2, 2P - 2, 2\beta), \quad (76)$$

depending on whether we are in the hi case or the lo case. Here β is some integer whose value does not effect the calculation.

Hi Case:

$$\begin{aligned} \Psi(\phi') - \Psi(\phi) - (1, 1, 1) &= \\ \frac{1}{2-P} \left(0, -2P, 2P + 2\beta \right) - (1, 1, 1) &= \\ (-1, -2A - 1, 2A - 1 + 2\beta(1 + A)) &= \\ 2\beta(0, 0, 1 + A) + (-1, 1, 1) + 2(0, A + 1, A - 1) &\in \Lambda_\Gamma. \end{aligned}$$

Notice that β plays no role at all in the final answer. To simplify the second calculation, we assume that $\beta = 0$.

Lo Case:

$$\begin{aligned} \Psi(\phi') - \Psi(\phi) - (1, 1, 1) &= \\ \frac{1}{2-P} \left(0, -2P + 2, 0 \right) - (1, 1, 1) &= \\ (-1, -A, -1) = (-1, 1, 1) - (0, 1 + A, 1 - A) - (0, 0, 1 + A) &\in \Lambda_\Gamma. \end{aligned}$$

This is what we wanted to prove.

At this point, we have reduced the Intertwining Theorem and the Hitset Theorem to the Geometric Claim.

9.10 Proof of the Geometric Claim

We will combine the Intertwining Formula with the Graph Reconstruction Formula. We are allowed to do this for the pair $(\zeta_\Gamma, \zeta_\Pi)$ by induction.

We introduce coordinates

$$\zeta_\Gamma = (a, b), \quad \Phi_\Pi(\zeta_\Pi) = (x, y, z, P)$$

. Let $[t] = t - \text{floor}(t)$.

Lemma 9.3

$$[a] = \left\lfloor \frac{x - y}{2 - P} \right\rfloor, \quad [b] = \left\lfloor \frac{-2 - P + P^2 + Px + 2y - 2Py}{2P - 4} \right\rfloor. \quad (77)$$

Proof: Define

$$\Psi \circ \Phi_\Pi(\zeta_\Pi) = (x^*, y^*, z^*, A).$$

For convenience, we repeat Equation 48 here:

$$\Psi(x, y, z, P) = \left[\frac{1}{2 - P} (x - y, -y - 1, z + P + 1, P) - (1, 0, 0, 0) \right]_\Lambda \quad (78)$$

We always take the $(-)$ option in Equation 48 because we are using the domain $\Upsilon \times [-1, 1]$ described in §9.8. The graph reconstruction formula tells us that

$$[a] = [x^*], \quad [b] = \left\lfloor \frac{y^* - Ax^*}{1 + A} \right\rfloor.$$

Combining this formula with Equation 78 and doing some algebra, we get Equation 77. ♠

The next result says that the formulas in Equation 77, which look messy, are actually as nice as possible.

Lemma 9.4 *Equation 77 induces an affine diffeomorphism from Υ to $[0, 1]^2$.*

Proof: Forgetting about the brackets, the corresponding map on the plane is an affine diffeomorphism Ω . The first coordinate of Ω is obviously constant along lines of slope 1. These lines are parallel to the diagonal sides of Υ . We

claim that the second coordinate of Ω is constant along lines parallel to the other two sides of Υ . To see this, we plug in the equation

$$y = \left(\frac{-P}{2-P} \right) x + c. \quad (79)$$

and observe that the resulting expression

$$f(c) = \frac{2+P-P^2}{4-2P} + \left(\frac{P-1}{2-P} \right) c \quad (80)$$

is independent of x .

The left and right sides of Υ are given by the equations $y = x$ and $y = x - (2 - P)$. Hence Ω maps the left and right sides of Υ respectively to the left and right sides of the integer unit square $[0, 1]^2$. The bottom and top sides of Υ are given by taking

$$c_0 = \frac{P-2}{2}, \quad c_1 = \frac{P-2}{2} + \frac{1-P}{2-P} \quad (81)$$

in Equation 79. We check that $f(c_0) = 1$ and $f(c_1) = 0$. Hence Ω maps the top and bottom of Υ respectively to the bottom and top of $[0, 1]^2$. ♠

The Geometric Claim follows immediately from the analysis in the previous lemma. It says that

$$\Lambda_\Gamma(H^{\text{hi}}) \cap \Upsilon = \Omega^{-1}([0, 1] \times [P, 1]), \quad \Lambda_\Gamma(H^{\text{lo}}) \cap \Upsilon = \Omega^{-1}([0, 1] \times [0, P]). \quad (82)$$

In light of Equation 77, this last equation is equivalent to the Geometric Claim.

This completes the proof of the Geometric Claim, and thereby completes the proof of both the Hitset Theorem and the Intertwining Theorem.

10 Correspondence of Polytopes

In this chapter we prove Statement 2 of the Pixellation Theorem modulo some integer linear algebra calculations. We also set up the kind of problem we need to solve in order to prove Statements 3,4, and 5 of the Pixellation Theorem. We fix some parameter A that is in the background of the whole discussion. Also, as in some previous chapters, we reserve the word *square* for unit integer squares.

10.1 Proof of Statement 2

Statement 2 of the Pixellation Theorem says that a grid full square is plaid trivial if and only if it is graph trivial.

The reduced triple partition \mathcal{RTP} consists of 218 polytopes in the fundamental domain $X_\Pi = [-1, 1]^3$. We call these polytopes Π_0, \dots, Π_{217} .

Lemma 10.1 *Suppose that Σ is a grid full square. If Σ is plaid trivial then Σ is graph trivial.*

Proof: In our listing, there are 6 polytopes in \mathcal{RTP} having null labels, namely Π_0, \dots, Π_5 . We observe that $\Psi(\Pi_j)$ is contained in a single polytope

$$\Gamma_j = \Gamma_{j,+} = \Gamma_{j,-}$$

in the graph partition, and that Γ_j is null labeled. (This is why $\Gamma_{j,+} = \Gamma_{j,-}$.)

Suppose that Σ is a grid full plaid trivial square for some parameter. Let ζ_Π be the center of Σ . Let ζ_Γ be the graph grid point in G_Γ which is contained in Σ .

By the Plaid Master Picture Theorem,

$$\Phi_\Pi(\zeta_\Pi) \subset \bigcup_{j=0}^5 \Pi_j.$$

By the Intertwining Theorem,

$$\Phi_\Gamma(\zeta_\Gamma) \subset \bigcup_{j=0}^5 \Psi(\Pi_j) \subset \bigcup_{j=0}^5 \Gamma_j.$$

By the Graph Master Picture Theorem, the portion of the arithmetic graph associated to ζ_Γ is trivial. That is, Σ is graph trivial. ♠

Lemma 10.2 *Suppose that Σ is a grid full square. If Σ is graph trivial then Σ is plaid trivial.*

Proof: We will prove the contrapositive: If Σ is plaid nontrivial then Σ is graph nontrivial. We observe that each of the polytopes Π_6, \dots, Π_{217} has a nontrivial label. We also observe the following:

- $\Psi(\Pi_j)$ is contained in a single graph polytope $\Gamma_{j,+}$ and a single graph polytope $\Gamma_{j,-}$ for $j = 6, \dots, 179$. The labels of these graph polytopes are all nontrivial
- $\Psi(\Pi_j)$ is contained in a single graph polytope $\Gamma_{j,-}$ and a union of two graph polytope $\Gamma_{j+,0}$ and $\Gamma_{j+,1}$ for $j = 180, \dots, 198$. The labels of these graph polytopes are all nontrivial.
- $\Psi(\Pi_j)$ is contained in a single graph polytope $\Gamma_{j,+}$ and a union of two graph polytope $\Gamma_{j-,0}$ and $\Gamma_{j-,1}$ for $j = 199, \dots, 217$. The labels of these graph polytopes are all nontrivial.

Combining the information listed above with the Plaid Master Picture Theorem, the Graph Master Picture Theorem, and the Intertwining Theorem in the same way as the previous proof, we get the conclusion of this lemma. ♠

10.2 A Sample Result

Let us press the method of the previous section a bit harder, in order to see both its power and its limitations. Figure 10.1 shows a particular arc of the plaid model. Depending on the way the triple is oriented, it corresponds to tiles in \mathcal{RTP} labeled NEWEWS or SWEWEN.

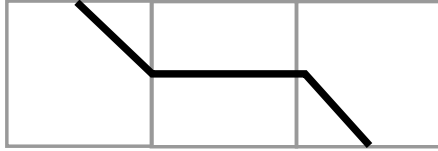


Figure 10.1: The triple of type NEWEWS or SWEWEN.

Lemma 10.3 (Sample) *Every time the triple of the type shown in Figure 10.1 appears in the arithmetic graph and the central square Σ is grid full, the two edges incident to the grid graph vertex in Σ are in $\mathcal{F}(0, 1)$ and $\mathcal{F}(0, -1)$.*

Proof: There are 6 polytopes in \mathcal{RTP} having the relevant labels. The ones labeled NEWNEWS are listed as $\Pi_7, \Pi_{138}, \Pi_{165}$. The ones labeled SWEWEN are listed as $\Pi_{103}, \Pi_{130}, \Pi_{159}$.

Recall that Ψ is the projective intertwining map. We check by direct computation that, for each $j \in \{7, 103, 130, 138, 159, 165\}$ there are polytopes $\Gamma_{j,+}$ and $\Gamma_{j,-}$ in the $(+)$ and $(-)$ graph PET partitions respectively so that

$$\Psi(\Pi_j) \subset \Gamma_{j,+} \cap \Gamma_{j,-}. \quad (83)$$

When we inspect the labels of these graph polytopes we observe that

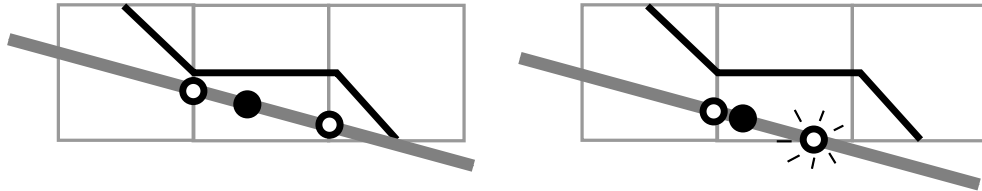
- The label of $\Gamma_{j,+}$ is always $(0, 1)$.
- The label of $\Gamma_{j,-}$ is always $(0, -1)$.

Now let us put this information together. Suppose we see the triple from Figure 10.1 in the plaid model for some parameter A . The rest of the discussion implicitly refers to the parameter A . Let ζ_Γ be the vertex of the graph grid G_Γ contained in the central square Σ of the triple. The same argument as in the previous section shows that

$$\Phi_\Gamma(\zeta_\Gamma) \in \bigcup_{j=7,103,130,138,159,165} \Gamma_{j,+} \cap \Gamma_{j,-}. \quad (84)$$

But then, by the Master Picture Theorem, the two edges incident to ζ_Γ are in $\mathcal{F}(0, 1)$ and $\mathcal{F}(0, -1)$. ♠

10.2 shows us the kind of conclusion we can draw from Lemma 10.3.



10.2: Some possible conclusions from Lemma 10.3.

Lemma 10.3 tells us that every time we see the triple in Figure 10.1, we see the arithmetic graph edges shown in (in grey) in 10.2. However, it might happen that one of these grey edges crosses the top or the bottom of the central square rather than the sides, as it the Pixellation Theorem suggests. Lemma 10.3 tells us the *local geometry* of the arithmetic graph but not how it crosses the edges of the central square. So eliminate the second option shown in 10.2 (as well as other bad options, we need to study how our machinery also determines the edge crossings.

In the rest of this chapter, we set up conventions and notation for the kind of problem we need to solve.

10.3 Fixing Orientations

Recall that there are both oriented and unoriented versions of the Plaid and Graph Master Picture Theorems. We have stated the Intertwining Theorem for the unoriented versions, because the proof is simpler. However, this forces us to deal with orientations in a somewhat *ad hoc* way.

As we mentioned above, there are 218 polytopes in RTP. Each of these polytopes has a 6 letter label which specifies an oriented arc of combinatorial length 3 in the plaid model. The catch is that we are using the small domain \widehat{X}/Λ_1 as the image of the plaid classifying map Φ_Π , rather than the double cover \widehat{X}/Λ_2 .

Thus, if $\zeta_\Pi \in G_\Pi$ is some point, the label of the polytope in \mathcal{RTP} containing $\Phi_\Pi(\zeta_\Pi)$ might specify the opposite orientation on the plaid arc through ζ_Π . More precisely, the assigned orientation is correct if and only if $\widehat{\Phi}_\Pi(\zeta_\Pi)$ is congruent mod Λ_2 to a point in the fundamental domain X_Π . Here $\widehat{\Phi}_\Pi$ is the lift of $\widehat{\Pi}$ to the double cover \widehat{X}/Λ_2 . At the same time, in order to figure out the orientations on the graph polygons, we would need to look at the lift $\widehat{\Phi}_\Gamma$ of the graph classifying map Φ_Γ .

Getting these orientations right is a tedious business, and we have a different way of dealing with it. We ignore the “true” orientations coming from the lifted maps and we simply make a guess as to how the plaid arcs correspond to the graph arcs. For example, in 10.2, it is pretty clear that the grey edge pointing left should be associated to the left half of the plaid triple.

Now we explain the convention in more detail, by way of example. Figure 10.3 shows an enhanced version of 10.2, specifically for Π_7 . Again, the label

of Π_7 is NEWNEWS, and this determines the orientation.

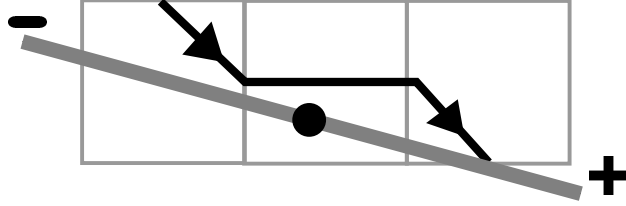


Figure 10.3: The case of Π_7 : a correspondence of type 1

We observe experimentally that the $(-)$ partition assigns the label $(0, -1)$, and this corresponds to the leftward pointing edge. Likewise, the $(+)$ partition assigns the label $(0, 1)$, and this corresponds to the rightward pointing edge. Thus, we associate the $(-)$ partition with the tail end of the triple and the $(+)$ partition with the head end. For this reason, we call Π_7 *type 1*. We would call Π_j *type 0* if, according to our experimental observations, the $(+)$ edge is associated with the tail and the $(-)$ edge is associated with the tail.

We guess the type for each of the 218 polytopes in the plaid triple partition, and these types are stored in the computer program. In most cases, as for Π_7 , the picture is completely obvious, and in a few cases, like the one shown in 10.2 for Π_{49} the picture is not quite as obvious but still pretty clear.

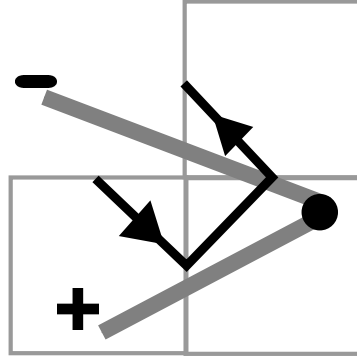


Figure 10.4: The case of Π_{48} : a correspondence of type 0.

Logically, it does not matter how we arrived at these guesses, or whether they agree with the true answer which can be cleaned by looking at the lifts. The point is simply that the proof runs to completion with the guesses made. In hindsight, our guesses surely agree with the true answer, but we do not need to prove this and we will not.

10.4 Edge Crossing Problems

To each index $i = 6, \dots, 218$ we associate what we call an *edge crossing problem*. We will first give the general definition and then we will work out the example of Π_7 .

Given Π_k , there corresponds a triple of squares $\Sigma_{-1}, \Sigma_1, \Sigma_1$ and an oriented plaid arc running through it, as in Figures 10.3 and 10.4. We label the squares so that Σ_1 is the head square in the type 1 case and the tail square in the type 0 case. In other words, the arithmetic graph edge associated to the (\pm) partition should point generally from Σ_0 to Σ_{\pm} for both types.

There are two kinds of edge crossing problems associated to P_k . One kind is labeled $(k, +, i, j, L)$. Here $L \in \{N, S, E, W\}$ is an edge of Σ_0 that the arithmetic graph edge $dT(i, j)$ associated to the $(+)$ partition could potentially cross (as in the right hand side of Figure 10.3) but according to the Pixellation Theorem is not supposed to cross. These crossing problems really only depend on the pair (Σ, Σ_+) . The other kind of edge crossing problem is labeled $(k, -, i, j, L)$, and has a similar explanation with $(-)$ in place of $(+)$.

Let's consider the case of P_7 . The two crossing problems are $(7, +, 0, 1, N)$ and $(7, -, 0, -1, S)$. The other two possibilities, namely $(7, +, 0, 1, E)$ and $(7, -, 0, -1, W)$, are the ones predicted by the Pixellation Theorem. They are not problems at all, but rather *goals*.

We have already mentioned that the first 6 of the plaid triple polytopes correspond to the trivial grid full squares. There are another 174 polytopes, labeled Π_6, \dots, Π_{179} , which have the property that there are unique graph polytopes $\Gamma_{k,+}$ and $\Gamma_{k,-}$ such that

$$\Psi(\Pi_k) \subset \Gamma_{k,\pm}. \quad (85)$$

Each of these contributes 2 edge crossing problems, giving a total of 348.

The 19 polytopes $\Pi_{180}, \dots, \Pi_{198}$ are such that

$$\Psi(\Pi_k) \subset \Gamma_{k,+,0} \cup \Gamma_{k,+,1}, \quad \Psi(\Pi_k) \subset \Gamma_{k,-}. \quad (86)$$

That is, $\Psi(\Pi_k)$ is contained in a union of two graph polytopes from the $(+)$ partition and 1 from the $(-)$ partition. In this case, there are two possible local picture of the arithmetic graph associated to this plaid triple. This does not bother us, as long as the edge crossings come out right. Each of these 19 polytopes contributes 3 edge crossing problems. This gives us another 57.

The 19 polytopes $\Pi_{199}, \dots, \Pi_{217}$ are such that

$$\Psi(\Pi_k) \subset \Gamma_{k,-,0} \cup \Gamma_{k,-,1}, \quad \Psi(\Pi_k) \subset \Gamma_{k,+}. \quad (87)$$

Each of these 19 polytopes contributes 3 edge crossing problems, giving yet another 57 crossing problems.

The grand total is 462 edge crossing problems. In the next chapter we will introduce the machinery needed to solve all these problems, so to speak. A *solution* amounts to a proof that the given case does not actually occur. Actually, we will be able to solve 416 of the problems. The remaining 46, in the cases where the pixellation really does fail, are involved in the catches for the offending edges discussed in the Pixellation Theorem. Once we have solved all the problems we can solve, and classified the exceptions, the rest of the Pixellation Theorem just comes down to inspecting the data generated by the program.

11 Edge Crossings

11.1 The Graph Method

Here we explain the first method we use for solving the edge crossing problems. We fix a parameter A throughout the discussion. Let G_Γ denote the grid graph. Let $\zeta_\Gamma \in G$ be some point, contained in a square Σ . As in previous chapters, the word *square* always means a unit integer square.

We assume that ζ_Γ is a nontrivial vertex of the arithmetic graph. Let e be one of the edges of the arithmetic graph incident to ζ_Γ . We think of e as a vector pointing from v out of Σ . From the Grid Geometry Lemma, we know that e crosses some edge of Σ . We say that e is of type (i, j, L) if $e = dT(i, j)$ and $L \in \{S, W, N, E\}$ is the label of the edge of Σ which e crosses.

Remark: We allow the possibility that e is of two types. This would happen if e crosses Σ at a vertex. We think that this never actually happens, but we have not ruled it out. In any case, this eventuality does not bother us.

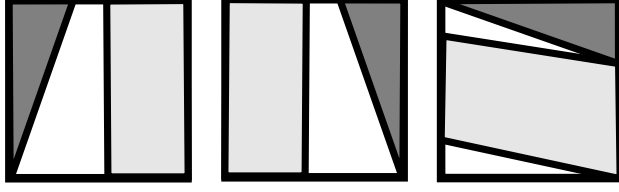
Let Φ_Γ denote the graph classifying map. We define

$$(x, y, z, A) = \Phi_\Gamma(\zeta_\Gamma) \tag{88}$$

Lemma 11.1 (Graph Avoidance) *The following is true.*

1. If $x \in (A, 1)$ then e is not of type $(-1, 0, W)$.
2. If $x \in (0, A)$ then e is not of type $(-1, 1, W)$.
3. If $y \in (A, 1)$ then e is not of type $(0, -1, N)$.
4. If $y \in (2A, 1 + A)$ then e is not of type $(0, 1, S)$.
5. If $x \in (1 - A, 1)$ then e is not of type $(1, -1, E)$.
6. If $x \in (0, 1 - A)$ then e is not of type $(1, 0, E)$.

Proof: We will treat the first three cases. The last three cases follow from symmetry. More precisely, reflection in the center of the square $[0, 1]^2$ carries the sets used to analyze Case N to the sets used to analyze Case 7-N. Figure 11.1 illustrates our arguments.



11.1: The first three cases

Case 1: We have

$$dT(-1, 0) = \left(-A, -\frac{1 + 2A - A^2}{1 + A} \right).$$

This vector points southwest and has slope greater than 1. So, in order for this edge to cross the west edge, it must lie in the triangle with vertices

$$(0, 0), \quad (0, 1) \quad \left(\frac{A^2 + A}{1 + 2A - A^2} \right).$$

We call this triangle *the danger zone*. The line through this third point and parallel to e contains the vertex between the south and west edges. The dark triangles in Figure 11.1 are hand-drawn versions of the danger zones in each case.

The Graph Reconstruction Formula tells us that the conditions $x \in (A, 1)$ correspond to the condition that the first coordinate of ξ_r lies in $(A, 1)$. The region of possibilities is the lightly shaded region on the left hand side of figure 11.1. As depicted in the figure, the two sets we have defined are disjoint.

Case 2: The argument is the same, except this time the danger zone has vertices

$$(1, 0), \quad (1, 1), \quad \left(\frac{4A}{4A - A^2} \right),$$

and the condition $x \in (0, A)$ corresponds to these same conditions on the first coordinate of ξ_r . Again, the two sets are disjoint. This is shown in the middle square of Figure 11.1.

Case 3: The argument is the same, except this time the danger zone has vertices

$$(0, 1), \quad (1, 1), \quad \left(1, \frac{1 - A}{1 + A} \right).$$

and the condition $y \in (A, 1)$ corresponds, *via* the Reconstruction Formula to ξ_Γ lying in the interior of the parallelogram with vertices

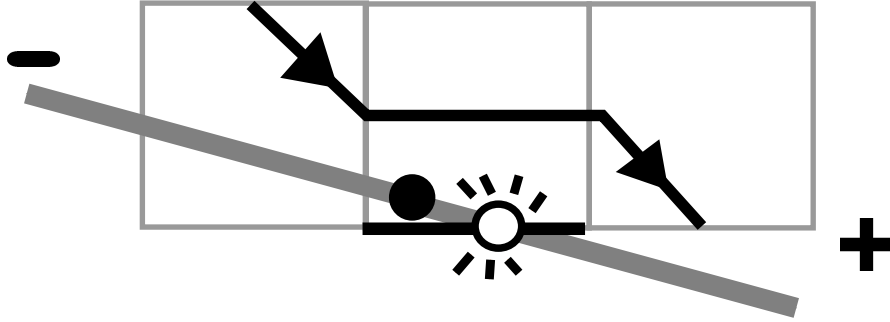
$$\left(0, \frac{A}{1+A}\right), \quad \left(0, \frac{1}{1+A}\right), \quad \left(1, \frac{1-A}{1+A}\right), \quad (0, 0).$$

Again, these sets are disjoint. This case is shown on the right side of Figure 11.1. ♠

Remark: In the previous result, the cases $(1, 1, N)$ and $(-1, -1, S)$ are missing. There is a similar result for these cases, but we will prove a result below that is more powerful and subsumes these cases. So, we ignore them here.

11.2 The Sample Result Revisited

In this section we explain how we solve the crossing problem $(7, +, , 0, 1, S)$. In other words, we are trying to rule out the bad crossing indicated on the right hand side of Figure 10.2, which we repeat here with enhanced labeling. We really need to solve 6 crossing



11.2: The crossing problem $(7, +, S)$.

The polytope $\Psi(\Pi_7)$ has 8 vertices:

- $(60, 60, 0, 30)/60$.
- $(60, 40, 20, 20)/60$.
- $(40, 40, 0, 20)/60$.
- $(60, 40, 0, 20,)/60$.

- $(60, 60, 0, 20)/60$.
- $(45, 45, 0, 15)/60$.
- $(60, 45, 15, 15)/60$.
- $(60, 45, 0, 15)/60$.

We have written the vertices this way so as to clear denominators. The factor of 60 works for every polytope in sight. (My program has a window which allows the user to see the vertices of any polytope in any of the partitions.)

Recalling that we coordinatize \hat{X} using the variables, note that

$$y \in [2A, 1 + 2A]. \quad (89)$$

for all vertices of $\Psi(\Pi_7)$. By convexity, this equation holds for all points, and we get strict inequality for points in the interior of $\Psi(\Pi_7)$.

It follows from the Master Picture Theorems and the Intertwining Theorem that

$$(x, y, z, A) = \Phi_\Gamma(\zeta_\Gamma) \in \text{interior}(\Psi(\Pi_y)). \quad (90)$$

Hence $y \in (2A, 1 + 2A)$. Case 4 of the Graph Avoidance Lemma, which pertains to the triple $(0, 1, S)$, solves this crossing problem.

The argument works the same way for all 6 crossing problems associated to the bad crossing shown in Figure 11.2. It follows from symmetry (or from a similar argument) that the 6 crossings associated to the other arithmetic graph edge in Figure 11.2 are also soluble. Thus, every time this pattern occurs in the plaid model for any parameter, and the central square is grid full, the central square is pixellated.

Remark: Sometimes we use the Graph Avoidance Lemma in a different way. To illustrate our other usage, we will solve the edge crossing problem $(198, +, -1, 1, E)$. This time it turns out that the criterion in the Graph Avoidance Lemma for $(1, -1, E)$ does not hold for $\Psi(\Pi_{198})$. However, it does hold for $\Gamma_{198,+,0}$, the relevant one of the two graph polytopes in the $(+)$ graph partition whose union contains $\Psi(\Pi_{198})$. So, again, we find that $\Phi_\Gamma(\xi_\Gamma)$ cannot lie in the region corresponding to a situation where the graph edge incident to ζ_Γ crosses E .

For all the relevant crossing problems on which we use the Graph Avoidance Lemma, we will either apply the criteria to $\Psi(\Pi)$ or to the relevant graph polytope Γ . In short, we will use the one method or the other.

11.3 The Plaid Method

Here we discuss a second method for solving crossing problems. In the discussion that follows, $L \in \{N, S, E, W\}$ stands for one of the edge labels. To 10 of the 16 pairs (i, j, L) . Let $\langle i, j, L \rangle$ denote the subset of \widehat{X} which assigns the edge $e = dT(i, j)$ to grid graph points ζ_Γ in such a way that e crosses the edge L of the square containing the point ζ_Γ . The Graph Avoidance Lemma can be interpreted as saying that certain regions in \widehat{X} avoid $\langle i, j, L \rangle$. For instance, the set $x \in (A, 1)$ is disjoint from $\langle -1, 0, W \rangle$.

Recall that X_Π^* is the hitset. We are going to associate a polytope $Z(i, j, L) \subset X_\Pi$ such that one of two things is true:

- If $P \cap Z(i, j, L) = \emptyset$ then $\Psi(P) \cap \langle i, j, L \rangle = \emptyset$.
- If $P \subset Z(i, j, L)$ then $\Psi(P \cap X_\Pi^*) \cap \langle i, j, L \rangle = \emptyset$.

In the first case, we call P an *excluder* and in the second case we call P a *confiner*. The other 6 pairs we simply ignore.

For each fixed parameter, our polytopes all have the form

$$Z(i, j, L) = Z'(i, j, L) \times [-1, 1], \quad (91)$$

Where $Z'(i, j, L)$ is a polygon in the xy plane. We will list 4 of the 10 sets. The other 5 are obtained from the first 5 *via* the following symmetry.

$$Z(-i, -j, L^{\text{opp}}) = -Z(i, j, L). \quad (92)$$

Here L^{opp} is defined to be the edge opposite L . For instance $E^{\text{opp}} = W$. We list the 5 polygons $Z'(i, j, L)$ as a function of the parameter A , and recall that $P = 2A/(1 + A)$. The first set is an excluder and the other 5 are confiners. Here are the sets:

- $Z'(1, 1, N)$: $(1 - P, 1 - P), (P - 1, P - 1), (P - 1, -1), (1 - P, -1)$.
- $Z'(1, 1, E)$: $(1 - P, 1 - P), (-1, -1), (1 - P, -1)$.
- $Z'(0, 1, S)$: $(-1, -1), (P - 1, P - 1), (1, P - 1), (1 - P, -1)$.
- $Z'(1, 0, E) = Z'(1, 1, E)$.
- $Z'(0, -1, W) = Z'(0, 1, S)$.

Conveniently, all these sets intersect the hitset inside the fundamental dipole Υ considered in §9.10. This makes our analysis easy.

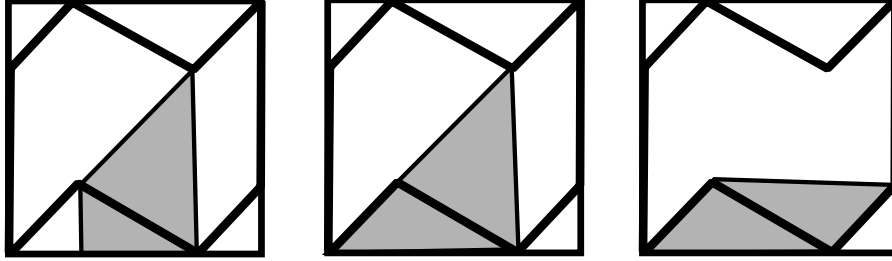


Figure 10.4: The barrier bases in action.

To establish our claims, we use the Plaid Reconstruction Formula, Equation 77, to map our sets into the unit square, and we check that the relevant image is disjoint from the set of positions in $[0, 1]^2$ where ζ_Γ can be placed so that $dT(i, j)$ crosses edge L . We called these sets the danger zones in the proof of the Graph Avoidance Lemma.

11.3.1 Case 1

Here we consider $(1, 1, N)$. Calculations like the one done in the proof of the Graph Avoidance Lemma show that the danger zone is the triangle with vertices

$$(1, 1), \quad (0, 1), \quad (0, P).$$

Let $Z'_*(1, 1, N)$ denote the intersection of $Z'(1, 1, N)$ with the planar projection of the hitset. The vertices of $Z'_*(1, 1, N)$ are

$$(P - 1, P - 1), \quad (1 - P, -1), \quad (1 - P, 1 - P).$$

Beautifully, the image of this triangle under the affine diffeomorphism from Equation 77 is exactly the danger zone.

11.3.2 Case 2

Here we consider $(1, 1, E)$. The danger zone is the complement of the triangle considered in Case 1. We have $Z'_+(1, 1, N) = Z'_+(1, 1, E)$. So, we have already computed the relevant affine image; it is the set $\Sigma_0(1, 1)$ from Case 1. But the interiors of $\Sigma_0(1, 1)$ and $\Sigma_1(1, 1)$ are disjoint: these two sets partition the unit square.

11.3.3 Case 3

Here we consider $(0, 1, S)$. The danger zone is the same as the one in Case 4 of the Graph Avoidance Lemma. It has vertices

$$(0, 0), \quad (1, 0), \quad (0, P).$$

The set $Z'_*(0, 1, Z)$ is the triangle with vertices

$$(P - 1, P - 1), \quad (1 - P, -1), \quad (1, P - 1).$$

The image of this set under the affine diffeomorphism is the triangle with vertices

$$(0, 1), \quad (1, 1), \quad (1, P).$$

This triangle is clearly disjoint from the danger zone.

11.3.4 Case 4

Here we consider $(1, 0, E)$. The danger zone has vertices

$$(1, 1), \quad (1, 0), \quad \left(\frac{1 + A - 2A^2}{1 + 2A - A^2} \right)$$

We have $Z'(1, 0, E) = Z'(1, 1, E)$. The analysis in Case 1 shows that the affine image of $Z'_+(1, 0, E)$ is the triangle with vertices

$$(1, 1), \quad (0, 1), \quad (0, P).$$

The interior of this set is clearly disjoint from the danger zone.

11.3.5 Case 5

Here we consider $(0, -1, W)$. The danger zone has vertices

$$(0, 0), \quad (1, 0), \quad (1, P).$$

We have $Z'(0, -1, W) = Z'(0, 1, S)$, the set from Case 3. As in Case 3, the vertices of the affine image of $Z'(0, -1, W)$ is the triangle with vertices

$$(0, 1), \quad (1, 1), \quad (1, P).$$

The interior of this set is disjoint from the danger zone.

11.4 Another Edge Crossing Problem

Here we solve another edge crossing problem, to illustrate the logic behind the use of the Plaid Method. We use the notation from above. One of the crossing problems is $(50, +, -1, -1, W)$. This time we find that $\Pi_{50} \subset Z(-1, -1, W)$. Therefore Hence

$$\Psi_{\Pi}(\zeta_{\Pi}) \subset Z(-1, -1, W). \quad (93)$$

The existence of ζ_{Γ} means that the relevant square Σ is grid full.

$$\Psi_{\Pi}(\zeta_{\Pi}) \subset Z(-1, -1, W) \cap X_{\Pi}^*. \quad (94)$$

By the Intertwining Theorem

$$\Phi_{\Gamma}(\zeta_{\Gamma}) \subset \Psi(Z(-1, -1, W) \cap X_{\Pi}^*). \quad (95)$$

By the confining property of $Z(-1, -1, W)$,

$$\Phi_{\Gamma}(\zeta_{\Gamma}) \notin \langle -1, -1, W \rangle. \quad (96)$$

This solves the crossing problem.

11.5 Out of Bounds

Sometimes none of the above methods works for a crossing problem, but then we notice that Π_k lies entirely outside the hitset Z_{Π}^* . In this case we call Π_k *out of bounds*. The corresponding crossing problem simply does not arise for a grid full square.

We will verify that Π_k is out of bounds by showing that

$$\Pi_k \subset \bigcup_{i=1}^4 B_i \times [-1, 1]. \quad (97)$$

Where B'_1, B'_2, B'_3, B'_4 are the following 4 triangles, described in terms of their vertices:

1. $B'_1 : (-1, -1), (P-1, -1), (P-1, P-1)$.
2. $B'_2 : (1-P, -1), (1, -1), (1, P-1)$.
3. $B'_3 = -B'_1$.

4. $B'_4 = -B'_2$.

Figure 11.5 shows how these triangles sit in relation to the planar projection of the hitset.

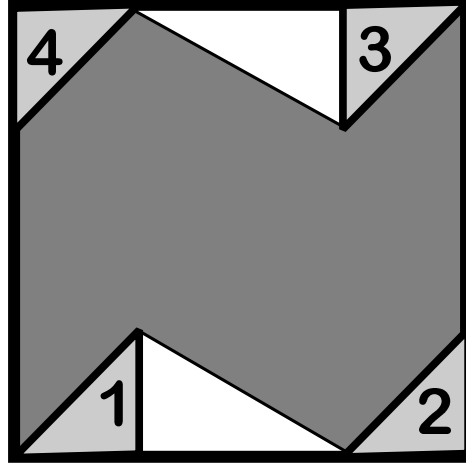


Figure 11,5: The out-of-bounds polygons in action.

Note that the union

$$B_i = \bigcup_{P \in [0,1]} (B'_i \times \{P\}) \quad (98)$$

is a convex polytope with integer coefficients. Here $P = 2A/(1+A)$ as usual. This, showing that $\Pi_k \subset B_i$ for some pair (k, i) is just a matter of integer linear algebra. We call the verification that $\Pi_k \subset B_i$ the *out of bounds test*.

12 Proof of the Pixellation Theorem

Pixellation Theorem. In this chapter, we prove Statements 3,4,5 of the Pixellation Theorem modulo certain integer computer calculations.

12.1 Solving Most of the Crossing Problems

Using the methods discussed in the last chapter, namely the Graph Method, the Plaid Method, and the Out of Bounds Test, we solve 416 of the 462 crossing problems. Each case is like one of the ones considered in the previous chapter, but there are too many to do by hand. In the next chapter we will explain the integer linear algebra tests we use to check each case.

There are 46 exceptional cases. Let's call these 46 cases *recalcitrant*. A few of the recalcitrant cases actually are soluble by more delicate methods - we would just need to look harder at the polytopes involved - but there isn't any problem in our proof with leaving them unsolved.

12.2 Proof of Statement 3

Figure 4.3 shows examples of an errant edge when the two squares are stacked side by side. We repeat the picture here. We will consider the picture on the right hand side of Figure 12.1 in detail. In this picture, the square with the dot is the central square and the top square is not part of the triple. So, we are only showing two of the three squares in the triple.

The codes associated to the figure on the right are either LLLEWS or SWELLL, depending on the orientation. Here $L \in \{N, S, E, W\}$ is a label we don't know. The corresponding errant edge must rise up at least 1 unit. This leaves $dT(1, -1)$ and $dT(1, 0)$ as the only possibilities.

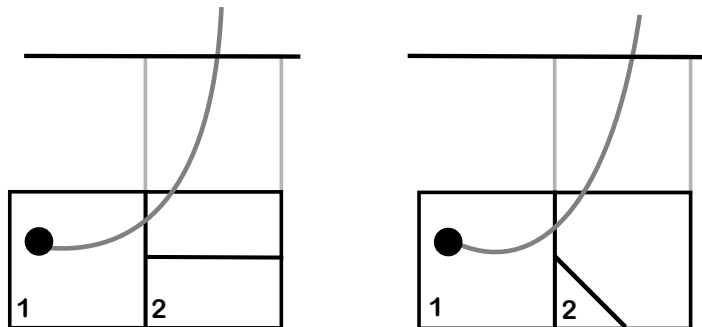


Figure 12.1: errant edges

From the correspondence of polytopes explained in §10, we know the complete list of labels associated to relevant ends of the relevant triples. We just check, by a quick computer search (and also by inspection) that the errant labels never arise. Thus, for instance, we never see the label $(1,0)$ associated to the head end of LLEWS or the tail end of SWELLL. We rule out the other possibilities similarly. Here is a list of the possible codes and the forbidden labels. To save space, we only list half the possibilities. The other half are obtained from these by 180 degree rotation. Also, of the half we do list, we only list the codes such that the corresponding errant edge would be associated to the head of the triple. So, we would list LLEWS only in our example above. Here is the list.

- LLEWS: $(1,0)$, $(1,-1)$.
- LLEWN: $(-1,0)$, $(-1,1)$.
- LLEWE: $(1,0)$, $(1,-1)$, $(-1,0)$, $(-1,1)$.
- LLLSNE: $(-1,-1)$, $(0,-1)$.
- LLLSNW: $(1,1)$, $(0,1)$.
- LLLSNS: $(-1,-1)$, $(1,1)$, $(0,1)$, $(0,-1)$.

We simply check that none of these bad situations actually arises. The rest of the proof of the Pixellation Theorem is devoted to proving Statements 3 and 4. This takes more work.

12.3 Proof of Statement 4

Statement 4 of the Pixellation Theorem says that two arithmetic graph edges incident to a vertex in a square never cross the same edge of that square. This result follows immediately for the 416 cases in which can solve the crossing problem: These cases are all pixellated and the edges in question cross the same sides as the plaid model segments. It just remains to deal with the 46 recalcitrant cases.

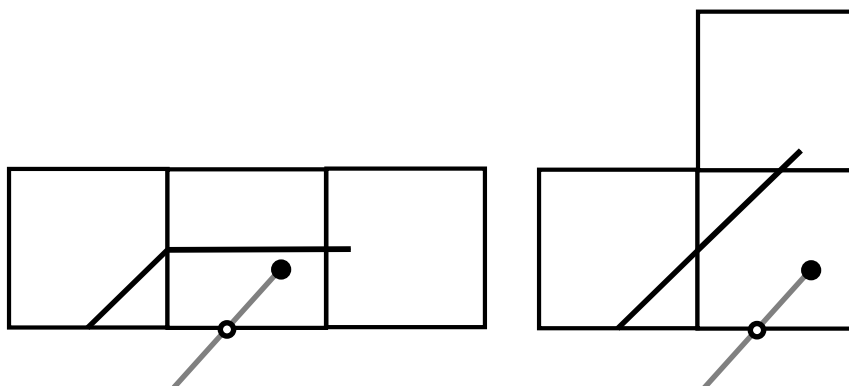


Figure 12.2: The recalcitrant cases

By direct inspection, we see that all of the recalcitrant cases are either pixellated or equivalent to the two cases shown in Figure 12.2. (By symmetry, we just have to inspect 23 of the 46 cases.) By *equivalent* we mean that the picture is meant to be taken up to rotations and reflections.

Now consider the arithmetic graph edges associated to the a recalcitrant case. The first edge, the one shown in Figure 12.2, is offending. The other edge is either offending or not. If the other edge is not offending, then it manifestly crosses a different edge of the central square. If the other edge is offending, and crosses the same edge as the first offending edge, then the picture must look like Figure 12.3.

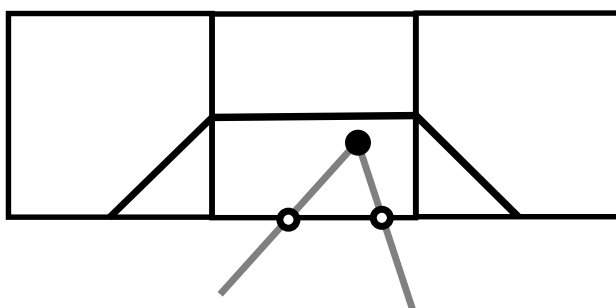


Figure 12.3: A double edge crossing

There are exactly two cases like this, corresponding to P_{34} and P_{173} . But, in both cases, we check that the polytope is involved in only one recalcitrant crossing problem. So, in these two cases, only one of the two edges is offending.

This takes care of all the possibilities.

12.4 Proof of Statement 5

Each recalcitrant case corresponds to a plaid triple. Using the curve-following dynamics discussed in §6.4, we check which plaid triples could attach to the one we have. We will illustrate what we mean by example and then state the general result.

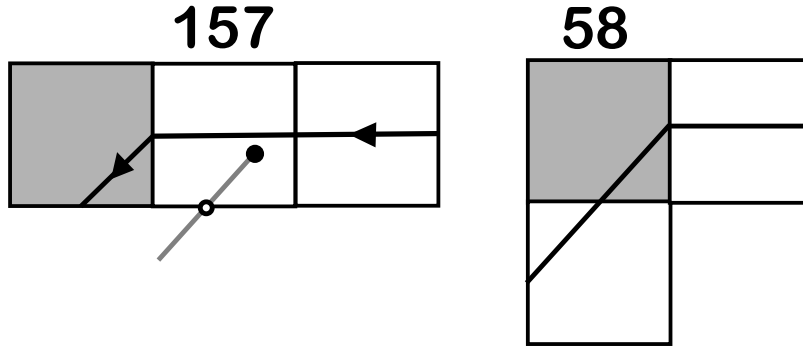


Figure 12.4: The triples corresponding to Π_{157} and Π_{58} .

One of the recalcitrant triples is $(157, -, -1, 0, S)$. The associated code for Π_{157} is EWEWES. Figure 12.4 shows the situation. The offending edge goes with the orientation of the plaid arc, and so we do the $(+)$ dynamics to figure out what happens to points in Π_{157} . That is, we consider the image $F(\Pi_{157})$. (In the other case, when the offending edge goes against the orientation, we would use the map F^{-1} .) We prove that

$$F(\Pi_{157}) \subset \Lambda(\Pi_{58}). \quad (99)$$

Here Λ is the plaid lattice.

We then check that Π_{58} is grid empty. This means that any unit integer square in the plaid model classified by Π_{58} is grid empty. Here we mean that Φ_Π maps the center of the square into Π_{58} . But then Equation 99 tells us that the square on the right and side of any plaid triple associated to Π_{157} is grid empty. We have shaded the trid empty squares.

Equation 99 says that every occurrence of a plaid triple associated to Π_{157} is conjoined, so speak, with a plaid triple associated to Π_{58} . We have also added in an extra square, even though we don't know the picture in this square. Figure 12.5 shows the situation.

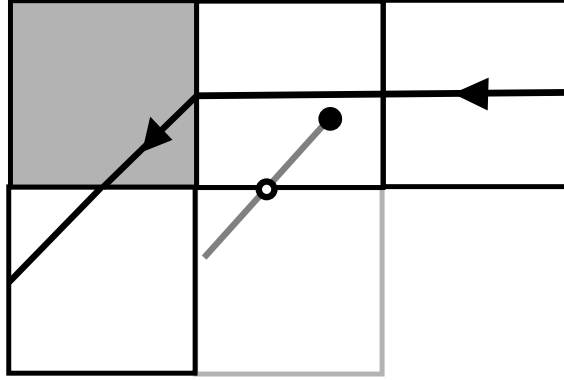


Figure 12.5: The plaid quadruple obtained by concatenating Π_{157} and Π_{38} .

When we look at the curve following dynamics for the other recalcitrant cases, we discover that the same thing always happens: The side square associated to the offending edge is grid empty. Up to isometry, the picture always looks like one of the cases of Figure 12.6.

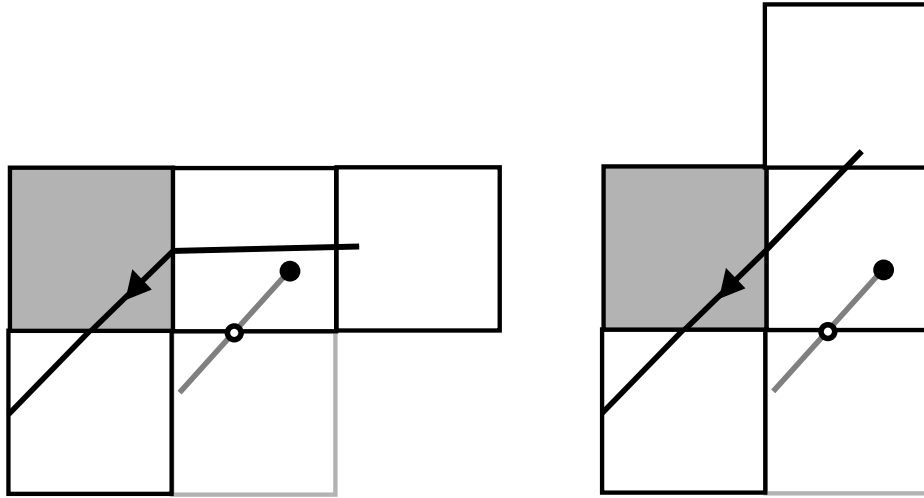


Figure 12.6: Concatenations for the recalcitrant triples

The only thing we need to do in order to finish the proof of Statements 3 and 4 is to analyze where the offending edge ends. There are 8 cases to consider, and the last 4 cases are rotates images of the first 4 cases. So, we will just consider the first 4 cases.

12.4.1 Case 1

In this case, the offending edge is $dT(-1, 0)$ and the picture is oriented as in Figure 12.6. There are 9 cases like this. We have

$$dT(0, -1) = \left(-A, \frac{A^2 - 2A - 1}{1 + A} \right).$$

For each of the 9 cases, we check that

$$\Psi(\Pi_k) \subset \{(x, y, z, A) | x \leq A\}. \quad (100)$$

By the Reconstruction Formula, the first coordinate of $(a, b) = \zeta_\Gamma$, the graph grid point contained in the relevant square, to satisfy $[a] < A$. But then the offending edge must cross over the thick vertical line shown in Figure 12.7 and end in one of the two indicated squares.

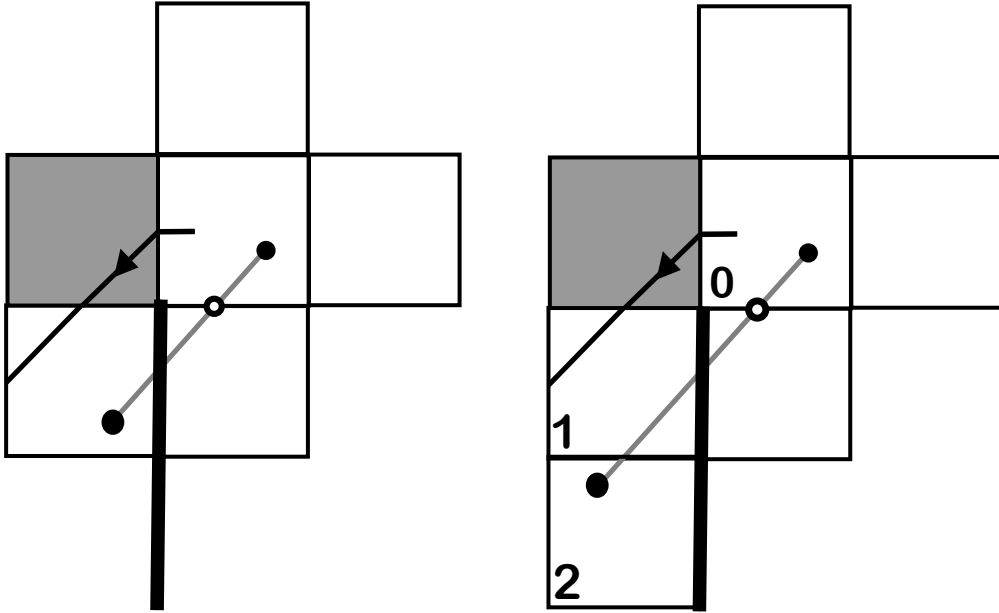


Figure 12.7: The two possible endings for the offending edge

We recognize the two cases as reflected versions of the catches in Figure 4.2. The proof is done in this case.

12.4.2 Case 2

In this case, the offending edge is $dT(-1, 0)$ and the picture is oriented as in Figure 12.8. There are 7 cases like this, and they all have the features shown in Figure 12.8.

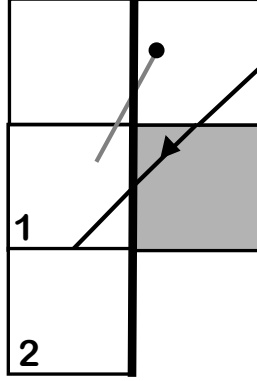


Figure 12.8: Cast 2

We check that Equation 100 holds in all 7 cases. Hence, the offending edge crosses the thick vertical line and ends in the squares marked 1 and 2. Again, we have the catches shown in Figure 4.2.

12.4.3 Case 3

In this case, the offending edge is $dT(0, -1) = (-1, P)$, and the picture is oriented as in Figure 12.9. There are 3 cases like this.

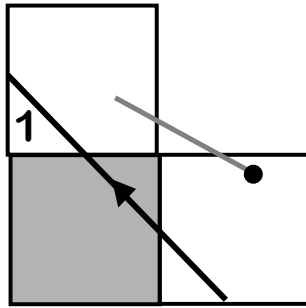


Figure 12.9: Case 3

This case is easy. We know that the offending edge crossed the top of the square it starts in, and given that the vector is $(-1, P)$, it must end in the square Σ_1 . This gives us the left hand catch in Figure 4.2, up to orientation.

12.4.4 Case 4

In this case, the offending edge is $dT(0, -1) = (-1, P)$, and the picture is oriented as in Figure 12.10. There are 4 cases like this.

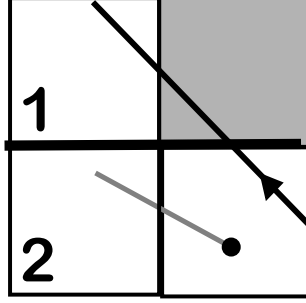


Figure 12.10: Case 4

In this case, the offending edge crosses the thick horizontal line provided that the coordinates (a, b) of ζ_Γ satisfy

$$b + Pa \geq 1 - P, \quad b \leq 1. \quad (101)$$

Notice that this is a weaker condition than $b + Pa \geq 1$, which is what we would have needed to solve the crossing problem. Using the Graph Reconstruction Formula, we have

$$a = x, \quad b = \frac{y - Ax}{1 + A} \quad (102)$$

Plugging this equation into Equation 101 and simplifying, we find that Equation 101 holds provided that

$$y \in [1 - A - Ax, 1 + A + Ax] \quad (103)$$

We check, for each of the cases, that $x \geq 0$ and $y \in [1 - A, 1 + A]$. This does the job for us. Thus, the offending edge ends in the square Σ_1 , and we get the catch on the left hand side of Figure 4.2.

In all cases, each offending edge has a catch. At the same time, each catch that appea

13 Computer Assisted Techniques

13.1 Operations on Polytopes

Clean Polytopes: Say that a *clean polytope* is a convex polytope in \mathbf{R}^4 with integer vertices, such that each vertex is the unique extreme point of some linear functional. In other words, a clean polytope is the convex hull of its (integer) vertices, and the convex hull of any proper subset of vertices is a proper subset. We always deal with clean polytopes. The polytopes in the plaid and graph triple partitions have all the properties mentioned above, except that their vertices are rational rather than integral. We fix this problem by scaling all polytopes in all partitions by a factor of 60.

Clean Polytope Test: Suppose we are given a finite number of integer points in \mathbf{R}^4 . Here is how we test that they are the vertices of a clean polytope. We consider all linear functionals of the form

$$L(x, y, z, A) = c_1x + c_2y + c_3z + c_4A, \quad |c_i| \leq N \quad (104)$$

and we wait until we have shown that each vertex is the unique maximum for one of the functionals. For the polytopes of interest to us, it suffices to take $N = 3$. In general, our test halts with success for some N if and only if the polytope is clean.

Disjointness Test: Here is how we verify that two clean polytopes P_1 and P_2 have disjoint interiors. We consider the same linear functionals as listed in Equation 104 and we try to find some such L with the property that

$$\max_{v \in V(P_1)} L(v) \leq \min_{v \in V(P_2)} L(v). \quad (105)$$

Here $V(P_k)$ denotes the vertex set of P_k . If this happens, then we have found a hyperplane which separates the one polytope from the other. This time we take $N = 5$.

Containment Test: Given clean polytopes P_1 and P_2 , here is how we verify that $P_1 \subset P_2$. By convexity, it suffices to prove that $v \in P_2$ for each vertex of P_1 . So, we explain how we verify that $P = P_2$ contains an integer point v . We do not have the explicit facet structure of P , though for another purposes (computing volumes) we do find it.

Let $\{L_k\}$ denote the set of all linear functionals determined by 4-tuples of vertices of P . Precisely, Given 4 vertices of P , say w_0, w_1, w_2, w_3 , and some integer point v , we take the 4×4 matrix whose first three rows are $w_i - w_0$ for $i = 1, 2, 3$ and whose last row is v . Then

$$L_{w_0, w_1, w_2, w_3}(v) = \det(M) \quad (106)$$

is the linear functional we have in mind.

If the vertices do not span a 3-dimensional space, then L will be trivial. This does not bother us. Also, some choices of vertices will not lead to linear functions which define a face of P . This does not bother us either. The point is that our list of linear functionals contains all the ones which do in fact define faces of P . We take our vertices in all orders, to make sure that we pick up every possible relevant linear functional. The computer does not mind this redundancy.

It is an elementary exercise to show that $v \notin P$ if and only if v is a unique extreme point amongst the set $\{v\} \cup V(P)$ for one of our linear functionals. Here $V(P)$ denotes the vertex set of P , as above. So, $v \in P$ if and only if v is never a unique extreme point for any of the linear functionals on our list.

Volume: First we explain how we find the codimension 1 faces of P . We search for k -tuples of vertices which are simultaneously in general position and the common extreme points for one of the linear functionals on our list. As long as $k \geq 4$, the list we find will be the vertices of one of the faces of P .

Now we explain how we compute the volume of P . This is a recursive problem. Let v_0 be the first vertex of P . Let F_1, \dots, F_k be the codimension 1 faces of P . Let P_j be the cone of F_j to v_0 . This is the same as the convex hull of $F_j \cup \{v_0\}$. Then

$$\text{vol}(V) = \sum_{j=1}^k \text{vol}(V_j). \quad (107)$$

If $v_0 \in V_j$ then the volume is 0. These extra trivial sums do not bother us.

To compute $\text{vol}(V_j)$ we let $w_{j0}, w_{j1}, w_{j2}, w_{j3}$ be the first 4 vertices of F_j . Let L_j be the associated linear functional. Then

$$4 \times \text{vol}(V_j) = L_j(v_0 - w_{j0}) \times \text{vol}(F_j). \quad (108)$$

We compute $\text{vol}(F_j)$ using the same method, one dimension down. That is, we cone all the facets of F_j to the point w_{j0} . It turns out that the

polyhedra $\{F_{ij}\}$ in the subdivision of F are either tetrahedra or pyramids with quadrilateral base. In case F_{ij} is a tetrahedron we compute $12\text{vol}(F_{ij})$ by taking the appropriate determinant and doubling the answer. In the other case, we compute 6 times the volume of each of the 4 sub-tetrahedron of F_{ij} obtained by omitting a vertex other than w_{0j} and then we add up these volumes. This computes $12\text{vol}(F_{ij})$ regardless of the cyclic ordering of the vertices around the base of F_{ij} .

When we add up all these contributions, we get $12 \text{ vol}(F_j)$. So, our final answer is $48 \text{ vol}(V)$. The reason we scale things up is that we want to have entirely integer quantities.

Potential Overflow Error: With regard to the volume method, a straightforward application of our method can cause an overflow error. We do the calculations using longs (a 64 bit representation of an integer) and the total number we get by adding up 218 smaller numbers is (barely) too large to be reliably represented. However, we observe that all the numbers we compute are divisible by 480. So, before adding each summand to the list, we divide out by 480. This puts us back into the representable range. Recalling that we have scaled up by 60, then computed 48 times the volume, then divided by 480, our final computation is

$$\Omega = 6^4 10^3 \tag{109}$$

times the true volume.

13.2 The Calculations

We work with 3 partitions and then a few extra polytopes.

The Plaid Partition: The plaid partition, described in §6 has 26 clean polytopes modulo the action of the plaid lattice Λ_1 . For each all i, j, k with $|i|, |j|, |k| \geq 3$, we check that each polytope P_k is disjoint from $\lambda_{i,j,k}(P_\ell)$, where $\lambda_{i,j,k}$ is the standard word in the generators of Λ_1 . Given that all the original polytopes intersect the fundamental domain, and given the sizes of the translations in Λ_1 , this check suffices to show that the orbit $\Lambda(\bigcup P_i)$ consists of polytopes with pairwise disjoint interiors and that the union of our polytopes $P_0 \cup \dots \cup P_{25}$ is contained in a fundamental domain for Λ_1 .

At the same time, we compute that

$$\sum_{i=0}^{25} \text{vol}(P_i) = 8. \quad (110)$$

Again, we compute that the scaled volume is 8Ω . This coincides with the volume of the fundamental domain $[-1, 1]^3 \times [0, 1]$ for Λ_1 .

We now know the following three things:

1. The union of the 26 plaid polytopes is contained in a fundamental domain.
2. The union of the 26 plaid polytopes has the same volume as a fundamental domain.
3. The Λ_1 orbit of the 26 plaid polytopes consists of polytopes having pairwise disjoint interiors.

We conclude from this that the Λ_1 orbit of the plaid polytopes P_0, \dots, P_{25} is a partition of \widehat{X} , as desired.

Remark: In view of the fact that we have already proved the Plaid Master Picture Theorem, these checks are really unnecessary, provided that we have correctly interpreted the geometric description of the plaid polytopes and copied down the points correctly. So, these calculations really serve as sanity checks.

The Graph Partitions: We just deal with the $(+)$ graph partition, because the $(-)$ graph partition is isometric to the $(+)$ partition. We make all the same calculations for the $(+)$ graph partition that we made for the plaid partition, and things come out the same way. Once again, the fact that things work out is a consequence of our Master Picture Theorem from [S0], but we made several changes to the polytopes in this paper. We swapped the first and third coordinates, and also translated. So, these calculations serve as sanity checks.

The Reduced Plaid Triple Partition: The reduced plaid triple partition consists of 218 convex rational polytopes, which we scale up by a factor of 60. The scaled polytopes are all clean. Using the above tests, we check

that the polytopes have pairwise disjoint interiors, and are all contained in the fundamental domain $X_{\Pi} = [-1, 1]^3 \times [0, 1]$. Finally, we check that the sum of the volumes is 8. This verifies that we really do have a partition.

There is one more important check we make. Each plaid triple polytope has a 6 letter code which tells how it is obtained as an intersection of the form $A_{-1} \cap A_0 \cap A_1$, where A_k is a polytope in the partition $F^{(k)}(\mathcal{P})$. Here \mathcal{P} is the plaid partition and F is the curve-following dynamics.

We check that each triple plaid Π_k is contained in the three polytopes that are supposed to contain it, and is disjoint from all the others in the plaid partition and its images under the forward and backward curve following map. This verifies that the plaid triple partition really is as we have defined it.

Nine Graph Doubles: We mentioned in §10 that sometimes it happens that $\Psi(\Pi_k)$ is not contained in a single graph polytope of one of the two partitions, but rather a union of two of them. This happens 19 times for the (+) partition and 19 times for the (−) partition. We call these unions of graph polytopes *doubles*.

We check that each graph double (when scaled up by a factor of 60) is clean, that each graph double indeed contains both of its constituent graph polytopes, and that the volume of the graph double is the sum of the volumes of the two constituents. This shows that the union of the two graph polytopes really is a clean convex polytope.

The Rest of the Calculations Each edge crossing problem either involves showing that some linear functional is positive on a polytope, or else that two clean polytopes have pairwise disjoint interiors, or that one clean polytope is contained in another. We simply run the tests and get the outcomes mentioned above. The same goes for the several recalcitrant cases done in connection with the proof of Statement 5 of the Pixellation Theorem given in the last chapter. Finally, checking that there are no errant edges just amounts to listing out the data and checking that there are no forbidden edge assignments. We also survey the assignments visually and see that there are no errant edges.

13.3 The Computer Program

In this last section I'll give a rough account of some of the main features of the program. The main purpose of this account is to show you the kinds of things the program can do. The later entries in this section are rather sketchy. They are designed to let you know what sorts of things the program can do, but they stop short of giving detailed instructions on how to get the program to do it. The program has its own documentation - every feature is explained - and this should help with the details.

13.3.1 Downloading the Program

My computer program can be downloaded from

<http://www.math.brown.edu/~res/Java/PLAID2.tar>

When you download the file, you get a tarred directory. I untar the directory with the Unix command **tar -xvf PLAID2.tar**. (Your system might be different.) Once this is done, you have a new directory called **PlaidModel**. The program resides in this directory and is spread out among many files.

13.3.2 Running and Compiling

The file **Main.java** is the main file. Assuming that the program is compiled already (and you would know by the presence of many .class files) compile the program with the command **javac *.java** and then you run the program with the command **java Main**. All this assumes, of course, that your computer can run Java programs. If everything works, a small and colorful window should pop up. This is the control panel. You can launch the other parts of the program from this window.

13.3.3 What to do first

The control panel has a smaller window which lists 10 pop-up windows. If you click on these buttons, additional windows will pop up. The first button you should press is the **Document** button. This will bring up a window which has information about the program. If you read the documentation, you will see how to operate the program.

13.3.4 Presets

The program has 4 preset modes. When you select the **preset** option on the **main** control panel, you bring up an auxiliary control panel called **presets**. This panel has 4 buttons:

- quasi-isomorphism theorem
- plaid master picture theorem
- graph master picture theorem
- plaid-graph correspondence

If you press one of these buttons, various windows will pop up, and they will be automatically set up to best show the advertised features. Moreover, documentation will appear which gives further instructions and explanations.

There is one irritating feature of the program which I should mention. The **preset** features work best when all the auxiliary pop-up windows are closed. If you press a **preset** when some the pop-up windows are already open, you run the risk of having duplicate windows open, and this causes problems for the program. When you want to use one of the preset buttons, you should close all the auxiliary windows.

13.3.5 Surveying the Data and Proofs

The files starting **Data** contain all the data for the polytope partitions. The file names give some idea of what the files contain. For instance, **Data-GraphPolytopes.java** contains the coordinates of the graph PET polytopes. Some of the files are harder to figure just from the names, but the files themselves have documentation.

The files starting **Proof** contain all the routines for the proof. Again, the names indicate the tests contained in the files. For instance **ProofVolume.java** contains the volume calculations for the partitions.

14 References

- [B] P. Boyland, *Dual billiards, twist maps, and impact oscillators*, Nonlinearity **9**:1411–1438 (1996).
- [DeB] N. E. J. De Bruijn, *Algebraic theory of Penrose’s nonperiodic tilings*, Nederl. Akad. Wentensch. Proc. **84**:39–66 (1981).
- [D] R. Douady, *These de 3-eme cycle*, Université de Paris 7, 1982.
- [DF] D. Dolopyat and B. Fayad, *Unbounded orbits for semicircular outer billiards*, Annales Henri Poincaré, to appear.
- [G] D. Genin, *Regular and Chaotic Dynamics of Outer Billiards*, Pennsylvania State University Ph.D. thesis, State College (2005).
- [GS] E. Gutkin and N. Simanyi, *Dual polygonal billiard and necklace dynamics*, Comm. Math. Phys. **143**:431–450 (1991).
- [H] W. Hooper, *Renormalization of Polygon Exchange Transformations arising from Corner Percolation*, Invent. Math. **191.2** (2013) pp 255-320
- [Ko] Kolodziej, *The antibilliard outside a polygon*, Bull. Pol. Acad Sci. Math. **37**:163–168 (1994).
- [M1] J. Moser, *Is the solar system stable?*, Math. Intelligencer **1**:65–71 (1978).
- [M2] J. Moser, *Stable and random motions in dynamical systems, with special emphasis on celestial mechanics*, Ann. of Math. Stud. 77, Princeton University Press, Princeton, NJ (1973).
- [N] B. H. Neumann, *Sharing ham and eggs*, Summary of a Manchester Mathematics Colloquium, 25 Jan 1959, published in Iota, the Manchester University Mathematics Students’ Journal.
- [S0] R. E. Schwartz, *Outer Billiard on Kites*, Annals of Math Studies **171** (2009)

- [S1] R. E. Schwartz, *Introducing the Plaid Model*, preprint 2015.
- [S2] R. E. Schwartz, *Unbounded orbits for the plaid model*, preprint 2015.
- [T1] S. Tabachnikov, *Geometry and billiards*, Student Mathematical Library 30, Amer. Math. Soc. (2005).
- [T2] S. Tabachnikov, *Billiards*, Société Mathématique de France, “Panoramas et Synthèses” 1, 1995
- [VS] F. Vivaldi and A. Shaidenko, *Global stability of a class of discontinuous dual billiards*, Comm. Math. Phys. **110**:625–640 (1987).